The Equations of Motion of the Post-Newtonian Compact Binary Inspirals As Gravitational Radiation Sources Under The Effective Field Theory Formalism

by

Zixin Yang

B.S. in Physics, Wuhan University, 2014

Submitted to the Graduate Faculty of

the Dietrich School of Arts and Sciences in partial fulfillment

of the requirements for the degree of

Doctor of Philosophy

University of Pittsburgh

2020

UNIVERSITY OF PITTSBURGH

KENNETH P. DIETRICH SCHOOL OF ARTS & SCIENCES

This dissertation was presented

by

Zixin Yang

It was defended on

April 30th 2020

and approved by

Adam Leibovich, Professor, University of Pittsburgh

Joseph Boudreau, Professor, University of Pittsburgh

Arthur Kosowsky, Professor, University of Pittsburgh

Ira Rothstein, Professor, Carnegie Mellon University

Eric Swanson, Professor, University of Pittsburgh

Dissertation Director: Adam Leibovich, Professor, University of Pittsburgh

The Equations of Motion of the Post-Newtonian Compact Binary Inspirals As Gravitational Radiation Sources Under The Effective Field Theory Formalism

Zixin Yang, PhD

University of Pittsburgh, 2020

The success of advanced LIGO/VIRGO detections of gravitational wave signals beginning in 2015 has opened a new window on the universe. Since April 2019, LIGO's third observing run has identified binary merger candidates with a rate of roughly one per week. In order to understand the properties of all the candidates, it is necessary to construct large template banks of gravitational waveforms. Future upgrades of the LIGO detectors and the next generation detectors with better sensitivity post challenges to the current calculations of waveform solutions. The improvement of the systematic and statistical uncertainties calls for higher accuracy in waveform modeling. It is also crucial to include more physical effects and cover the full parameter space for the future runs.

This thesis focuses on the equations of motion of the post-Newtonian compact binary inspirals as gravitational wave sources. The second post-Newtonian order corrections to the radiation reaction is calculated using the Effective Field Theory formalism. The analytical solutions to the equations of motion and spin precession equations are obtained using the dynamical renormalization group method up to the leading order in spin-orbit effects and radiation reaction.

Table of Contents

List of Figures

Preface

This preface is dedicated to acknowledge the countless help I have received during my Ph.D. program. First and foremost, I would like to thank my advisor, Professor Adam Leibovich, who has been a tremendous mentor for me. I could not have accomplished this Ph.D. without his patience, motivation, immense knowledge, and most importantly, his continuous guidance and support. The joy and enthusiasm he has for his research is contagious and motivational, and will be a life-long inspiration for me. Forever shall I remain indebted to him.

I would like to express my deepest appreciation to my committee who have played crucial roles in my graduate study: Ira Rothstein, Arthur Kosowsky, Joseph Boudreau and Eric Swanson. They have passed on knowledge that would benefit me throughout the career.

1.0 Introduction

A worldwide network of gravitational wave (GW) detectors is being developed to observe the ripples in the fabric of space-time passing through the earth. This includes the ground-based laser interferometers GEO600, LIGO, and VIRGO collaborations currently in operation, and the under-construction space-based observatory LISA and cryogenic detector KAGRA in Japan. The successful detection of gravitational waves from inspiraling black holes (BH) and neutron stars (NS) by the LIGO and VIRGO collaborations directly and spectacularly confirmed one of the predictions of Einstein's Theory of General Relativity. As a generic prediction of metric theories of gravity, BH or NS coalescence is a strong source of GWs for interferometric detectors. To successfully identify and analyze the gravitational wave signals, it is necessary to construct a systematic description of the binary black hole dynamics and waveforms during coalescence. A set of expected waveforms characterized by the intrinsic parameters of the compact binary within the astrophysically interesting region of the parameter space forms a waveform template bank [1–3]. Using these precise waveform templates, a matched filtering technique is used to discover the weak GW signals buried in the detector noise. Templates with higher accuracy will help us extract physical information from the observed events to gain further knowledge of the black hole or neutron star properties. This thesis focuses on the analytical post-Newtonian dynamics of binary gravitational waves to higher orders of precision, using the effective field theory techniques.

1.1 Compact Binary Systems and the Post-Newtonian Expansions

Compact objects, in the context of astronomy, refer to massive stars with high density, including neutron stars and black holes. The compact stars are usually formed in the final stages of stellar evolution. A compact binary system consists of two compact objects, orbiting around a common center-of-mass under the gravitational interactions with each other. This thesis focuses only on black holes but neutron stars are similar. Due to general relativity, the

binary black hole system emits weak gravitational radiation. And the gravitational waves carrying energy away causes the loss of the total system energy. The radiated energy is compensated by the shrinking of the orbital radius and the increase of the orbital frequency. Eventually, the binary black holes spiral into one another, forming a single black hole. This entire process is called the binary coalescence.

The inspiral stage of the coalescence lasts a very long time compared to the orbital period. As the orbital radius gradually reaches its innermost stable circular orbit, the binary becomes relativistically dynamically unstable as the stars getting closer and closer. The two objects plunge into each other and form a single BH in the next stage called merger. The merger phase is a highly nonlinear dynamic process. GW signals are the strongest and reach the peak value at this time. Immediately followed is the ringdown phase, during which the largely deformed black hole radiates away most of the distortions and leaves a stable final Kerr black hole.

In this thesis, we study the inspiraling binary dynamics as solutions of the Einstein field equations. The nonlinear structure of general relativity limits the possibility of exact solutions. The post-Newtonian formalism is one of the approximation methods that attempt to extract information from GR under certain conditions. Binary systems are described by Newtonian gravity in flat space-time. For moderately relativistic systems, post-Newtonian corrections to the Newtonian equations of motion in powers of the source velocities v are taken into account. This type of approximation has been developed by Einstein [4], and later by Droste, de Sitter and Lorentz [5–7], and has produced fruitful classical results.

The post-Newtonian assumptions include that the sources are slowly moving and weakly self-gravitated. The non-relativistic expansion is in terms of v/c, the ratio of source velocity and the speed of light. For a self-gravitated binary system with total mass M we have $(v/c)^2 \sim R_S/r$, where $R_S = 2GM/c^2$ is the Schwarzschild radius of the source and r is the orbital radius. The post-Newtonian expansion uses sufficiently small v/c and R_S/r as the expansion parameter and denotes the post-Newtonian terms of order $(v/c)^n$ by $\frac{n}{2}$PN. Even though the formalism is built on a small velocity expansion, the sources can get very relativistic, especially in the last few orbits of the inspiral. Eventually the expansion breaks down and other methods must be explored. Therefore, it is necessary to obtain higher orders

post-Newtonian waveforms for more accurate descriptions of the binary dynamics.

1.2 Gravitational Waves from Compact Binaries

The existence of gravitational waves was predicted from general relativity by Einstein in 1916 [8]. Gravitational waves appears in the linearized gravity theory that expands the Einstein equations around the flat Minkowski metric $\eta_{\mu\nu}$. A small space-time perturbation $h_{\mu\nu}$, defined as $g_{\mu\nu} = \eta_{\mu\nu} + h_{\mu\nu}$, satisfies the wave equation

$$\Box \bar{h}_{\mu\nu} = -\frac{16\pi G}{c^4} T_{\mu\nu}, \tag{1.1}$$

where $\bar{h}_{\mu\nu} = h_{\mu\nu} - \frac{1}{2}\eta_{\mu\nu}\eta^{\alpha\beta}h_{\alpha\beta}$ and $T_{\mu\nu}$ is the stress-energy tensor of the source. The physical picture can be portrayed as the source binary moving in flat space-time along the trajectories determined by the mutual influence of the source masses and the Newtonian background.

Gravitational waves carry energy flux and momenta away from the sources. Once generated, they propagate almost unimpeded except for the redshift effects. The scattering and absorption of gravitational waves are negligible due to the small cross-sections from the extremely weak couplings. Therefore, the observed gravitational waves contain fundamental information about the original binary systems. A proper and precise waveform model is crucial to the understanding of black holes and the nature of gravity itself.

The dynamics of the binary BHs are usually divided into three zones according to typical length scale: The internal zone with length scale R_s, the potential zone with orbital radius r, and the radiation zone with GW typical wavelength $\lambda \sim r/v$. For non-relativistic sources the hierarchy of the energy scales is $\lambda^{-1} \ll r^{-1} \ll r_s^{-1}$ in natural units.

In the post-Newtonian formalism, the binary motion is conserved until 2PN. Gravitational waves enter into play at the order of 2.5PN through the radiation reaction force. At the level of the binary equations of motion, the post-Newtonian expansion can be written as

$$\mathbf{a}^i = \mathbf{a}^i_{\text{Newtonian}} + \mathbf{a}^i_{\text{1PN}} + \mathbf{a}^i_{\text{2PN}} + \mathbf{a}^i_{\text{RR}} + ..., \tag{1.2}$$

where $\mathbf{a}^i_{\rm RR}$ is the leading order radiation reaction at 2.5PN. Gravitational radiation reaction is an analog of the Abraham-Lorentz-Dirac force or the radiation damping force in electromagnetism, which is a recoil force on an accelerating charged particle due to the emission of electromagnetic radiation.

In gravity, radiation reaction was first studied by Burke and Thorne in 1970 [9, 10]. They used an asymptotic matched expansion between the potential zone and the radiation zone. The leading terms in the radiation reaction arise from mass quadrupole moments and subleading contributions from all mass and current multipoles of the source. The 1PN correction of radiation reaction, which is the 3.5PN correction to the equations of motion, has been calculated in [11]. In Chapter 3, this thesis discusses the 2PN calculation of the radiation reaction force in the formalism of effective field theory.

1.3 Spinning Extended Objects in Gravity

A rotating black hole, or Kerr black hole, is a black hole that carries intrinsic angular momentum S, referred to as the spin of the black hole. The experimental observations and analyses show that stellar-mass black holes can be generically close to being maximally spinning [12, 13]. We will adopt the notation for spin variables such that

$$S_a = G m_a^2 \chi_a, \tag{1.3}$$

where m_a is the mass of the object $a = 1, 2$ and χ_a is the dimensionless spin parameter, maximally rotating black holes have $\chi \sim 1$.

The inclusion of black hole spins induces nontrivial effects to the binary dynamics. The equations of motion become more complicated as a consequence of the extra six degrees of freedom from the three-dimensional spin vectors for each compact body. The magnitude of the black hole spins are usually much smaller compared to the binary orbital angular momentum $L = \nu M |\mathbf{r} \times \mathbf{v}|$, where $\nu = m_1 m_2 / M^2$. Therefore, the spin is treated perturbatively with a distinction among the linear spin-orbit (SO) effects, the quadratic spin-spin (SS) effects, and the possible higher orders terms in spin.

The leading contributions from spin-orbit effects enter the equations of motion at 1.5PN and spin-spin effects enter at 2PN, which are before the 2.5PN radiation reaction force [14]. The post-Newtonian equations of motion expansion (1.2) then becomes

$$\mathbf{a}^i = \mathbf{a}^i_{\rm Newtonian} + \mathbf{a}^i_{\rm 1PN} + \mathbf{a}^i_{\rm SO} + \mathbf{a}^i_{\rm 2PN} + \mathbf{a}^i_{\rm SS} + \mathbf{a}^i_{\rm RR} + ..., \tag{1.4}$$

When the spin vectors are not aligned with the orbital momentum, the spin effects lead to the precession of the orbital plane. In this circumstance, the orientation of the orbital plane varies with time. Thus the observed waveform, which depends on the orbital orientation with respect to the detector, will modulate due to the spin-induced orbital precession.

The spin vectors themselves evolve following the spin precession equations

$$\frac{{\rm d}\mathbf{S}_a}{{\rm d}t} = \mathbf{\Omega}_a \times \mathbf{S}_a, \tag{1.5}$$

where $\mathbf{\Omega}_a$ is the precession vector of the conserved-norm spin variable S_a. The total angular momentum $\mathbf{J} = \mathbf{L} + \mathbf{S}_1 + \mathbf{S}_2$ is conserved unless the dissipative effects are taken into account. In Chapter 4, this thesis gives a detailed analytical solutions to the binary equations of motion including the leading order SO effect and radiation reaction, and the solutions to the spin precession equations, utilizing a new method [15] called dynamical renormalization group method.

The thesis is arranged as follows. After this introduction, in Chapter 2, we outline the effective field theory for radiative gravity. With a brief summary of the multipole expansion and the non-conservative variation principle of action, we give an example calculation of the radiation reaction force in the EFT formalism. In Chapter 3, we use the EFT framework to compute the mass quadrupole moment, the equation of motion, and the power loss of inspiralling compact binaries at second order in the PN approximation. We present expressions for the stress-energy pseudo-tensor components of the binary system to the PN orders needed for this calculation. In Chapter 4, we calculate the real-space trajectory and spin precession of a generic spinning compact binary inspiral at any time instant using the dynamical renormalization group formalism. This method leads to closed-form analytic solutions to the binary motion through treating radiation reaction as perturbations and resumming the secular growth of perturbative terms. We consider the spin-orbit effects

at leading order and the 2.5PN radiation reaction without orbit averaging or precession averaging for arbitrary individual masses and spin magnitudes and orientations.

As of this writing, the relevant publications can be found in Refs. [16, 17]

2.0 Non-Relativistic General Relativity and The Effective Field Theory Formalism

For theories that have natural separations among several energy/distance scales, Effective Field Theory (EFT) methods offer tools to decouple the physics at these different scales. In general, there are two distinct approaches to build an EFT. The first one is a "top-down" procedure, where the high energy theory is fully understood, and the effects of heavy physics on low energy observables are of interest. In this case, integrating out the heavier physics and matching onto a low energy theory provides a systematic manner to simplify the calculations. The applications include, for instance, Heave Quark Effective Theory and Non-relativistic QCD. However, when the full theory is unknown, or the matching is too complicated, a "bottom-up" approach is sometimes taken. In this approach, an effective action or Lagrangian is constructed by writing down possible operators consistent with the fundamental properties of the theory, such as symmetries, equations of motion, and degrees of freedom. An example of bottom-up effective theory is chiral perturbation theory.

The EFT approach to the binary inspiral problem, proposed by Goldberger and Rothstein [18], is a top-down EFT approach that is a Lagrangian formalism of non-relativistic general relativity within the PN expansion. The EFT framework provides manifest power counting in the velocity v, the PN expansion parameter. Calculated using the field theory language of Feynman rules and Feynman diagrams, the EFT approach considerably simplifies the calculations and presents a physical understanding in the picture of the interactions of potential gravitons and radiation gravitons. Currently, the binary dynamics has been calculated up to 4PN for non-spinning systems and extended to spin effects by the EFT approach. This chapter presents an outline for the EFT approach to the post-Newtonian gravitational dynamics.

2.1 Effective Field Theory of Compact Binary Inspirals

As mentioned in the introduction, the three characteristic scales of binary inspiral are the internal structure scale R_s, the orbital radius r, and the radiation wavelength r/v. The gravitational wave observables to be detected appear from the radiation zone at the scale of r/v. To integrate out the two intermediate scales using EFT methods, the theory adopts the point particle interacting with the gravitational fields. The resulting EFT of gravity contains a potential mode mediating the forces that form the bound system, and a radiation mode propagating out from the source.

The EFT formulation starts with an action of the relativistic point particles coupled with gravity

$$S_{\mathit{eff}}[x^\mu, g_{\mu\nu}] = S_{EH}[g] + S_{pp}[x, g], \tag{2.1}$$

where S_{EH} is the Einstein-Hilbert action

$$S_{EH} = -2m_{Pl}^2 \int \mathrm{d}^4x\sqrt{g}R(x), \tag{2.2}$$

and $m_{pl}^{-2} = 32\pi G_N$ and $R(x)$ is the Ricci scalar. S_{pp} is given by

$$S_{pp} = -\sum_a m_a \int \mathrm{d}\tau_a + ..., \tag{2.3}$$

where m_a is the mass of the point particle a. The point particles living on the worldline are parametrized by the proper time $\mathrm{d}\tau_a^2 = g_{\mu\nu}x_a^\mu x_a^\nu$. The ellipsis includes any possible curvature dependent terms, and the corrections to the action involving spin degrees of freedom that are introduced in Section 1.3.

Recall that, in linearized gravity, the gravitational field is defined to be a small perturbation from flat space-time through $g_{\mu\nu} = \eta_{\mu\nu} + h_{\mu\nu}/m_{Pl}$. The momenta carried by the gravitons $h_{\mu\nu}$ can be split up into two regions. The first region, scaling as $k^\mu \to (k^0 \sim v/r, \mathbf{k} \sim 1/r)$, is the potential gravitons mediating the nearly instantaneous exchanges between the point particles. These gravitons can never be on-shell since their $k^2 \sim 1/r$. The other region of momenta that scales as $k^\mu \to (k^0 \sim v/r, \mathbf{k} \sim v/r)$ corresponds to the radiation gravitons that can appear on-shell and propagate to the observers.

The potential gravitons are never on-shell and cannot propagate, and therefore do not appear in the physics at long distance that can be detected from the earth. To integrate out the potential modes, it is useful to decompose the gravitational field as

$$h_{\mu\nu}(x) = \bar{h}_{\mu\nu}(x) + H_{\mu\nu}(x), \tag{2.4}$$

where $\bar{h}_{\mu\nu}$ is the radiation graviton field and $H_{\mu\nu}$ is the potential graviton field. The scalings of the graviton fields are then

$$\left(\partial_\alpha \bar{h}_{\mu\nu} \sim \frac{v}{r}\bar{h}_{\mu\nu}\right), \qquad \text{and} \qquad \left(\partial_0 H_{\mu\nu} \sim \frac{v}{r}H_{\mu\nu}, \quad \partial_i H_{\mu\nu} \sim \frac{1}{r}H_{\mu\nu}\right). \tag{2.5}$$

To unify the power counting of the derivatives acting on the fields such that $\partial_\mu \sim v/r$, it is convenient to rewrite $H_{\mu\nu}$ in the momentum space as

$$H_{\mu\nu}(x^0, \mathbf{x}) = \int \frac{\mathrm{d}^3\mathbf{k}}{(2\pi)^3} e^{i\mathbf{k}\cdot\mathbf{x}} H_{\mathbf{k}\mu\nu}(x^0), \tag{2.6}$$

where $H_{\mathbf{k}\mu\nu}(x^0)$ is the spatial Fourier transformed field of $H_{\mu\nu}(x^0, \mathbf{x})$. In this definition the hard momenta $\mathbf{k} \sim 1/r$ are detached from radiation length scale $x^\mu \sim v/r$.

The action S_{eff} is matched onto the long-distance NR EFT containing $\bar{h}_{\mu\nu}$ and the worldline x_a^μ by integrating out the potential gravitons through the path integral

$$e^{iS_{\mathrm{NR}}[x_a,\bar{h}]} = \int \mathcal{D}H e^{iS_{EH}[\bar{h}+H]} e^{iS_{pp}[x,\bar{h}+H]} e^{iS_{\mathrm{GF}}}, \tag{2.7}$$

where S_{GF} is a gauge fixing term. It is chosen by adopting the background field method to preserve the gauge invariance of the action $S_{\mathrm{NR}}[x_a, \bar{h}]$, which gives

$$S_{\mathrm{GF}} = m_{Pl}^2 \int \mathrm{d}^4x \sqrt{\bar{g}} \Gamma^\mu \Gamma_\mu, \tag{2.8}$$

where $\bar{g}$ is the determinant of the background metric $\bar{g}_{\mu\nu} = \eta_{\mu\nu} + \bar{h}_{\mu\nu}/M_{Pl}$, and $\Gamma_\mu = D_\alpha H_\mu^\alpha - \frac{1}{2} D_\mu H_\alpha^\alpha$ with the covariant derivative D_μ with respect to $\bar{g}_{\mu\nu}$.

The Feynman rules and the propagators for the gravitons can be read off from the effective action. Expanding the point particle action in (2.3) in powers of the particle three-velocities $\mathbf{v}$, the worldline Lagrangian can be written as

$$L_{pp} = \sum_a \frac{m_a}{m_{Pl}} \Bigg[-\frac{1}{2}H^{00} - \frac{1}{2}\bar{h}^{00} - \frac{1}{2}H_{0i}\mathbf{v}_{ai} - \frac{1}{2}\bar{h}_{0i}\mathbf{v}_{ai} - \frac{1}{4}H^{00}\mathbf{v}_a^2$$

$$- \frac{1}{4}\bar{h}^{00}\mathbf{v}_a^2 - \frac{1}{2}H_{ij}\mathbf{v}_{ai}\mathbf{v}_{aj} - \frac{1}{2}\bar{h}_{ij}\mathbf{v}_{ai}\mathbf{v}_{aj} + ...\Big], \tag{2.9}$$

where the gravitons $H^{\mu\nu}(x^0, \mathbf{x}_a(x^0))$ and $\bar{h}^{\mu\nu}(x^0, \mathbf{x}_a(x^0))$ are evaluated on the point particle worldline.

The relevant $\mathcal{O}(H^2)$ terms to determine the potential propagator in the action are

$$S_{H^2} = \frac{1}{2}\int \mathrm{d}x^0 \frac{\mathrm{d}^3\mathbf{x}}{(2\pi)^3}\Big[\mathbf{k}^2 H_{\mathbf{k}\mu\nu}H^{\mu\nu}_{-\mathbf{k}} - \frac{\mathbf{k}^2}{2}H_{\mathbf{k}}H_{-\mathbf{k}} - \partial_0 H_{\mathbf{k}\mu\nu}\partial_0 H^{\mu\nu}_{-\mathbf{k}} + \frac{1}{2}\partial_0 H_{\mathbf{k}}\partial_0 H_{-\mathbf{k}}\Big], \tag{2.10}$$

where $H_{\mathbf{k}} = H^{\alpha}_{\alpha\mathbf{k}}$. The last two terms associated with the partial derivative of x_0 are power suppressed by a factor of v^2 with respect to the first two terms that are proportional to $\mathbf{k}^2$. The propagator of $H_{\mathbf{k}\mu\nu}$ derived from the $\mathbf{k}^2$ terms can be written as

$$\langle H_{\mathbf{k}\mu\nu}(x^0)H_{\mathbf{q}\alpha\beta}(y^0) = -\frac{i}{\mathbf{k^2}}(2\pi)^3\delta^3(\mathbf{k}+\mathbf{q})\delta(x^0-y^0)P_{\mu\nu;\alpha\beta}, \tag{2.11}$$

where the tensor structure $P_{\mu\nu;\alpha\beta} = \frac{1}{2}\Big(\eta_{\mu\alpha}\eta_{\nu\beta} + \eta_{\nu\alpha}\eta_{\mu\beta} - \frac{2}{d-2}\eta_{\mu\nu}\eta_{\alpha\beta}\Big)$ with the space-time dimension d.

Besides the interactions involving point particle sources, the Feynman rules for the n-graviton vertices can be derived from the Einstein-Hilbert action (2.2) and the gauge fixing term (2.8). For instance, the three-graviton vertices involving three potential gravitons receive contribution only from S_{EH} since S_{GF} contains only $\mathcal{O}(H^2)$ terms. Expanding $\sqrt{g}g^{\mu\nu}$ and $R_{\mu\nu}$ from the Einstein-Hilbert action to the H^3,

$$\begin{aligned}\sqrt{g}g^{\mu\nu}R_{\mu\nu} \to\ & \eta^{\mu\nu}R^{(3)}_{\mu\nu} \\ & + \Big(-H^{\mu\nu} + \frac{1}{2}\eta^{\mu\nu}H\Big)R^{(2)}_{\mu\nu} \\ & + \Big(H^{\mu\alpha}H^{\nu}_{\alpha} - \frac{1}{2}H^{\mu\nu}H + \frac{1}{8}\eta^{\mu\nu}H^2 - \frac{1}{4}\eta^{\mu\nu}H_{\alpha\beta}H^{\alpha\beta}\Big)R^{(1)}_{\mu\nu} + \mathcal{O}(H^4),\end{aligned} \tag{2.12}$$

where the expansions of the Ricci tensor are

$$R^{(1)}_{\mu\nu} = -\frac{1}{2}\partial_\alpha\partial^\alpha H_{\mu\nu} + \frac{1}{2}\partial_\alpha\partial_\mu H^{\alpha}_{\nu} + \frac{1}{2}\partial_\alpha\partial_\nu H^{\alpha}_{\mu} - \frac{1}{2}\partial_\nu\partial_\mu H, \tag{2.13}$$

$$\begin{aligned}R^{(2)}_{\mu\nu} =& -\frac{1}{4}\partial_\alpha H\partial^\alpha H_{\mu\nu} + \frac{1}{2}\partial_\beta H^{\beta}_{\alpha}\partial^\alpha H_{\mu\nu} + \frac{1}{2}H^{\alpha\beta}\partial_\beta\partial_\alpha H_{\mu\nu} - \frac{1}{2}H^{\alpha\beta}\partial_\beta\partial_\mu H_{\nu\alpha} - \frac{1}{2}H^{\alpha\beta}\partial_\beta\partial_\nu H_{\mu\alpha} \\ & - \frac{1}{2}\partial_\alpha H_{\nu\beta}\partial^\beta H^{\alpha}_{\mu} + \frac{1}{2}\partial_\beta H_{\nu\alpha}\partial^\beta H^{\alpha}_{\mu} + \frac{1}{4}\partial_\alpha H\partial_\mu H^{\alpha}_{\nu} - \frac{1}{2}\partial_\beta H^{\beta}_{\alpha}\partial_\mu H^{\alpha}_{\nu} + \frac{1}{2}H^{\alpha\beta}\partial_\mu\partial_\nu H_{\alpha\beta} \\ & + \frac{1}{4}\partial_\mu H^{\alpha\beta}\partial_\nu H_{\alpha\beta} + \frac{1}{4}\partial_\alpha H\partial_\nu H^{\alpha}_{\mu} - \frac{1}{2}\partial_\beta H^{\beta}_{\alpha}\partial_\nu H^{\alpha}_{\mu},\end{aligned} \tag{2.14}$$

$$
\begin{aligned}
R^{(3)}_{\mu\nu} = &+\frac{1}{4}H^{\alpha\gamma}\partial_\gamma H\partial^\alpha H_{\mu\nu} - \frac{1}{4}H^{\alpha\gamma}\partial_\gamma H\partial_\mu H_{\nu\alpha} - \frac{1}{4}H^{\alpha\gamma}\partial_\gamma H\partial_\nu H_{\mu\alpha} - \frac{1}{2}H^{\alpha\gamma}\partial^\alpha H^\beta_\mu\partial_\gamma H_{\nu\beta} \\
&- \frac{1}{2}H^{\alpha\gamma}\partial_\beta H^\beta_\gamma\partial^\alpha H_{\mu\nu} + \frac{1}{2}H^{\alpha\gamma}\partial^\alpha H^\beta_\mu\partial_\beta H_{\nu\gamma} - \frac{1}{2}H^{\alpha\gamma}H^\beta_\alpha\partial_\beta\partial_\gamma H_{\mu\nu} + \frac{1}{2}H^{\alpha\gamma}H^\beta_\alpha\partial_\beta\partial_\mu H_{\nu\gamma} \\
&+ \frac{1}{2}H^{\alpha\gamma}H^\beta_\alpha\partial_\beta\partial_\nu H_{\mu\gamma} + \frac{1}{2}H^{\alpha\gamma}\partial^\beta H_{\mu\alpha}\partial_\gamma H_{\nu\beta} - \frac{1}{2}H^{\alpha\gamma}\partial^\beta H_{\mu\alpha}\partial_\beta H_{\nu\gamma} - \frac{1}{2}H^{\alpha\gamma}\partial_\gamma H_{\alpha\beta}\partial^\beta H_{\mu\nu} \\
&+ \frac{1}{4}H^{\alpha\gamma}\partial_\beta H_{\alpha\gamma}\partial^\beta H_{\mu\nu} + \frac{1}{2}H^{\alpha\gamma}\partial_\beta H^\beta_\gamma\partial_\mu H_{\nu\alpha} + \frac{1}{2}H^{\alpha\gamma}\partial_\gamma H_{\alpha\beta}\partial_\mu H^\beta_\nu - \frac{1}{4}H^{\alpha\gamma}\partial_\beta H_{\alpha\gamma}\partial_\mu H^\beta_\nu \\
&- \frac{1}{2}H^{\alpha\gamma}H^\beta_\alpha\partial_\mu\partial_\nu H_{\gamma\beta} - \frac{1}{2}H^{\alpha\gamma}\partial_\mu H^\beta_\alpha\partial_\nu H_{\gamma\beta} + \frac{1}{2}H^{\alpha\gamma}\partial_\beta H^\beta_\gamma\partial_\nu H_{\mu\alpha} + \frac{1}{2}H^{\alpha\gamma}\partial_\gamma H_{\alpha\beta}\partial_\nu H^\beta_\mu \\
&- \frac{1}{4}H^{\alpha\gamma}\partial_\beta H_{\alpha\gamma}\partial_\nu H^\beta_\mu. \qquad (2.15)
\end{aligned}
$$

In this form the Feynman rules can be extracted by substituting the derivatives on $H_{\mu\nu}$ by the corresponding momenta from $H_{\mathbf{k}\mu\nu}$. The three-graviton vertex appears in the calculation of the first-order post-Newtonian gravitational potential. Figure 2.1 shows all the diagrams that contribute to the 1PN two-body potential. The sum of these diagram gives the 1PN Lagrangian first derived by Einstein, Infeld and Hoffmann using a different method [19],

$$
L_{\rm EIH} = \frac{1}{8}\sum_a m_a\mathbf{v}_a^4 + \frac{G_N m_1 m_2}{2|\mathbf{x}_1-\mathbf{x}_2|}\left[3(\mathbf{v}_1^2+\mathbf{v}_2^2) - 7(\mathbf{v}_1\cdot\mathbf{v}_2) - (\mathbf{v}_1\cdot\mathbf{n})(\mathbf{v}_2\cdot\mathbf{n})\right] - \frac{G_N^2 M m_1 m_2}{2|\mathbf{x}_1-\mathbf{x}_2|^2}, \qquad (2.16)
$$

where $\mathbf{n}$ is the normal vector of the orbital radius vector $\mathbf{n} = (\mathbf{x}_1-\mathbf{x}_2)/|\mathbf{x}_1-\mathbf{x}_2|$ and M is the total mass $M = m_1+m_2$.

2.2 Gravitational Radiation and The Multipole Expansion

The diagrams in Fig. 2.1 that generate the gravitational interaction between the point binaries contain no external radiation graviton $\bar{h}_{\mu\nu}$. The Feynman diagrams with external legs of $\bar{h}_{\mu\nu}$ coupled to the particle worldline or potential gravitons can be constructed from the action (2.7).

The Feynman rules of the vertices involving radiation gravitons are generated similarly through expanding $S_{EH}[\bar{h}+H]+S_{GF}[\bar{h}+H]$. For instance, the three-graviton vertex involving radiation mode in Fig. 2.2, can be derived in the same manner as the three-potential-graviton vertex in Sec. 2.1.

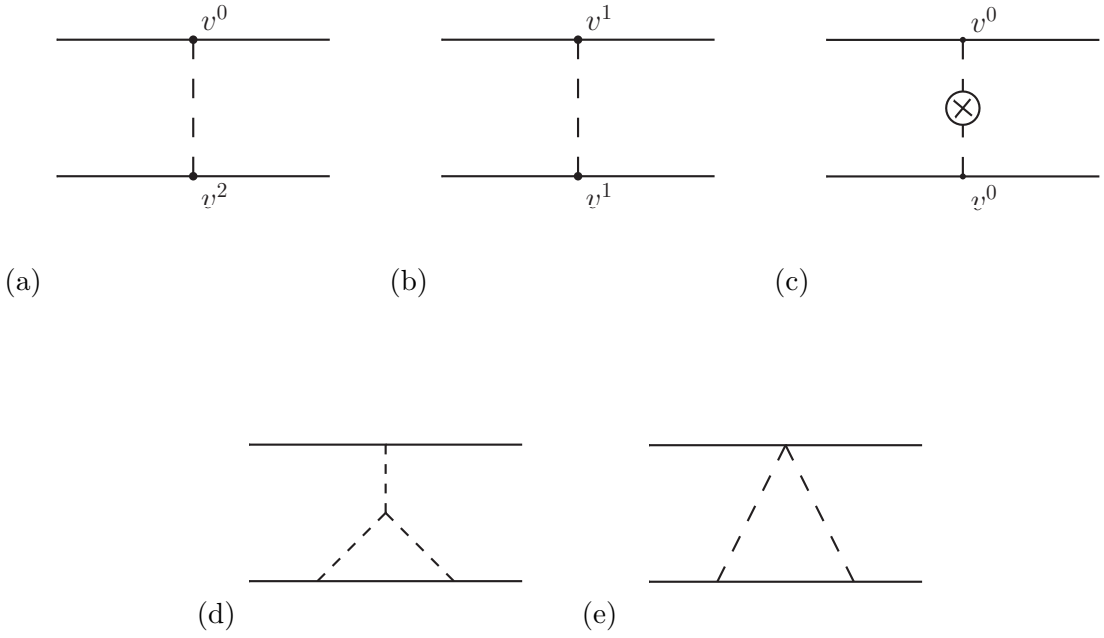

Figure 2.1: Diagrams contributing to the 1PN two-body potential, omitting their mirror diagrams. The solid lines represent the point particle worldline. The dashed lines denote the potential gravitons. The v^1 and v^2 corrections to the worldline coupling in (a) and (b) refer to the higher order terms in the worldline Lagrangian (2.9). The $\otimes$ on the propagator in (c) stands for the potential graviton kinetic term insertion from the two terms involving ∂_0 in (2.10). The three-graviton vertex appears in (d). The power counting of (a)-(c) are of $\mathcal{O}(G_N v^2)$ and (d)-(e) are of $\mathcal{O}(G_N^2)$.

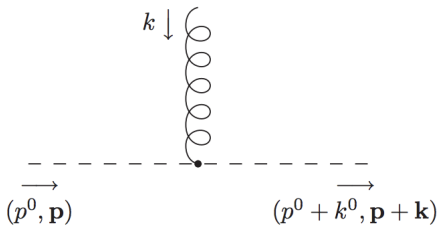

Figure 2.2: The three-graviton vertex involving two potential gravitons and a radiation graviton in the curly line.

However, the potential field in (2.2) poses problems to the manifest power counting in the radiation graviton EFT. The graviton with momentum $\mathbf{p}+\mathbf{k}$ has a propagator proportional to $1/(\mathbf{p}+\mathbf{k})^2$ that can be expanded in powers of v as

$$\frac{1}{(\mathbf{p}+\mathbf{k})^2} = \frac{1}{\mathbf{p}^2}\Big(1 - \frac{2\mathbf{p}\cdot\mathbf{k}}{\mathbf{p}^2} + ...\Big), \tag{2.17}$$

where $\mathbf{p} \sim 1/r$ and $\mathbf{k} \sim v/r$. Then the potential graviton propagator becomes an infinite series in powers of v that shows no manifest power counting. It is necessary to multipole-expand the interactions between the radiation field and potentials or point particle at the level of action,

$$\bar{h}_{\mu\nu}(x^0, \mathbf{x}) = \bar{h}_{\mu\nu}(x^0, \mathbf{X}) + \delta\mathbf{x}_i \partial_i \bar{h}_{\mu\nu}(x^0, \mathbf{x}) + \frac{1}{2}\delta\mathbf{x}_i \delta\mathbf{x}_j \partial_i\partial_j \bar{h}_{\mu\nu}(x^0, \mathbf{x}) + ..., \tag{2.18}$$

where $\mathbf{X}$ is an arbitrary reference point and $\delta\mathbf{x} = \mathbf{x} - \mathbf{X}$. For simplicity $\mathbf{X}$ is usually defined to be the center-of-mass of the binary system at the origin,

$$\mathbf{x}^i_{cm} = \frac{\int \mathrm{d}^3\mathbf{x}\; T^{00}(x^0, \mathbf{x})\; \mathbf{x}^i}{\int \mathrm{d}^3\mathbf{x}\; T^{00}(x^0, \mathbf{x})} = 0, \tag{2.19}$$

where T^{00} is the 00-component of $T^{\mu\nu}$, the stress-energy pseudo-tensor that contains all the potential contributions from the Einstein-Hilbert action and worldline couplings. The source term of the single graviton emission in the effective action is written as [20]

$$\Gamma[\bar{h}] = -\frac{1}{2m_{Pl}} \int \mathrm{d}^4x\; T^{\mu\nu}(x)\bar{h}_{\mu\nu}(x). \tag{2.20}$$

The off-shell gravitational wave amplitude is written in terms of $T^{\mu\nu}(x)$,

$$\mathcal{A}^{\mu\nu} = -\frac{1}{2m_{Pl}} \int \mathrm{d}^4x \; T^{\mu\nu}(x) e^{-ikx}, \tag{2.21}$$

and thus the Ward identity leads to the conservation law $\partial_\mu T^{\mu\nu} = 0$.

The radiation field $\bar{h}_{\mu\nu}$ in the source action in (2.20) can be substituted by the Taylor expansion in (2.18). Then the Taylor expanded action is expressed in terms of manifestly gauge invariant operators in order to obtain the multipole expansion of the action. In the case of general relativity, the gauge invariant quantities are the Riemann tensor, the Ricci tensor, the Ricci scalar, and the covariant derivatives. The multipole expansion form of the EFT action can be written as

$$S_{\mathrm{NR}}[x_a, \bar{h}] = \int \mathrm{d}t \left[-M(t) + \sum_{\ell=2} \left(\frac{1}{\ell!} I^L(t) \nabla_{L-2} E_{i_{\ell-1} i_\ell} - \frac{2\ell}{(\ell+1)!} J^L(t) \nabla_{L-2} B_{i_{\ell-1} i_\ell} \right) \right], \tag{2.22}$$

where $L = (i_1 i_2 ... i_\ell), L-2 = (i_1 ... i_{\ell-2})$, and $I^L(t)$, $J^L(t)$ are the mass type and current type multipole moments. The multipole moments are coupled to E_{ij} and B_{ij}, which are given by

$$E_{ij} = C_{i0j0} = \frac{1}{2m_{Pl}} \Big(\partial_0 \partial_j \bar{h}_{0i} + \partial_0 \partial_i \bar{h}_{0j} - \partial_i \partial_j \bar{h}_{00} - \partial_0^2 \bar{h}_{ij} \Big) + \mathcal{O}(\bar{h}^2) \tag{2.23a}$$

$$B_{ij} = \frac{1}{2} \epsilon_{imn} C_{0jmn} = \frac{1}{2m_{Pl}} \epsilon_{imn} \Big(\partial_0 \partial_n \bar{h}_{jm} + \partial_j \partial_m \bar{h}_{0n} \Big) + \mathcal{O}(\bar{h}^2). \tag{2.23b}$$

These are the electric and magnetic components of the Weyl tensor $C_{\mu\nu\alpha\beta}$, the traceless part of the Riemann tensor.

Matching the multipole expansion of the action (2.22) and the Taylor expanded (2.20) determines the expressions of the multipole moments as the Wilson coefficients of the EFT [21],

$$\begin{aligned}
I^L = & \sum_{p=0}^{\infty} \frac{(2\ell+1)!!}{(2p)!!(2\ell+2p+1)!!} \left(1 + \frac{8p(\ell+p+1)}{(\ell+1)(\ell+2)} \right) \left[\int \mathrm{d}^3\mathbf{x} \, \partial_t^{2p} T^{00}(x^0, \mathbf{x}) \mathbf{x}^{2p} \mathbf{x}^L \right]^{\mathrm{STF}} \\
& + \sum_{p=0}^{\infty} \frac{(2\ell+1)!!}{(2p)!!(2\ell+2p+1)!!} \left(1 + \frac{4p}{(\ell+1)(\ell+2)} \right) \left[\int \mathrm{d}^3\mathbf{x} \, \partial_t^{2p} T^{aa}(x^0, \mathbf{x}) \mathbf{x}^{2p} \mathbf{x}^L \right]^{\mathrm{STF}} \\
& - \sum_{p=0}^{\infty} \frac{(2\ell+1)!!}{(2p)!!(2\ell+2p+1)!!} \frac{4}{\ell+1} \left(1 + \frac{2p}{\ell+2} \right) \left[\int \mathrm{d}^3\mathbf{x} \, \partial_t^{2p+1} T^{0a}(x^0, \mathbf{x}) \mathbf{x}^{2p} \mathbf{x}^{aL} \right]^{\mathrm{STF}}
\end{aligned}$$

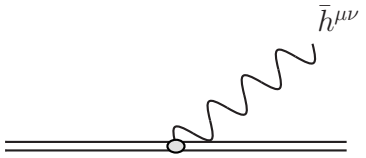

Figure 2.3: The diagram of the linear source action after integrating out the potential gravitons. The double line indicates that the EFT scales beyond the orbital scale r.

$$+\sum_{p=0}^{\infty}\frac{(2\ell+1)!!}{(2p)!!(2\ell+2p+1)!!}\frac{2}{(\ell+1)(\ell+2)}\left[\int \mathrm{d}^3\mathbf{x}\,\partial_t^{2p+2}T^{ab}(x^0,\mathbf{x})\mathbf{x}^{2p}\mathbf{x}^{abL}\right]^{\mathrm{STF}} \tag{2.24a}$$

$$J^L=\sum_{p=0}^{\infty}\frac{(2\ell+1)!!}{(2p)!!(2\ell+2p+1)!!}\left(1+\frac{2p}{\ell+2}\right)\left[\int \mathrm{d}^3\mathbf{x}\,\epsilon^{k_\ell ba}\partial_t^{2p}T^{0a}(x^0,\mathbf{x})\mathbf{x}^{2p}\mathbf{x}^{bL-1}\right]^{\mathrm{STF}}$$
$$-\sum_{p=0}^{\infty}\frac{(2\ell+1)!!}{(2p)!!(2\ell+2p+1)!!}\frac{1}{\ell+2}\left[\int \mathrm{d}^3\mathbf{x}\,\epsilon^{k_\ell ba}\partial_t^{2p+1}T^{ac}(x^0,\mathbf{x})\mathbf{x}^{2p}\mathbf{x}^{bcL-1}\right]^{\mathrm{STF}}, \tag{2.24b}$$

where STF stands for symmetric trace-free part of the enclosing tensor structure. The radiated power loss is given by

$$P=\sum_{\ell=2}^{\infty}\frac{G(\ell+1)(\ell+2)}{\ell(\ell-1)\ell!(2\ell+1)!!}\left\langle\left(\frac{\mathrm{d}^{\ell+1}I^L}{\mathrm{d}t^{\ell+1}}\right)^2\right\rangle+\sum_{\ell=0}^{\infty}\frac{4G\ell(\ell+2)}{(\ell-1)(\ell+1)!(2\ell+1)!!}\left\langle\left(\frac{\mathrm{d}^{\ell+1}J^L}{\mathrm{d}t^{\ell+1}}\right)^2\right\rangle. \tag{2.25}$$

The spatial Fourier transform of $T^{\mu\nu}(x^0,\mathbf{x})$ gives

$$T^{\mu\nu}(x^0,\mathbf{k})=\sum_{n=0}^{\infty}\frac{(-i)^n}{n!}\left(\int \mathrm{d}^3\mathbf{x}\;T^{\mu\nu}(x^0,\mathbf{x})\mathbf{x}^{i_1}...\mathbf{x}^{i_n}\right)\mathbf{k}^{i_1}...\mathbf{k}^{i_n}, \tag{2.26}$$

by Taylor expanding $\int \mathrm{d}^3\mathbf{x}\;T^{\mu\nu}(x^0,\mathbf{x})e^{i\mathbf{k}\cdot\mathbf{x}}$ about small $\mathbf{k}\cdot\mathbf{x}\sim v$. Each term in the expansion is associated to a sum of Feynman diagrams up to the corresponding order in $\mathbf{k}\cdot\mathbf{x}$, with the amplitude given by

$$i\mathcal{A}_h(x^0,\mathbf{k})=-\frac{i}{2m_{Pl}}\epsilon^*_{\mu\nu}(\mathbf{k},h)T^{\mu\nu}(x^0,\mathbf{k}). \tag{2.27}$$

The multipole moments are obtained by substituting the stress energy tensor components $T^{\mu\nu}$ read off from the amplitude $\mathcal{A}_h$. The radiation EFT action (2.22) leads to the type of diagrams in Fig. 2.3. At this stage, the effective action for the binary system is replaced by a series of multipole moments on the worldline interacting with the radiation fields.

2.3 Classical Mechanics For Non-conservative Systems

Hamilton's principle of stationary action and the Euler-Lagrange equations derived from the action integral give the differential equations of motion to various physics systems in classical mechanics. The formulation of Hamilton's principle requires boundary conditions in time to determine the dynamical evolution of the system. For generic non-conservative problems, including gravitational radiations, the final configurations rely on the dynamics of the system and thus, Hamilton's principle is not applicable.

In the conservative sector of the worldline effective action, the sum of the advanced and retarded Green's function is symmetric in time as they satisfy boundary conditions according to Sturm-Liouville theory. It is necessary to develop a suitable action principle to accommodate the dissipative effects, including gravitational radiations in the effective action, which are time-asymmetric processes.

The principle of stationary non-conservative action [22, 23] is a variational principle that allows for non-conservative time-irreversible processes to be included at the level of the action. This path-integral formalism only depends on initial conditions, while the final states are dynamically determined by the evolution of the system. It is similar to the "in-in", or the closed time path functional formalism in the nonequilibrium quantum theory, which relies on the evolution of expectation values of field operators $\langle in|\hat{\mathcal{O}}|in\rangle$ and their correlation functions.

For a general dynamical system with a set of N generalized coordinates $\mathbf{q}(\mathbf{t}) = \{q^I(t)\}_{I=1}^N$ and velocities $\dot{\mathbf{q}}(t) = \{\dot{q}^I(t)\}_{I=1}^N$, the action of the system is the time integral of the Lagrangian along a trajectory $\mathbf{q}(t)$ from the initial time t_i to the final time t_f,

$$S[\mathbf{q}] = \int_{t_i}^{t_f} \mathrm{d}t L(\mathbf{q}, \dot{\mathbf{q}}, t) \tag{2.28}$$

To break the time reversal symmetry, a double copy of the coordinate set is introduced in order to describe dissipation in this formalism and the degrees of freedom are doubled as

$$q^I(t) \to \big(q_1^I(t), q_2^I(t)\big), \tag{2.29}$$

and similar doubling on the velocities. Fig. 2.4 shows the schematic diagram of the doubled degrees of freedom. The trajectories $\mathbf{q}_1(t)$ and $\mathbf{q}_2(t)$ evolve from the specified initial conditions

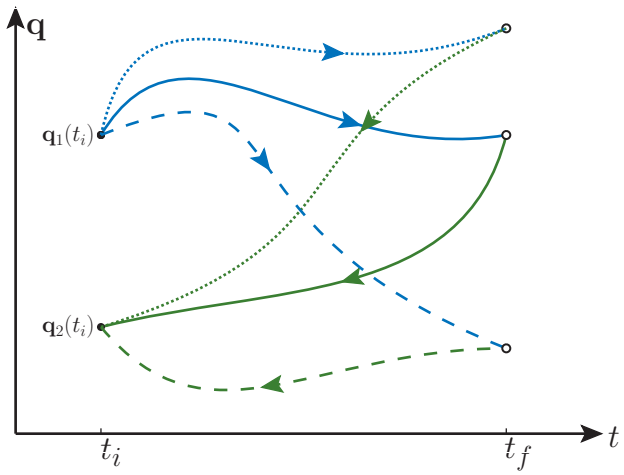

Figure 2.4: The trajectories $\mathbf{q}_1$ and $\mathbf{q}_2$ in the constructed non-conservative Lagrangian with the doubled degrees of freedom. Only the initial conditions are specified, and final states satisfy the equality conditions. The arrows indicate the time integral directions for the Lagrangian. Solid lines and dashed lines correspond to the paths with a stationary action and the varied paths through configuration space.

at $t = t_i$ to some final time $t = t_f$ where the values of $\mathbf{q}_1(t_f)$ and $\mathbf{q}_2(t_f)$ are determined by the dynamics. The arrows on the paths represent the direction for the time integration of the Lagrangian. The dynamics for the doubled variable is described by the new action

$$\begin{aligned} S[\mathbf{q}_1, \mathbf{q}_2] &= \int_{t_i}^{t_f} \mathrm{d}t L(\mathbf{q}_1, \dot{\mathbf{q}}_1, t) + \int_{t_f}^{t_i} \mathrm{d}t L(\mathbf{q}_2, \dot{\mathbf{q}}_2, t) + \int_{t_i}^{t_f} \mathrm{d}t K(\mathbf{q}_1, \mathbf{q}_2, \dot{\mathbf{q}}_1, \dot{\mathbf{q}}_2, t) \\ &= \int_{t_i}^{t_f} \mathrm{d}t \Big[L(\mathbf{q}_1, \dot{\mathbf{q}}_1, t) - L(\mathbf{q}_2, \dot{\mathbf{q}}_2, t) + K(\mathbf{q}_1, \mathbf{q}_2, \dot{\mathbf{q}}_1, \dot{\mathbf{q}}_2, t) \Big], \end{aligned} \tag{2.30}$$

and the new Lagrangian is

$$\Lambda(\mathbf{q}_1, \mathbf{q}_2, \dot{\mathbf{q}}_1, \dot{\mathbf{q}}_2, t) = L(\mathbf{q}_1, \dot{\mathbf{q}}_1, t) - L(\mathbf{q}_2, \dot{\mathbf{q}}_2, t) + K(\mathbf{q}_1, \mathbf{q}_2, \dot{\mathbf{q}}_1, \dot{\mathbf{q}}_2, t). \tag{2.31}$$

The first two terms $L = L(\mathbf{q}_1, \dot{\mathbf{q}}_1, t) - L(\mathbf{q}_2, \dot{\mathbf{q}}_2, t)$ accounts for the conservative sector in which the double coordinates $\mathbf{q}_1$ and $\mathbf{q}_2$ are decoupled from each other. The last term on the right-hand side K contains all the non-conservative effects that are not derivable from a potential energy. Therefore, K can be considered as a non-conservative potential. It can

be shown that K is anti-symmetric under the interchange of the history labels $1 \leftrightarrow 2$ in the action,

$$K(\mathbf{q}_1, \mathbf{q}_2, \dot{\mathbf{q}}_1, \dot{\mathbf{q}}_2, t) = -K(\mathbf{q}_2, \mathbf{q}_1, \dot{\mathbf{q}}_2, \dot{\mathbf{q}}_1, t), \tag{2.32}$$

thus K mush vanish when $\mathbf{q}_1 = \mathbf{q}_2$.

The canonical momentum conjugate to $\mathbf{q}_1$ is defined as

$$\pi_{1,I}(\mathbf{q}_1, \mathbf{q}_2, \dot{\mathbf{q}}_1, \dot{\mathbf{q}}_2, t) = \frac{\partial \Lambda}{\partial \dot{q}_1^I(t)} = \frac{\partial L(\mathbf{q}_1, \dot{\mathbf{q}}_1, t)}{\partial \dot{q}_1^I} + \frac{\partial K}{\partial \dot{q}_1^I(t)}, \tag{2.33}$$

and similarly for the second history

$$\pi_{2,I}(\mathbf{q}_1, \mathbf{q}_2, \dot{\mathbf{q}}_1, \dot{\mathbf{q}}_2, t) = -\frac{\partial \Lambda}{\partial \dot{q}_2^I(t)} = \frac{\partial L(\mathbf{q}_2, \dot{\mathbf{q}}_2, t)}{\partial \dot{q}_2^I} - \frac{\partial K}{\partial \dot{q}_2^I(t)}. \tag{2.34}$$

It is convenient to switch the history variables from $(1, 2)$ to $\pm$ with

$$q_+^I \equiv \frac{q_1^I + q_2^I}{2}, \qquad q_-^I \equiv q_1^I - q_2^I. \tag{2.35}$$

The physical limit is defined as

$$q_+^I \to q^I, \qquad q_-^I \to 0, \tag{2.36}$$

such that the histories $q_1^I = q_2^I = q^I$ and $\dot{q}_1^I = \dot{q}_2^I = \dot{q}^I$.

The variation to the effective action becomes

$$\left.\frac{\delta S_{\mathit{eff}}[q_+^I, q_-^I]}{\delta q_-^I}\right|_{\mathrm{PL}} = 0, \tag{2.37}$$

where PL stands for taking the physical limit to ensure that the two histories match with each other at the final time. The physical limit does not fix the values of the final states, instead it makes sure that both paths are the same as the physical one after all variations are performed. The variational principle leads to the Euler-Lagrangian equations

$$0 = \int_{t_i}^{t_f} \mathrm{d}t \left\{ \frac{\partial \Lambda}{\partial q_-^I} - \frac{\mathrm{d}}{\mathrm{d}t} \frac{\partial \Lambda}{\partial \dot{q}_-^I} \right\}_{\mathrm{PL}}. \tag{2.38}$$

The equations of motion for the non-conservative dynamics of $\mathbf{q}(t)$ can be expressed in terms of L and K,

$$\frac{\mathrm{d}}{\mathrm{d}t}\frac{\partial L}{\partial \dot{q}^I_-} - \frac{\partial L}{\partial q^I_-} = \left[\frac{\partial K}{\partial q^I_-} - \frac{\mathrm{d}}{\mathrm{d}t}\frac{\partial K}{\partial \dot{q}^I_-}\right]_{PL} \equiv Q_I(q^J, \dot{q}^J, t), \tag{2.39}$$

where Q^I is defined as the generalized non-conservative force due to the non-conservative potential K. Applying the non-conservative variation principle to the effective action $S_{\rm NR}[x_a, \bar{h}]$ computed from the corresponding Feynman diagrams is the next step in the procedure to obtain gravitational radiation reaction in the next section.

2.4 Gravitational Radiation Reaction In EFT Framework

The radiation reaction force is calculated through the Feynman diagrams such as the ones shown in Fig. 2.5. The electric and magnetic parts of the Weyl curvature tensor E_{ij} and B_{ij} in (2.22) that contain the radiation fields are integrated out in these diagrams. As an example, we present here a detail calculation of the current octupole coupling diagram in momentum space. This diagram contributes to the 2PN corrections to the radiation reaction. Starting from the couplings of the current octupole moment and the magnetic part of the Weyl tensor, the amplitude of the diagram can be written as

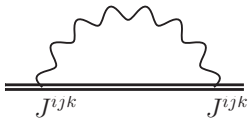

$$= \frac{1}{2}\left(-\frac{i}{4}\right)^2 \int \mathrm{d}t\mathrm{d}t' J_A^{ijk}(t)\langle \partial_k B^A_{ij}(t)\partial_l B^B_{mn}(t')\rangle J_B^{lmn}(t') \tag{2.40}$$

Here A and B are the history indices that label the copy of the worldine. Using the expansion of B_{ij} in (2.23), the two-point function in (2.40) in the radiation field momentum space is given by

$$\begin{aligned}&\langle \partial_k B^A_{ij}(t)\partial_l B^B_{mn}(t')\rangle \\ =&\epsilon_{iab}\epsilon_{mcd}\langle\left(iq_0\mathbf{q}_a\mathbf{q}_k\bar{h}^A_{bj} - i\mathbf{q}_j\mathbf{q}_a\mathbf{q}_k\bar{h}^A_{0b}\right)\left(-iq_0\mathbf{q}_c\mathbf{q}_l\bar{h}^B_{nd} + i\mathbf{q}_n\mathbf{q}_c\mathbf{q}_l\bar{h}^B_{0d}\right)\rangle\end{aligned} \tag{2.41}$$

(a) (b)

Figure 2.5: The Feynman diagrams that contribute to the radiation reaction from the mass type and current type multipole moments.

where $q = (q^0, \mathbf{q}) \sim v/r$ is the momentum carried by the radiation graviton. With the $\bar{h}_{\mu\nu}$ propagator $\langle \bar{h}^A_{\mu\nu} \bar{h}^B_{\alpha\beta} \rangle = D^{AB}(q) P_{\mu\nu;\alpha\beta}$, the effective action becomes

$$iS_{eff} = -\pi G \int \mathrm{d}t\mathrm{d}t' J_A^{ijk}(t) J_B^{lmn}(t') \int \frac{\mathrm{d}^4 q}{(2\pi)^4} e^{-iq_0(t-t')} D^{AB}(q) \times \epsilon_{iab}\epsilon_{mcd} \left(q_0^2 \mathbf{q}_a \mathbf{q}_c \mathbf{q}_k \mathbf{q}_l P_{bj;nd} + \mathbf{q}_a \mathbf{q}_c \mathbf{q}_j \mathbf{q}_k \mathbf{q}_l \mathbf{q}_n P_{0b;0d} \right). \quad (2.42)$$

In the $\pm$ history indices basis, the matrix of the propagator is

$$D^{AB} = \begin{pmatrix} 0 & -iD_{adv} \\ -iD_{ret} & 0 \end{pmatrix} \quad (2.43)$$

with $D_{adv}(t, t') = D_{ret}(t', t)$ to further simplify (2.42) to be

$$S_{eff} = \frac{\pi G}{2} \int \mathrm{d}t\mathrm{d}t' J_+^{ijk}(t) J_-^{ijk}(t') \int \frac{\mathrm{d}^4 q}{(2\pi)^4} e^{-iq_0(t-t')} \frac{1}{(q_0 + i\epsilon)^2 - \mathbf{q}^2} \left(\frac{2}{15} q_0^2 \mathbf{q}^4 - \frac{4}{105} \mathbf{q}^6 \right), \quad (2.44)$$

where the property of the octupole being symmetric and traceless is applied to drop and combine a number of terms. Contour integration with respect to the three-momentum $\mathbf{q}$ leaves the action as

$$S_{eff} = -\frac{iG}{84} \int \mathrm{d}t\mathrm{d}t' J_+^{ijk}(t) J_-^{ijk}(t') \int \frac{\mathrm{d}q_0}{2\pi} e^{-iq_0(t-t')} q_0^7$$

$$= -\frac{iG}{84}\int \mathrm{d}t\mathrm{d}t' J_+^{ijk}(t)J_-^{ijk}(t')\int \frac{\mathrm{d}q_0}{2\pi}(i\partial_t)^7 e^{-iq_0(t-t')} \tag{2.45}$$
$$= \frac{G}{84}\int \mathrm{d}t J_-^{ijk}(t)J_{+ijk}^{(7)}(t).$$

The leading order current octupole $J_\pm^{ijk}(t)$ can be written in terms of the $\mathbf{x}_{a\pm}$ variables as

$$J_-^{ijk} = \sum_{a,b} m_a \Big[\epsilon^{iml}(\mathbf{x}_{a+}^j\mathbf{x}_{a+}^k\mathbf{x}_{a+}^m\mathbf{v}_{a-}^l + \mathbf{x}_{a+}^j\mathbf{x}_{a+}^k\mathbf{x}_{a-}^m\mathbf{v}_{a+}^l + \mathbf{x}_{a+}^j\mathbf{x}_{a-}^k\mathbf{x}_{a+}^m\mathbf{v}_{a+}^l$$
$$+ \mathbf{x}_{a-}^j\mathbf{x}_{a+}^k\mathbf{x}_{a+}^m\mathbf{v}_{a+}^l)\Big]_{\mathrm{STF}} + \mathcal{O}(\mathbf{x}_{a-}^3), \tag{2.46a}$$
$$J_+^{ijk} = \sum_{a,b} m_a \Big[\epsilon^{iml}\mathbf{x}_{a+}^j\mathbf{x}_{a+}^k\mathbf{x}_{a+}^m\mathbf{v}_{a+}^l\Big]_{\mathrm{STF}} + \mathcal{O}(\mathbf{x}_{a-}^2), \tag{2.46b}$$

where only the $\mathcal{O}(\mathbf{x}_{a-}^0)$ and $\mathcal{O}(\mathbf{x}_{a-})$ terms are kept for the next step. Finally the equations of motion is obtained through the non-conservative variation principle applied to the action in (2.45),

$$F_a^i(t) = \left[\frac{\partial L_{eff}}{\partial \mathbf{x}_{ai-}} - \frac{\mathrm{d}}{\mathrm{d}t}\left(\frac{\partial L_{eff}}{\partial \dot{\mathbf{x}}_{ai-}}\right)\right]_{\mathrm{PL}}, \tag{2.47}$$

where $F_a^i(t)$ is the radiation reaction force. From (2.46), (2.45) and (2.47), the acceleration $\mathbf{a} = \mathbf{a}_1 - \mathbf{a}_2 = \mathbf{F}_1(t)/m_1 - \mathbf{F}_2(t)/m_2$ due to J^{ijk} interaction contribution in the center-of-mass

frame is then

$$\begin{aligned}
\mathbf{a}^i_{\rm CO} =&\frac{1404M^2\nu^2\dot{r}^7\mathbf{x}^i}{r^4} - \frac{2106M^2\nu^3\dot{r}^7\mathbf{x}^i}{r^4} - \frac{234M^2\nu\dot{r}^7\mathbf{x}^i}{r^4} + \frac{1482M^2\nu^3\dot{r}^6\mathbf{v}^i}{r^3} + \frac{494M^2\nu\dot{r}^6\mathbf{v}^i}{3r^3}\\
&- \frac{988M^2\nu^2\dot{r}^6\mathbf{v}^i}{r^3} + \frac{4314M^2\mathbf{v}^2\nu^3\dot{r}^5\mathbf{x}^i}{r^4} + \frac{1438M^2\mathbf{v}^2\nu\dot{r}^5\mathbf{x}^i}{3r^4} + \frac{360M^3\nu^2\dot{r}^5\mathbf{x}^i}{r^5}\\
&- \frac{2876M^2\mathbf{v}^2\nu^2\dot{r}^5\mathbf{x}^i}{r^4} - \frac{540M^3\nu^3\dot{r}^5\mathbf{x}^i}{r^5} - \frac{60M^3\nu\dot{r}^5\mathbf{x}^i}{r^5} + \frac{1820M^2\mathbf{v}^2\nu^2\dot{r}^4\mathbf{v}^i}{r^3}\\
&+ \frac{492M^3\nu^3\dot{r}^4\mathbf{v}^i}{r^4} + \frac{164M^3\nu\dot{r}^4\mathbf{v}^i}{3r^4} - \frac{2730M^2\mathbf{v}^2\nu^3\dot{r}^4\mathbf{v}^i}{r^3} - \frac{910M^2\mathbf{v}^2\nu\dot{r}^4\mathbf{v}^i}{3r^3}\\
&- \frac{328M^3\nu^2\dot{r}^4\mathbf{v}^i}{r^4} + \frac{12220M^2\mathbf{v}^4\nu^2\dot{r}^3\mathbf{x}^i}{7r^4} + \frac{33414M^3\mathbf{v}^2\nu^3\dot{r}^3\mathbf{x}^i}{35r^5} + \frac{11138M^3\mathbf{v}^2\nu\dot{r}^3\mathbf{x}^i}{105r^5}\\
&+ \frac{4232M^4\nu^3\dot{r}^3\mathbf{x}^i}{35r^6} + \frac{4232M^4\nu\dot{r}^3\mathbf{x}^i}{315r^6} - \frac{18330M^2\mathbf{v}^4\nu^3\dot{r}^3\mathbf{x}^i}{7r^4} - \frac{6110M^2\mathbf{v}^4\nu\dot{r}^3\mathbf{x}^i}{21r^4}\\
&- \frac{22276M^3\mathbf{v}^2\nu^2\dot{r}^3\mathbf{x}^i}{35r^5} - \frac{8464M^4\nu^2\dot{r}^3\mathbf{x}^i}{105r^6} + \frac{1350M^2\mathbf{v}^4\nu^3\dot{r}^2\mathbf{v}^i}{r^3} + \frac{150M^2\mathbf{v}^4\nu\dot{r}^2\mathbf{v}^i}{r^3}\\
&+ \frac{2524M^3\mathbf{v}^2\nu^2\dot{r}^2\mathbf{v}^i}{5r^4} + \frac{272M^4\nu^2\dot{r}^2\mathbf{v}^i}{5r^5} - \frac{900M^2\mathbf{v}^4\nu^2\dot{r}^2\mathbf{v}^i}{r^3} - \frac{3786M^3\mathbf{v}^2\nu^3\dot{r}^2\mathbf{v}^i}{5r^4}\\
&- \frac{1262M^3\mathbf{v}^2\nu\dot{r}^2\mathbf{v}^i}{15r^4} - \frac{408M^4\nu^3\dot{r}^2\mathbf{v}^i}{5r^5} - \frac{136M^4\nu\dot{r}^2\mathbf{v}^i}{15r^5} + \frac{2970M^2\mathbf{v}^6\nu^3\dot{r}\mathbf{x}^i}{7r^4}\\
&+ \frac{330M^2\mathbf{v}^6\nu\dot{r}\mathbf{x}^i}{7r^4} + \frac{1420M^3\mathbf{v}^4\nu^2\dot{r}\mathbf{x}^i}{7r^5} + \frac{128M^4\mathbf{v}^2\nu^2\dot{r}\mathbf{x}^i}{35r^6} + \frac{344M^5\nu^3\dot{r}\mathbf{x}^i}{35r^7} + \frac{344M^5\nu\dot{r}\mathbf{x}^i}{315r^7}\\
&- \frac{1980M^2\mathbf{v}^6\nu^2\dot{r}\mathbf{x}^i}{7r^4} - \frac{2130M^3\mathbf{v}^4\nu^3\dot{r}\mathbf{x}^i}{7r^5} - \frac{710M^3\mathbf{v}^4\nu\dot{r}\mathbf{x}^i}{21r^5} - \frac{192M^4\mathbf{v}^2\nu^3\dot{r}\mathbf{x}^i}{35r^6}\\
&- \frac{64M^4\mathbf{v}^2\nu\dot{r}\mathbf{x}^i}{105r^6} - \frac{688M^5\nu^2\dot{r}\mathbf{x}^i}{105r^7} + \frac{540M^2\mathbf{v}^6\nu^2\mathbf{v}^i}{7r^3} + \frac{774M^3\mathbf{v}^4\nu^3\mathbf{v}^i}{5r^4} + \frac{86M^3\mathbf{v}^4\nu\mathbf{v}^i}{5r^4}\\
&+ \frac{2368M^4\mathbf{v}^2\nu^2\mathbf{v}^i}{105r^5} + \frac{688M^5\nu^2\mathbf{v}^i}{105r^6} - \frac{810M^2\mathbf{v}^6\nu^3\mathbf{v}^i}{7r^3} - \frac{90M^2\mathbf{v}^6\nu\mathbf{v}^i}{7r^3} - \frac{516M^3\mathbf{v}^4\nu^2\mathbf{v}^i}{5r^4}\\
&- \frac{1184M^4\mathbf{v}^2\nu^3\mathbf{v}^i}{35r^5} - \frac{1184M^4\mathbf{v}^2\nu\mathbf{v}^i}{315r^5} - \frac{344M^5\nu^3\mathbf{v}^i}{35r^6} - \frac{344M^5\nu\mathbf{v}^i}{315r^6},
\end{aligned} \tag{2.48}$$

where $\dot{r} = \mathbf{n}\cdot\mathbf{v}$ and $\nu = (m_1 \times m_2)/M^2$. The same procedure applied to the other multipole moments and the PN corrections from the potential interactions to the corresponding moments leads to the equations of motion at 4.5PN due to the radiation reaction force.

2.5 Dynamical Renormalization Group Method

The choice of the BH coalescence model is critical for determining the waveform. The last few orbits of the inspiral phase through the merger and ringdown of the BH coalescence

have been simulated by Numerical Relativity [24, 25]. There have been developments on the analytic understandings for merger and ringdown [26]. The slowly-orbiting long inspiral phase can be studied analytically using post-Newtonian (PN) perturbation theory with small velocity and weak field approximations. BH dynamics is described by the Newtonian-like equations of motion in the form of the acceleration of the binary constituents. During the inspiral, the binary slowly loses energy and angular momentum to gravitational radiation starting at 2.5PN [9, 10]. Higher order corrections up to 4PN in the conservative sector have been calculated [27–35]. Solving for the motions is the fundamental step in obtaining the waveforms and deriving the evolution of the theoretical physical measurements in time, such as the GW phase directly measured by the detectors and power loss due to gravitational radiations.

The exact solutions to the motions can be found by numerically integrating these nonlinearly-coupled ordinary differential equations. However, in calculations of template banks, each point in the intrinsic parameter space representing a waveform with different initial conditions requires a new numerical computation. The sample rate of the corresponding waveform directly depends on the precision and step sizes of the solutions of the motions. The discrete nature of the computational solutions also brings the issue of the distance between the templates in the parameter space, which may result in the loss in signal-to-noise ratio due to the mismatch of the template in the match-filter of the signal data. Since the third observing run of LIGO and Virgo are having a weekly rate of observed events, a faster and more accurate way of computation in the signal analysis is critical, with even larger rates expected with future upgrades. A fully analytic waveform solution with continuous parameters would certainly increase the calculation efficiency for template-based data analysis.

In [15], Galley and Rothstein applied a method called the Dynamical Renormalization Group (DRG) formalism to calculate the analytic solutions to compact binary inspiral equations of motions. This method generates closed-form solutions to the binary real space trajectory without any orbit averaging. The binary equations of motion (1.2) under the post-Newtonian formalism is a series of second-order ordinary differential equations. The equations expressed in terms of the dynamical degrees of freedom can be derived from various methods including the EFT formalism introduced in the previous sections. The DRG method

treats the radiation reactions starting at 2.5PN as PN perturbations to the conservative quasi-circular orbits. The renormalization group method is applied to systematically resum the secularly growing terms in the perturbative solutions of the binary orbital radius $r(t)$, accumulated orbital phase $\phi(t)$ and orbital frequency $\omega(t)$.

To derive the DRG solutions to the equations of motion

$$\begin{aligned}\mathbf{a}^i &= \mathbf{a}^i_{\rm Newtonian} + \mathbf{a}^i_{\rm RR} \\ &= -\frac{M}{r^2}\hat{\boldsymbol{n}} + \frac{M^2\nu}{15r^4}\dot{r}\Big(\frac{136M}{r} + 72\boldsymbol{v}^2\Big)\boldsymbol{r} - \frac{8M^2\nu}{5r^3}\Big(\frac{3M}{r} + \boldsymbol{v}^2\Big)\boldsymbol{v},\end{aligned} \tag{2.49}$$

we start with a background circular orbit and consider the radiation reaction force as a small perturbation to the nearly circular orbit. The Newtonian orbit is described by $M = \Omega_B^2 R_B^3$ with the constant radius R_B and the constant angular frequency Ω_B. The perturbations to the background orbit as a result of the radiation scale as $\delta r(t) \sim v^5 R_B$ and $\delta\omega(t) \sim v^5\Omega_B$ and the physical solutions can be written as

$$r(t) = R_B + \delta r(t), \qquad\qquad \omega(t) = \Omega_B + \delta\omega(t). \tag{2.50}$$

Substituting into (2.49) and expanding to the leading order in δr and $\delta\omega$, the solutions to the perturbations are

$$\delta r(t) = -\frac{64\nu}{5}R_B^6\Omega_B^6(t-t_0) + A_B\sin\left(\Omega_B(t-t_0) + \Phi_B\right), \tag{2.51}$$

$$\delta\omega(t) = \frac{96\nu}{5}R_B^5\Omega_B^7(t-t_0) - \frac{2\Omega_B A_B}{R_B}\sin\left(\Omega_B(t-t_0) + \Phi_B\right), \tag{2.52}$$

where $A_B \sim v^5 R_B$ and Φ_B are integration constants that can be determined from the initial condition at time t_0. The terms that grows with $(t-t_0)$ spoil the power counting of the perturbations as t evolves away from the initial t_0. These are the secular divergences to be eliminated using the renormalization group method.

The bare parameters R_B, Ω_B, A_B and Φ_B can be split into renormalized parameters and counter-terms

$$\begin{aligned}R_B(t_0) &= R_R(\tau) + \delta_R(\tau, t_0), \\ \Omega_B(t_0) &= \Omega_R(\tau) + \delta_\Omega(\tau, t_0), \\ \Phi_B(t_0) &= \Phi_R(\tau) + \delta_\Phi(\tau, t_0), \\ A_B(t_0) &= A_R(\tau) + \delta_A(\tau, t_0),\end{aligned} \tag{2.53}$$

where a new time parameter τ is defined as the arbitrary renormalization scale. The renormalization scale is introduced into the solutions by writing $(t-t_0)=(t-\tau)+(\tau-t_0)$. By fixing the counter-terms to cancel the secular divergences, we can find that

$$\begin{aligned}
\delta_R(\tau,t_0) &= \frac{64\nu}{5}R_R^6\Omega_R^6(\tau-t_0),\\
\delta_\Omega(\tau,t_0) &= -\frac{96\nu}{5}R_R^5\Omega_R^7(\tau-t_0),\\
\delta_\Phi(\tau,t_0) &= -\Phi_R(\tau-t_0)+\frac{48\nu}{5}R_R^5\Omega_R^7(\tau-t_0)^2.
\end{aligned} \tag{2.54}$$

The renormalization scale is chosen to be $\tau=t$ at the observation time to minimize the t-dependence of the physical solutions to be

$$\begin{aligned}
r(t) =& R_R(t)+A_R(t)\sin\Phi_R(t),\\
\omega(t) =& \Omega_R(t)-\frac{2\Omega_R(t)A_R(t)}{R_R(t)}\sin\Phi_R(t),\\
\phi(t) =& \Phi_R(t)+\frac{2A_R(t)}{R_R(t)}\cos\Phi_R(t).
\end{aligned} \tag{2.55}$$

Finally the time dependence of the renormalized parameters is determined by the RG equations. Since the bare parameters are independent of τ,

$$0=\frac{\mathrm{d}R_B}{\mathrm{d}\tau}=\frac{\mathrm{d}}{\mathrm{d}\tau}R_R(\tau)+\frac{\mathrm{d}\delta_R}{\mathrm{d}\tau} \tag{2.56}$$

and similarly for the others. The RG equations for the parameters are

$$\begin{aligned}
\frac{\mathrm{d}R_R}{\mathrm{d}\tau} =& -\frac{64\nu}{5}R_R^6(\tau)\Omega_R^6(\tau),\\
\frac{\mathrm{d}\Omega_R}{\mathrm{d}\tau} =& \frac{96\nu}{5}R_R^5(\tau)\Omega_R^7(\tau),\\
\frac{\mathrm{d}\Phi_R}{\mathrm{d}\tau} =& \Omega_R(\tau),\\
\frac{\mathrm{d}A_R}{\mathrm{d}\tau} =& 0.
\end{aligned} \tag{2.57}$$

The solutions to the RG equations combined with the physical solutions in (2.55) give the resummed solution to the leading order inspiral dynamics of (2.49) valid up to $t-t_0\sim\frac{1}{\nu v^5\Omega_B}$. The accuracy of the resummed perturbative solution can be systematically improved by calculating at "two-loop". The calculation is done by including two insertions of the leading

order radiation reaction and renormalizing the perturbations at $\mathcal{O}(v^{10})$, based on the previous one-loop result of $\mathcal{O}(v^5)$ perturbation resummation.

Compared to the adiabatic solutions, the DRG solutions are much better at describing the small oscillations and avoid the ambiguity in specifying the initial data. The DRG method also provides systematic ways to include post-Newtonian corrections to the radiation reaction force and spin effects. In Chapter 4, the DRG method is applied to the spinning binary inspiral equations of motion and spin precession equations.

3.0 Second Post-Newtonian Order Radiative Dynamics

The goal of this section is to determine the 2PN correction to the mass quadrupole moment, which comes from various moments of the stress-energy pseudo-tensor. Each such contribution starts at different order in the PN expansion and only a few of these contributions can be derived from known quantities. We also derive the equation of motion of the binary system at 2PN order in the appendix B. Note that this acceleration was calculated previously in the EFT approach in [36], where the authors worked with Kaluza-Klein variables [37] in conjunction with harmonic coordinates. The 2PN acceleration derived here, on the other hand, is written in the linearized (background) harmonic gauge, which leaves a gauge invariant effective action for the radiation field after the potential modes are integrated out, and can be used in combination with previous results obtained in the EFT approach where the linearized harmonic gauge was used. Our results constitute the final missing part necessary for the computation of the next-to-next-to-leading order radiation reaction force as well as for the construction of spinning templates at 2.5 PN for the phase and 3PN for the amplitude. These computations are ongoing and will be reported in a subsequent publication.

3.1 Radiation Sector

The radiation action, which describes arbitrary gravitational wave sources in the long wavelength approximation, can be written in a diffeomorphism invariant way in terms of multipoles. Specifically, it is a derivative expansion where higher order terms are suppressed by powers of the ratio between the size of the binary system over the wavelength of the radiation emitted. In the center-of-mass frame, the action of the radiation sector is [20]

$$S_{rad}\left[\bar{h}, x_a\right] = -\int dt\sqrt{\bar{g}_{00}}\Big[m + \frac{1}{2}L_{ij}\omega_0^{ij} + \sum_{l=2}^{\infty}\Big(\frac{1}{l!}I^L\nabla_{L-2}E_{i_{l-1}i_l} - \frac{2l}{(2l+1)!}J^L\nabla_{L-2}B_{i_{l-1}i_l}\Big)\Big], \tag{3.1}$$

where a multi-index representation $L = i_1...i_l$ is used. The first two terms generate the Kerr background in which the gravitational waves propagate. The multipole moments, which constitute the source of radiation, are coupled to the electric and the magnetic components of the Weyl tensor.

To determine the moments, one performs a matching between the effective action (3.1) in the long wavelength limit and the action valid below the orbital scale, which depends on both radiation and potential modes of the gravitational field. The latter action is used in order to compute the one-graviton emission amplitude. As a result, by definition the resulting action takes the form

$$\Gamma\left[\bar{h}\right] = -\frac{1}{2m_{Pl}}\int d^4x T^{\mu\nu}\bar{h}_{\mu\nu}, \tag{3.2}$$

where $T^{\mu\nu}$ is the stress-energy pseudotensor of the system. Relations from the Ward identity $\partial_\mu T^{\mu\nu} = 0$ as well as the on-shell equations of motion can be used to bring both actions (3.1) and (3.2) in a comparable form. After that, a general form for the mass quadrupole moment is obtained in terms of the components of the stress-energy pseudotensor and its derivatives,

$$\begin{aligned} I^{ij} = \sum_{p=0}^{\infty}\frac{5!!}{(2p)!!(5+2p)!!}\Bigg\{&\left(1+\frac{2p(3+p)}{3}\right)\left[\int d^3\mathbf{x}\partial_0^{2p}T^{00}\mathbf{x}^{2p}\mathbf{x}^i\mathbf{x}^j\right]_{TF} \\ &+\left(1+\frac{p}{3}\right)\left[\int d^3\mathbf{x}\partial_0^{2p}T^{ll}\mathbf{x}^{2p}\mathbf{x}^i\mathbf{x}^j\right]_{TF} - \frac{4}{3}\left(1+\frac{p}{2}\right)\left[\int d^3\mathbf{x}\partial_0^{2p+1}T^{0l}\mathbf{x}^{2p}\mathbf{x}^l\mathbf{x}^i\mathbf{x}^j\right]_{TF} \\ &+\frac{1}{6}\left[\int d^3\mathbf{x}\partial_0^{2p+2}T^{kl}\mathbf{x}^{2p}\mathbf{x}^k\mathbf{x}^l\mathbf{x}^i\mathbf{x}^j\right]_{TF}\Bigg\}, \end{aligned} \tag{3.3}$$

where TF stands for trace-free[1]. For the exact expressions for the multipole moments in all orders in the PN expansion, see [38]. The leading-order contribution to the mass quadrupole moment comes from just one term

$$I^{ij}_{0PN} = \left[\int d^3\mathbf{x}T^{00}_{0PN}\mathbf{x}^i\mathbf{x}^j\right]_{TF} = \sum_a m_a\left[\mathbf{x}^i_a\mathbf{x}^j_a\right]_{TF}, \tag{3.4}$$

while its 1PN correction [20] is given by four different contributions of the components of the stress-energy pseudotensor:

$$I^{ij}_{1PN} = \left[\int d^3\mathbf{x}T^{00}_{1PN}\mathbf{x}^i\mathbf{x}^j\right]_{TF} + \left[\int d^3\mathbf{x}T^{ll}_{0PN}\mathbf{x}^i\mathbf{x}^j\right]_{TF}$$

[1]More precisely, the multipole moments are symmetric trace-free (STF) quantities, but we are supressing the "S" in the label to avoid redundancy since the general expression for the quadrupole moment is explicitly written as a symmetric tensor already.

$$
\begin{aligned}
&-\frac{4}{3}\left[\int d^3\mathbf{x}\partial_0 T^{0l}_{0PN}\mathbf{x}^l\mathbf{x}^i\mathbf{x}^j\right]_{TF}+\frac{11}{42}\left[\int d^3\mathbf{x}\partial_0^2 T^{00}_{0PN}\mathbf{x}^2\mathbf{x}^i\mathbf{x}^j\right]_{TF}\\
&=\sum_a m_a\left[\left(\frac{3}{2}\mathbf{v}_a^2-\sum_{b\neq a}\frac{Gm_b}{r}\right)\mathbf{x}_a^i\mathbf{x}_a^j+\frac{11}{42}\frac{d^2}{dt^2}\left(\mathbf{x}_a^2\mathbf{x}_a^i\mathbf{x}_a^j\right)-\frac{4}{3}\frac{d}{dt}\left(\mathbf{x}_a\cdot\mathbf{v}_a\mathbf{x}_a^i\mathbf{x}_a^j\right)\right]_{TF}.
\end{aligned}
\tag{3.5}
$$

The 2PN correction to the leading order mass quadrupole moment is given by

$$
\begin{aligned}
I^{ij}_{2PN}=&\left[\int d^3\mathbf{x}T^{00}_{2PN}\mathbf{x}^i\mathbf{x}^j\right]_{TF}+\left[\int d^3\mathbf{x}T^{ll}_{1PN}\mathbf{x}^i\mathbf{x}^j\right]_{TF}-\frac{4}{3}\left[\int d^3\mathbf{x}\partial_0 T^{0l}_{1PN}\mathbf{x}^l\mathbf{x}^i\mathbf{x}^j\right]_{TF}\\
&+\frac{1}{6}\left[\int d^3\mathbf{x}\partial_0^2 T^{kl}_{0PN}\mathbf{x}^k\mathbf{x}^l\mathbf{x}^i\mathbf{x}^j\right]_{TF}+\frac{11}{42}\left[\int d^3\mathbf{x}\partial_0^2 T^{00}_{1PN}\mathbf{x}^2\mathbf{x}^i\mathbf{x}^j\right]_{TF}\\
&+\frac{2}{21}\left[\int d^3\mathbf{x}\partial_0^2 T^{ll}_{0PN}\mathbf{x}^2\mathbf{x}^i\mathbf{x}^j\right]_{TF}-\frac{1}{7}\left[\int d^3\mathbf{x}\partial_0^3 T^{0l}_{0PN}\mathbf{x}^2\mathbf{x}^l\mathbf{x}^i\mathbf{x}^j\right]_{TF}\\
&+\frac{23}{1512}\left[\int d^3\mathbf{x}\partial_0^4 T^{00}_{0PN}\mathbf{x}^4\mathbf{x}^i\mathbf{x}^j\right]_{TF}+I^{ij}_{1PN}\left(\mathbf{a}_{1PN}\right).
\end{aligned}
\tag{3.6}
$$

Notice that the last term in the expression above arises from two terms in the second line of (3.5) after using the equations of motion. While T^{00}_{0PN} and T^{0l}_{0PN} are trivial, the higher PN order components T^{00}_{2PN}, T^{0i}_{1PN}, T^{ll}_{1PN} have yet to be obtained in the EFT formalism.

3.2 Higher Order Stress-energy Tensors

Introducing the partial Fourier transform of the stress-energy pseudotensor $T^{\mu\nu}(t,\mathbf{k})=\int d^3x T^{\mu\nu}(t,\mathbf{x})\,e^{-i\mathbf{k}\cdot\mathbf{x}}$, we consider the long wavelength limit $\mathbf{k}\to 0$ to write

$$
T^{\mu\nu}(t,\mathbf{k})=\sum_{n=0}^{\infty}\frac{(-i)^n}{n!}\left(\int d^3\mathbf{x}T^{\mu\nu}(t,\mathbf{x})\,\mathbf{x}^{i_1}...\mathbf{x}^{i_n}\right)\mathbf{k}_{i_1}...\mathbf{k}_{i_n},
\tag{3.7}
$$

where each term in this expansion corresponds to a sum of Feynman diagrams that scale as a definite power of the parameter v. This partial Fourier transform is convenient since Feynman graphs are more easily handled in momentum space and, with the pseudotensor written in this way, we can read off the contributions to the mass quadrupole moment (3.6), the ultimate goal of this chapter.

3.2.1 2PN correction to T^{00}

The leading order and the next-to-leading order temporal components of the pseudotensor, obtained in [20] using the EFT techniques summarized in the previous section, are given by

$$T^{00}_{0PN}(t,\mathbf{k}) = \sum_a m_a e^{-i\mathbf{k}\cdot\mathbf{x}_a}, \tag{3.8}$$

$$T^{00}_{1PN}(t,\mathbf{k}) = \left[\sum_a \frac{1}{2} m_a \mathbf{v}_a^2 - \sum_{a\neq b} \frac{G m_a m_b}{2r} + O(\mathbf{k}) + ...\right] e^{-i\mathbf{k}\cdot\mathbf{x}_a}. \tag{3.9}$$

If we take into account the zeroth order term of the exponential expanded in the radiation momentum $\mathbf{k}$, we see that the leading order pseudotensor provides the total mass whereas the next-to-leading order represents the Newtonian energy of a dynamical two-body system. These quantities scale as mv^0 and mv^2, respectively. Hence, to obtain the 2PN correction to the leading order T^{00}, we have to calculate all Feynman diagrams that contribute to the one-graviton $\bar{h}_{00}$ emission and enter at order v^4.

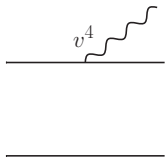

Figure 3.1: No graviton exchange between the two particles, one external $\bar{h}^{00}$ momentum.

The simplest contribution to the second PN correction for the temporal component of the stress-energy pseudotensor is illustrated in Fig. 3.1 and comes from the source action term. Comparing this diagram against (3.2), we extract the following contribution to the pseudotensor

$$T^{00}_{Fig1}(t,\mathbf{k}) = \sum_a \frac{3}{8} m_a \mathbf{v}_a^4 e^{-i\mathbf{k}\cdot\mathbf{x}_a}. \tag{3.10}$$

By expanding the exponential up to the second order in the radiation momentum $\mathbf{k}$, we read off the contribution for the mass quadrupole moment:

$$\int d^3\mathbf{x} T^{00}_{Fig1} \left[\mathbf{x}^i \mathbf{x}^j\right]_{TF} = \sum_a \frac{3}{8} m_a \mathbf{v}_a^4 \left[\mathbf{x}_a^i \mathbf{x}_a^j\right]_{TF}. \tag{3.11}$$

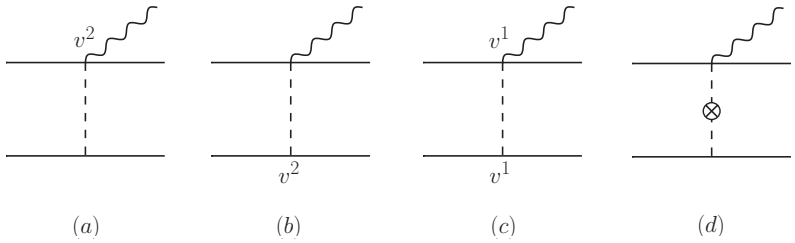

Figure 3.2: One-graviton exchange with external $\bar{h}^{00}$ momentum.

The diagrams that contain the exchange of one potential graviton are shown in Fig. 3.2 and are composed by the couplings between the source action terms(A.1- A.6) and also the propagator (A.15) and its correction (A.16). Notice that we need not separate out all of the various terms that arise in the Feynman rules into different orders in the PN expansion as is done in the appendix. We also calculated covariantly vertices, as is done when calculating in the Post-Minkowskian (PM) expansion (see e.g. [39]), and then expand in v, as a calculational check. However, for pedagogical purposes we have separated Feynman rules into give orders in the PN expansion. The results from Fig. 3.2 is given by

$$T^{00}_{Fig2a}(t,\mathbf{k}) = \sum_{a\neq b}\frac{5}{2}\frac{Gm_am_b}{r}\mathbf{v}_a^2 e^{-i\mathbf{k}\cdot\mathbf{x}_a}, \tag{3.12a}$$

$$T^{00}_{Fig2b}(t,\mathbf{k}) = \sum_{a\neq b}\frac{3}{2}\frac{Gm_am_b}{r}\mathbf{v}_b^2 e^{-i\mathbf{k}\cdot\mathbf{x}_a}, \tag{3.12b}$$

$$T^{00}_{Fig2c}(t,\mathbf{k}) = -\sum_{a\neq b}4\frac{Gm_am_b}{r}\mathbf{v}_a\cdot\mathbf{v}_b e^{-i\mathbf{k}\cdot\mathbf{x}_a}, \tag{3.12c}$$

$$T^{00}_{Fig2d}(t,\mathbf{k}) = \sum_{a\neq b}\frac{Gm_am_b}{2r}\left(-\mathbf{a}_b^i\mathbf{r}^i + \mathbf{v}_b^2 - (\mathbf{v}_b\cdot\mathbf{n})^2\right)e^{-i\mathbf{k}\cdot\mathbf{x}_a}. \tag{3.12d}$$

Leaving

$$\int d^3\mathbf{x}T^{00}_{Fig2a-2d}\left[\mathbf{x}^i\mathbf{x}^j\right]_{TF} = \sum_{a\neq b}\frac{Gm_am_b}{2r}\left[\left(5\mathbf{v}_a^2 + 4\mathbf{v}_b^2 - 8\mathbf{v}_a\cdot\mathbf{v}_b - \mathbf{a}_b\cdot\mathbf{r} - (\mathbf{v}_b\cdot\mathbf{n})^2\right)\mathbf{x}_a^i\mathbf{x}_a^j\right]_{TF}. \tag{3.13}$$

Note the implicit dependence on the indices a, b in the quantities $\mathbf{r} = \mathbf{x}_a - \mathbf{x}_b$, $r = |\mathbf{r}|$ and $\mathbf{n} = \frac{\mathbf{r}}{r}$ inside the sum.

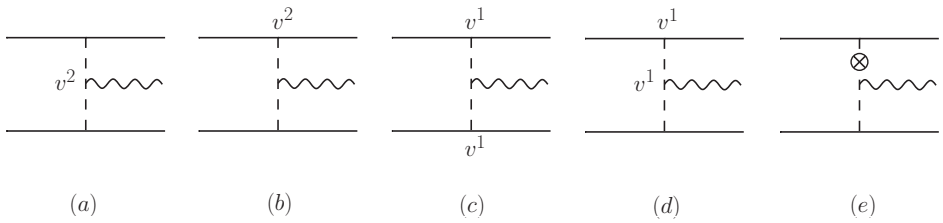

Figure 3.3: Diagrams with two potential gravitons coupled to $\bar{h}_{00}$.

The graphs in Fig. 3.3 are composed by the source terms (A.1- A.3) together with the vertices (A.17- A.21) and (A.16). Note that we multipole expand the denominators in $\mathbf{k}/\mathbf{q} \sim v$

$$\frac{1}{\mathbf{q}^2\left(\mathbf{q}+\mathbf{k}\right)^2} = \frac{1}{\mathbf{q}^4} - \frac{2\left(\mathbf{q}\cdot\mathbf{k}\right)}{\mathbf{q}^6} + \frac{4\left(\mathbf{q}\cdot\mathbf{k}\right)^2}{\mathbf{q}^8} + ..., \tag{3.14}$$

In calculating the contributions to the mass quadrupole sourced by the temporal components of the pseudotensor at 2PN, we are allowed to drop terms depending on $\mathbf{k}^2$ in the expansion of the denominator, since those terms contribute to the trace part of the mass quadrupole, which is removed in the definition of the STF moment. The results are organized in orders of the radiation momentum, as it is shown below:

$$\begin{aligned}
T^{00}_{Fig3a}\left(t,\mathbf{k}\right) = \sum_{a\neq b}\frac{Gm_am_b}{4r}e^{-i\mathbf{k}\cdot\mathbf{x}_a}\Big\{&2\left(\mathbf{v}^2+\mathbf{a}\cdot\mathbf{r}-\dot{r}^2\right)+5\mathbf{v}_a\cdot\mathbf{v}_b-5\mathbf{v}_a\cdot\mathbf{n}\mathbf{v}_b\cdot\mathbf{n}\\
&+i\mathbf{k}^i\left[\left(\mathbf{v}^2+\mathbf{a}\cdot\mathbf{r}-\dot{r}^2+\frac{5}{2}\mathbf{v}_a\cdot\mathbf{v}_b-\frac{5}{2}\mathbf{v}_a\cdot\mathbf{n}\mathbf{v}_b\cdot\mathbf{n}\right)\mathbf{r}^i\right.\\
&\left.+\left(\frac{1}{2}r\dot{r}+\frac{5}{2}\mathbf{v}_b\cdot\mathbf{r}\right)\mathbf{v}_b^i-\left(2r\dot{r}+\frac{5}{2}\mathbf{v}_b\cdot\mathbf{r}\right)\mathbf{v}_a^i-r^2\left(\mathbf{a}_a^i+\mathbf{a}_b^i\right)\right]\\
&+\frac{1}{6}\mathbf{k}^i\mathbf{k}^j\left[-\left(2\mathbf{v}^2+5\mathbf{v}_a\cdot\mathbf{v}_b-2\dot{r}^2-5\mathbf{v}_a\cdot\mathbf{n}\mathbf{v}_b\cdot\mathbf{n}+2\mathbf{a}\cdot\mathbf{r}\right)\mathbf{r}^i\mathbf{r}^j\right.\\
&+\left(4\mathbf{v}_a\cdot\mathbf{r}+\mathbf{v}_b\cdot\mathbf{r}\right)\mathbf{v}_a^i\mathbf{r}^j-\left(2\mathbf{v}_a\cdot\mathbf{r}+8\mathbf{v}_b\cdot\mathbf{r}\right)\mathbf{v}_b^i\mathbf{r}^j\\
&\left.+r^2\left(-4\mathbf{v}^i\mathbf{v}^j-7\mathbf{v}_a^i\mathbf{v}_b^j+2\mathbf{a}_a^i\mathbf{r}^j+4\mathbf{a}_b^i\mathbf{r}^j\right)\right]\Big\}+O\left(\mathbf{k}^3\right)+...,
\end{aligned} \tag{3.15}$$

$$T^{00}_{Fig3b}\left(t,\mathbf{k}\right) = -\sum_{a\neq b}\frac{Gm_am_b}{r}e^{-i\mathbf{k}\cdot\mathbf{x}_a}\left[\frac{7}{4}\mathbf{v}_b^2+\frac{3}{4}\mathbf{v}_a^2-\frac{i}{2}\mathbf{k}^i\mathbf{v}_b^2\mathbf{r}^i\right.$$

$$+\frac{1}{2}\mathbf{k}^i\mathbf{k}^j\left(\frac{1}{2}\mathbf{v}_b^2\mathbf{r}^i\mathbf{r}^j+2\mathbf{r}^2\mathbf{v}_b^i\mathbf{v}_b^j\right)\Big]+O\left(\mathbf{k}^3\right)+..., \tag{3.16}$$

$$T^{00}_{Fig3c}\left(t,\mathbf{k}\right)=\sum_{a\neq b}\frac{2Gm_am_b}{r}e^{-i\mathbf{k}\cdot\mathbf{x}_a}\left(2\mathbf{v}_a\cdot\mathbf{v}_b+\mathbf{k}^i\mathbf{k}^j\mathbf{r}^2\mathbf{v}_a^i\mathbf{v}_b^j\right)+O\left(\mathbf{k}^3\right)+..., \tag{3.17}$$

$$\begin{aligned}T^{00}_{Fig3d}\left(t,\mathbf{k}\right)=-\sum_{a\neq b}\frac{2Gm_am_b}{r}e^{-i\mathbf{k}\cdot\mathbf{x}_a}\Big\{&-\frac{i}{2}\mathbf{k}^i\left[2\mathbf{r}^2\mathbf{a}_a^i+2\mathbf{v}_a^i\left(\mathbf{v}_b\cdot\mathbf{r}+\mathbf{v}_a\cdot\mathbf{r}\right)\right]\\&-\frac{1}{2}\mathbf{k}^i\mathbf{k}^j\left[\mathbf{r}^2\left(\mathbf{v}_a^i\mathbf{v}_a^j-\mathbf{v}_a^i\mathbf{v}_b^i-\mathbf{r}^j\mathbf{a}_a^i\right)-\mathbf{v}_a^i\mathbf{r}^j\left(\mathbf{v}_a\cdot\mathbf{r}+\mathbf{v}_b\cdot\mathbf{r}\right)\right]\Big\}+O\left(\mathbf{k}^3\right)+...,\end{aligned} \tag{3.18}$$

$$\begin{aligned}T^{00}_{Fig3e}\left(t,\mathbf{k}\right)=-\sum_{a\neq b}\frac{Gm_am_b}{4r}e^{-i\mathbf{k}\cdot\mathbf{x}_a}\Big\{&6\left(-\mathbf{a}_b\cdot\mathbf{r}+\mathbf{v}_b^2-\left(\mathbf{v}_b\cdot\mathbf{n}\right)^2\right)\\&-\frac{3i}{2}\mathbf{k}^i\left[\left(\mathbf{a}_b\cdot\mathbf{r}-\mathbf{v}_b^2+\left(\mathbf{v}_b\cdot\mathbf{n}\right)^2\right)\mathbf{r}^i-2\mathbf{v}_b\cdot\mathbf{r}\mathbf{v}_b^i+\mathbf{r}^2\mathbf{a}_b^i\right]\\&-\frac{1}{2}\mathbf{k}^i\mathbf{k}^j\left[\left(-\mathbf{a}_b\cdot\mathbf{r}+\mathbf{v}_b^2-\left(\mathbf{v}_b\cdot\mathbf{n}\right)^2\right)\mathbf{r}^i\mathbf{r}^j+4\mathbf{v}_b\cdot\mathbf{r}\mathbf{v}_b^i\mathbf{r}^j\right.\\&\left.-2\mathbf{r}^2\mathbf{a}_b^i\mathbf{r}^j+2\mathbf{r}^2\mathbf{v}_b^i\mathbf{v}_b^j\right]\Big\}+O\left(\mathbf{k}^3\right)+...\cdot\end{aligned} \tag{3.19}$$

Together, these quantities provide us with the following contribution,

$$\begin{aligned}\int d^3\mathbf{x}T^{00}_{Fig3a-3e}\left[\mathbf{x}^i\mathbf{x}^j\right]_{TF}=\sum_{a\neq b}\frac{Gm_am_b}{12r}\Big[&\left(-2\mathbf{v}_a^2-35\mathbf{v}_b^2+26\mathbf{v}_a\cdot\mathbf{v}_b-10\mathbf{v}_a\cdot\mathbf{n}\mathbf{v}_b\cdot\mathbf{n}\right.\\&\left.+3\left(\mathbf{v}_a\cdot\mathbf{n}\right)^2+12\left(\mathbf{v}_b\cdot\mathbf{n}\right)^2-4\dot{r}^2+\mathbf{a}_a\cdot\mathbf{r}+8\mathbf{a}_b\cdot\mathbf{r}\right)\mathbf{x}_a^i\mathbf{x}_a^j\\&+\left(\mathbf{v}_a^2+\mathbf{v}_a\cdot\mathbf{v}_b-5\mathbf{v}_a\cdot\mathbf{n}\mathbf{v}_b\cdot\mathbf{n}+3\left(\mathbf{v}_a\cdot\mathbf{n}\right)^2-2\dot{r}^2+\mathbf{a}_a\cdot\mathbf{r}\right)\mathbf{x}_a^i\mathbf{x}_b^j\\&+\left(\mathbf{v}_a\cdot\mathbf{r}+\mathbf{v}_b\cdot\mathbf{r}\right)\left(-20\mathbf{v}_a^i\mathbf{x}_a^j+26\mathbf{v}_a^i\mathbf{x}_b^j\right)\\&+\mathbf{r}^2\left(2\mathbf{v}_a^i\mathbf{v}_a^j-\mathbf{v}_a^i\mathbf{v}_b^j-22\mathbf{a}_a^i\mathbf{x}_a^j-23\mathbf{a}_a^i\mathbf{x}_b^j\right)\Big]_{STF}.\end{aligned} \tag{3.20}$$

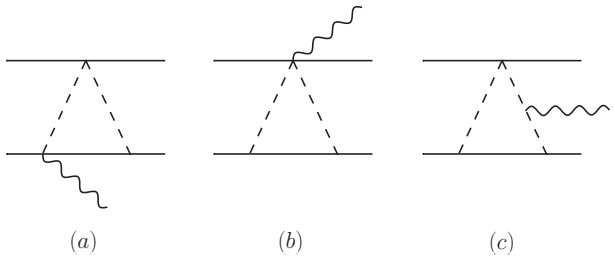

Figure 3.4: Two-potential-graviton exchange with external $\bar{h}^{00}$ momentum.

Contributions from Fig. 3.4 are composed of the source terms (A.1), (A.4), (A.8) and (A.9) and yield

$$T^{00}_{Fig4a}(t,\mathbf{k}) = \sum_{a\neq b} \frac{G^2 m_a^2 m_b}{r^2} e^{-i\mathbf{k}\cdot\mathbf{x}_a}, \tag{3.21a}$$

$$T^{00}_{Fig4b}(t,\mathbf{k}) = \sum_{a\neq b} \frac{3G^2 m_a m_b^2}{2r^2} e^{-i\mathbf{k}\cdot\mathbf{x}_a}, \tag{3.21b}$$

$$T^{00}_{Fig4c}(t,\mathbf{k}) = -\sum_{a\neq b} \frac{3G^2 m_a m_b m}{2r^2} e^{-i\mathbf{k}\cdot\mathbf{x}_a}, \tag{3.21c}$$

which gives us

$$\int d^3\mathbf{x} T^{00}_{Fig4a-4c} \left[\mathbf{x}^i\mathbf{x}^j\right]_{TF} = -\sum_{a\neq b} \frac{G^2 m_a^2 m_b}{2r^2} \left[\mathbf{x}_a^i\mathbf{x}_a^j\right]_{TF}. \tag{3.22}$$

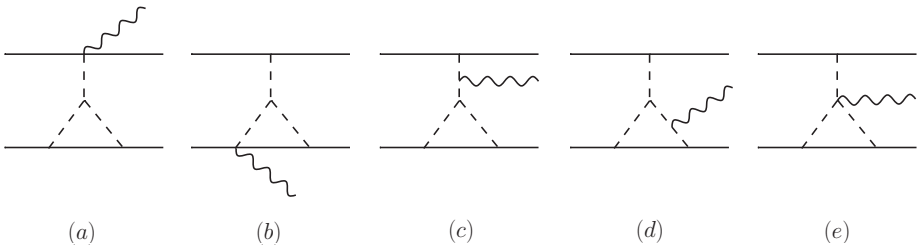

Figure 3.5: Three-potential-graviton exchange with external $\bar{h}^{00}$ momentum.

The diagrams illustrated in Fig. 3.5, are composed of the three-potential-graviton vertices (A.28- A.30) as well as the three-potential-one-radiation-graviton vertex (A.32- A.33) in composition with (A.1) and (A.4) contribute to T^{00}_{2PN}. These diagrams give:

$$T^{00}_{Fig5a}(t,\mathbf{k}) = -\sum_{a\neq b}\frac{G^2 m_a m_b^2}{r^2}e^{-i\mathbf{k}\cdot\mathbf{x}_a}, \tag{3.23a}$$

$$T^{00}_{Fig5b}(t,\mathbf{k}) = -\sum_{a\neq b}\frac{2G^2 m_a^2 m_b}{r^2}e^{-i\mathbf{k}\cdot\mathbf{x}_a}, \tag{3.23b}$$

$$T^{00}_{Fig5c}(t,\mathbf{k}) = -\sum_{a\neq b}\frac{G^2 m_a^2 m_b}{r^2}e^{-i\mathbf{k}\cdot\mathbf{x}_a}\left(\frac{1}{2}-\frac{7}{2}i\mathbf{k}^i\mathbf{r}^i+\frac{5}{3}\mathbf{k}^i\mathbf{k}^j\mathbf{r}^i\mathbf{r}^j\right)+O\left(\mathbf{k}^3\right)+..., \tag{3.23c}$$

$$T^{00}_{Fig5d}(t,\mathbf{k}) = \sum_{a\neq b}\frac{G^2 m_a^2 m_b}{r^2}e^{-i\mathbf{k}\cdot\mathbf{x}_a}\left(5-2i\mathbf{k}^i\mathbf{r}^i+\frac{2}{3}\mathbf{k}^i\mathbf{k}^j\mathbf{r}^i\mathbf{r}^j\right)+O\left(\mathbf{k}^3\right)+..., \tag{3.23d}$$

$$T^{00}_{Fig5e}(t,\mathbf{k}) = -\sum_{a\neq b}\frac{G^2 m_a m_b^2}{2r^2}e^{-i\mathbf{k}\cdot\mathbf{x}_a}. \tag{3.23e}$$

Keeping terms to second order in the radiation momentum we have

$$\int d^3\mathbf{x}T^{00}_{Fig5a-5e}\left[\mathbf{x}^i\mathbf{x}^j\right]_{TF} = \sum_{a\neq b}\frac{G^2 m_a m_b}{r^2}\left[\frac{3}{2}\left(m_a-m_b\right)\mathbf{x}_a^i\mathbf{x}_a^j - m_a\mathbf{x}_a^i\mathbf{x}_a^j + 2m_a\mathbf{x}_b^i\mathbf{x}_b^j\right]_{TF}. \tag{3.24}$$

Summing the contributions (3.11), (3.13), (3.20), (3.22) and (3.24), the total contribution of T^{00}_{2PN} to the mass quadrupole is

$$\begin{aligned}
&\int d^3\mathbf{x}T^{00}_{2PN}\left[\mathbf{x}^i\mathbf{x}^j\right]_{TF}\\
&=\sum_a\frac{3}{8}m_a\mathbf{v}_a^4\left[\mathbf{x}_a^i\mathbf{x}_a^j\right]_{TF}+\sum_{a\neq b}\frac{Gm_am_b}{12r}\left[\left(28\mathbf{v}_a^2-11\mathbf{v}_b^2-22\mathbf{v}_a\cdot\mathbf{v}_b-10\mathbf{v}_a\cdot\mathbf{n}\mathbf{v}_b\cdot\mathbf{n}\right.\right.\\
&\quad+3\left(\mathbf{v}_a\cdot\mathbf{n}\right)^2+6\left(\mathbf{v}_b\cdot\mathbf{n}\right)^2-4\dot{r}^2+\mathbf{a}_a\cdot\mathbf{r}+2\mathbf{a}_b\cdot\mathbf{r}+12\frac{Gm_a}{r}+6\frac{Gm_b}{r}\Big)\mathbf{x}_a^i\mathbf{x}_a^j\\
&\quad+\left(\mathbf{v}_a^2+\mathbf{v}_a\cdot\mathbf{v}_b-5\mathbf{v}_a\cdot\mathbf{n}\mathbf{v}_b\cdot\mathbf{n}+3\left(\mathbf{v}_a\cdot\mathbf{n}\right)^2-2\dot{r}^2+\mathbf{a}_a\cdot\mathbf{r}-12\frac{Gm_a}{r}\right)\mathbf{x}_a^i\mathbf{x}_b^j\\
&\quad\left.+\left(\mathbf{v}_a\cdot\mathbf{r}+\mathbf{v}_b\cdot\mathbf{r}\right)\left(-20\mathbf{v}_a^i\mathbf{x}_a^j+26\mathbf{v}_a^i\mathbf{x}_b^j\right)+\mathbf{r}^2\left(2\mathbf{v}_a^i\mathbf{v}_a^j-\mathbf{v}_a^i\mathbf{v}_b^j-22\mathbf{a}_a^i\mathbf{x}_a^j-23\mathbf{a}_a^i\mathbf{x}_b^j\right)\right]_{STF}.
\end{aligned} \tag{3.25}$$

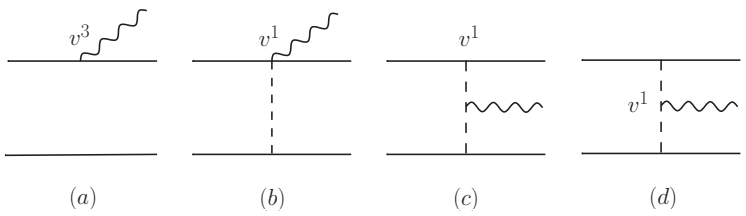

Figure 3.6: All diagrams that contribute to T^{0i}_{1PN}.

3.2.2 1PN correction to T^{0i}

The leading order T^{0i} component was obtained in [20] is

$$T^{0i}_{0PN}(t,\mathbf{k}) = \sum_a m_a \mathbf{v}^i_a e^{-i\mathbf{k}\cdot\mathbf{x}_a}. \tag{3.26}$$

The 1PN correction enter at v^3 and are shown in Fig. 3.6.

To extract the T^{0i} contributions to the mass quadrupole moment, which is the third term in (3.6), the expansion of the denominator of vertices in Fig. 3.6c-3.6d has to be carried out to third order. In addition, $\mathbf{k}^2$ terms can not be dropped, since they contribute terms that cannot be included in the trace part of the quadrupole.

Comparing the diagrams illustrated in Fig. 3.6, which are composed of (A.1, A.2, A.10, A.11) together with (A.15), (A.22) and (A.23) we find

$$T^{0l}_{Fig6a}(t,\mathbf{k}) = \sum_a \frac{m_a}{2}\mathbf{v}^l_a \mathbf{v}^2_a e^{-i\mathbf{k}\cdot\mathbf{x}_a}, \tag{3.27}$$

$$T^{0l}_{Fig6b}(t,\mathbf{k}) = \sum_{a\neq b} \frac{Gm_a m_b}{r}\mathbf{v}^l_a e^{-i\mathbf{k}\cdot\mathbf{x}_a}, \tag{3.28}$$

$$\begin{aligned} T^{0l}_{Fig6c}(t,\mathbf{k}) = \sum_{a\neq b} \frac{Gm_a m_b}{r} e^{-i\mathbf{k}\cdot\mathbf{x}_a} \Big[& -2\mathbf{v}^l_a + 2i\mathbf{k}^i \left(\mathbf{v}^i_a \mathbf{r}^l - \mathbf{r}^i \mathbf{v}^l_a\right) + \mathbf{k}^i\mathbf{k}^j \left(\mathbf{r}^i\mathbf{r}^j\mathbf{v}^l_a - \mathbf{v}^i_a\mathbf{r}^j\mathbf{r}^l\right) \\ & + \frac{i}{6}\mathbf{k}^i\mathbf{k}^j\mathbf{k}^k \left(\mathbf{r}^2\delta^{ij}\mathbf{v}^k_a\mathbf{r}^l - \mathbf{r}^2\delta^{il}\mathbf{v}^j_a\mathbf{r}^k - 2\mathbf{v}^i_a\mathbf{r}^j\mathbf{r}^k\mathbf{r}^l + 2\mathbf{r}^i\mathbf{r}^j\mathbf{r}^k\mathbf{v}^l_a\right)\Big] + O\left(\mathbf{k}^4\right) + ..., \end{aligned} \tag{3.29}$$

$$
\begin{aligned}
T^{0l}_{Fig6d}(t,\mathbf{k}) = \sum_{a\neq b}\frac{Gm_am_b}{4r}e^{-i\mathbf{k}\cdot\mathbf{x}_a}\Bigg\{&\mathbf{v}_a^l+\mathbf{v}_b^l-\frac{1}{r^2}(\mathbf{v}_a+\mathbf{v}_b)\cdot\mathbf{r}\mathbf{r}^l\\
&-\frac{i}{2}\mathbf{k}^i\left(3r\dot{r}\delta^{il}-\mathbf{r}^i\left(\mathbf{v}_a^l+\mathbf{v}_b^l\right)+\mathbf{v}^i\mathbf{r}^l+\frac{1}{r^2}(\mathbf{v}_a+\mathbf{v}_b)\cdot\mathbf{r}\mathbf{r}^i\mathbf{r}^l\right)\\
&+\frac{1}{6}\mathbf{k}^i\mathbf{k}^j\Big[-5\mathbf{r}^2\left(\mathbf{v}_a^i+\mathbf{v}_b^i\right)\delta^{jl}+(4\mathbf{v}_a\cdot\mathbf{r}-5\mathbf{v}_b\cdot\mathbf{r})\,\mathbf{r}^i\delta^{jl}+\left(\mathbf{v}_a^i-2\mathbf{v}_b^i\right)\mathbf{r}^j\mathbf{r}^l\\
&+\left(\mathbf{v}_a^l+\mathbf{v}_b^l\right)\left(\frac{1}{2}\delta^{ij}\mathbf{r}^2-\mathbf{r}^i\mathbf{r}^j\right)+(\mathbf{v}_a\cdot\mathbf{r}+\mathbf{v}_b\cdot\mathbf{r})\left(\frac{1}{2}\delta^{ij}\mathbf{r}^l+\frac{1}{r^2}\mathbf{r}^i\mathbf{r}^j\mathbf{r}^l\right)\Big]\\
&-\frac{i}{24}\mathbf{k}^i\mathbf{k}^j\mathbf{k}^k\Big[\delta^{kl}\left(6\mathbf{r}^2\mathbf{v}_a^i\mathbf{r}^j+14\mathbf{r}^2\mathbf{v}_b^i\mathbf{r}^j-5\mathbf{v}_a\cdot\mathbf{r}\mathbf{r}^i\mathbf{r}^j+7\mathbf{v}_b\cdot\mathbf{r}\mathbf{r}^i\mathbf{r}^j\right)\\
&+\delta^{ij}\mathbf{r}^2\left(3\delta^{kl}\mathbf{v}_a\cdot\mathbf{r}-3\delta^{kl}\mathbf{v}_b\cdot\mathbf{r}-\mathbf{r}^k\mathbf{v}_b^l-\mathbf{r}^k\mathbf{v}_a^l+\mathbf{v}_a^k\mathbf{r}^l-\mathbf{v}_b^k\mathbf{r}^l\right)\\
&-\delta^{ij}(\mathbf{v}_a\cdot\mathbf{r}+\mathbf{v}_b\cdot\mathbf{r})\,\mathbf{r}^k\mathbf{r}^l+\mathbf{r}^i\mathbf{r}^j\mathbf{r}^k\left(\mathbf{v}_a^l+\mathbf{v}_b^l\right)+\left(3\mathbf{v}_b^i-\mathbf{v}_a^i\right)\mathbf{r}^j\mathbf{r}^k\mathbf{r}^l\\
&-\frac{1}{r^2}(\mathbf{v}_a+\mathbf{v}_b)\cdot\mathbf{r}\mathbf{r}^i\mathbf{r}^j\mathbf{r}^k\mathbf{r}^l\Big]\Bigg\}+O\left(\mathbf{k}^4\right)+...\cdot
\end{aligned}
\tag{3.30}
$$

Expanding the exponentials up to the third order in the radiation momentum, we get

$$
\begin{aligned}
&\int d^3\mathbf{x}\partial_0 T^{0l}_{1PN}\mathbf{x}^l\left[\mathbf{x}^i\mathbf{x}^j\right]_{TF}\\
&=\sum_a\frac{d}{dt}\left[\frac{1}{2}m_a\mathbf{v}_a^2\mathbf{v}_a\cdot\mathbf{x}_a\mathbf{x}_a^i\mathbf{x}_a^j\right]_{TF}\\
&\quad+\sum_{a\neq b}\frac{d}{dt}\Bigg\{\frac{Gm_am_b}{12r}\Big[\left(8\mathbf{r}^2-20\mathbf{r}\cdot\mathbf{x}_b\right)\mathbf{v}_a^i\mathbf{x}_a^j+\left(20\mathbf{r}^2-22\mathbf{r}\cdot\mathbf{x}_b\right)\mathbf{v}_a^i\mathbf{x}_b^j\\
&\quad+\left(22\mathbf{v}_a\cdot\mathbf{x}_a-30\mathbf{v}_b\cdot\mathbf{x}_a-8\mathbf{v}_a\cdot\mathbf{x}_b+8\mathbf{v}_b\cdot\mathbf{x}_b-\frac{2}{r^2}(\mathbf{v}_a+\mathbf{v}_b)\cdot\mathbf{r}\mathbf{r}\cdot\mathbf{x}_b\right)\mathbf{x}_a^i\mathbf{x}_a^j\\
&\quad+\left(9\mathbf{v}_a\cdot\mathbf{x}_a-7\mathbf{v}_a\cdot\mathbf{x}_b-\frac{1}{r^2}(\mathbf{v}_a+\mathbf{v}_b)\cdot\mathbf{r}\mathbf{r}\cdot\mathbf{x}_b\right)\mathbf{x}_a^i\mathbf{x}_b^j\Big]\Bigg\}_{STF}.
\end{aligned}
\tag{3.31}
$$

3.2.3 1PN correction to T^{ii}

The leading order T^{ii} component obtained in [20] has the form

$$
T^{ii}_{0PN}(t,\mathbf{k})=\left(\sum_a m_a\mathbf{v}_a^2-\sum_{a\neq b}\frac{Gm_am_b}{2r}+O(\mathbf{k})+...\right)e^{-i\mathbf{k}\cdot\mathbf{x}_a}.
\tag{3.32}
$$

Notice that, while T^{0i}_{0PN} in (3.26) is down by v^1 relative to T^{00}_{0PN} in (3.8), the leading order spatial component (3.32) is down by v^2 compared to T^{00}_{0PN}, this fixes the PN hierarchy among the components T^{00}, T^{i0} and T^{ij} of the pseudotensor.

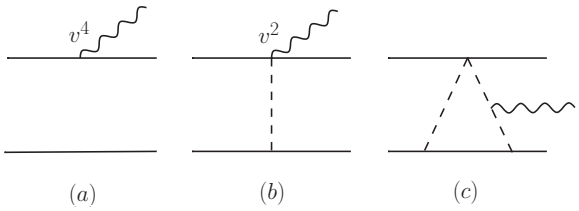

Figure 3.7: Diagrams with $\bar{h}^{ii}$ external momentum.

To obtain T^{ii}_{1PN} as well as its contributions to I^{ij}_{2PN} we have to compute all diagrams that enter at v^4 with one $\bar{h}^{ii}$ external momentum. To compute the spatial component of the pseudotensor and to extract its contribution to the mass quadrupole moment we have to carry out the expansions up to the second order in the radiation momentum. $\mathbf{k}^2$ may be dropped as in section 3.2.1.

The diagrams illustrated in Fig. 3.7, involve (A.1, A.8, A.12, A.13), (A.15) and (A.24) give

$$T^{ll}_{Fig7a}(t,\mathbf{k}) = \sum_a \frac{m_a}{2}\mathbf{v}_a^4 e^{-i\mathbf{k}\cdot\mathbf{x}_a}, \tag{3.33a}$$

$$T^{ll}_{Fig7b}(t,\mathbf{k}) = \sum_{a\neq b} \frac{Gm_am_b}{r}\mathbf{v}_a^2 e^{-i\mathbf{k}\cdot\mathbf{x}_a}, \tag{3.33b}$$

$$T^{ll}_{Fig7c}(t,\mathbf{k}) = -\sum_{a\neq b} \frac{G^2m_am_bm}{2r^2} e^{-i\mathbf{k}\cdot\mathbf{x}_a}. \tag{3.33c}$$

It is straightforward to extract the contribution for the mass quadrupole moment by expanding the exponentials up to the second order in the radiation momentum,

$$\int d^3\mathbf{x} T^{ll}_{Fig7a-7c}\left[\mathbf{x}^i\mathbf{x}^j\right]_{TF} = \sum_a \frac{m_a}{2}\mathbf{v}_a^4\left[\mathbf{x}_a^i\mathbf{x}_a^j\right]_{TF} + \sum_{a\neq b}\frac{Gm_am_b}{r}\left(\mathbf{v}_a^2 - \frac{Gm}{2r}\right)\left[\mathbf{x}_a^i\mathbf{x}_a^j\right]_{TF}. \tag{3.34}$$

The computation of T^{ii}_{1PN} follows from the diagrams shown in Fig. 3.8 which involve (A.1- A.3) and (A.15, A.16, A.24- A.27),

$$T^{ll}_{Fig8a}(t,\mathbf{k}) = \sum_{a\neq b}\frac{3Gm_am_b}{4r}e^{-i\mathbf{k}\cdot\mathbf{x}_a}\left\{2\mathbf{v}^2 + \mathbf{v}_a\cdot\mathbf{v}_b - 2\dot{r}^2 - \frac{1}{r^2}\mathbf{v}_a\cdot\mathbf{r}\mathbf{v}_b\cdot\mathbf{r} + 2\mathbf{a}\cdot\mathbf{r}\right.$$

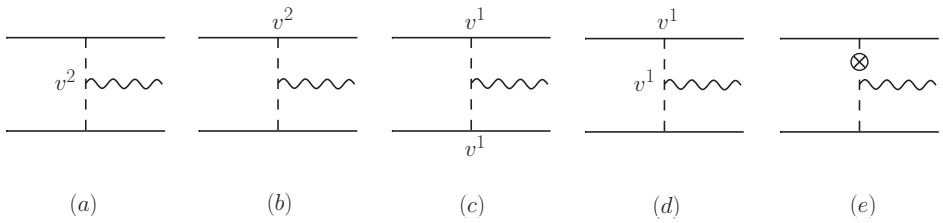

Figure 3.8: One potential graviton exchange with $\bar{h}^{ii}$ external momentum.

$$
\begin{aligned}
&+\frac{i}{2}\mathbf{k}^i\left[\left(2\mathbf{v}^2+\mathbf{v}_a\cdot\mathbf{v}_b-2\dot{r}^2-\frac{1}{r^2}\mathbf{v}_a\cdot\mathbf{r}\mathbf{v}_b\cdot\mathbf{r}+2\mathbf{a}\cdot\mathbf{r}\right)\mathbf{r}^i\right.\\
&\left.+\mathbf{v}_b^i\left(4\mathbf{v}_b\cdot\mathbf{r}-3\mathbf{v}_a\cdot\mathbf{r}\right)+\mathbf{v}_a^i\left(3\mathbf{v}_b\cdot\mathbf{r}-4\mathbf{v}_a\cdot\mathbf{r}\right)-2r^2\left(\mathbf{a}_a^i+\mathbf{a}_b^i\right)\right]\\
&+\frac{1}{6}\mathbf{k}^i\mathbf{k}^j\left[\left(-2\mathbf{v}^2-\mathbf{v}_a\cdot\mathbf{v}_b-2\mathbf{a}\cdot\mathbf{r}+2\dot{r}^2+\frac{1}{r^2}\mathbf{v}_a\cdot\mathbf{r}\mathbf{v}_b\cdot\mathbf{r}\right)\mathbf{r}^i\mathbf{r}^j\right.\\
&+\left(6\mathbf{v}_a\cdot\mathbf{r}-8\mathbf{v}_b\cdot\mathbf{r}\right)\mathbf{v}_b^i\mathbf{r}^j+\left(4\mathbf{v}_a\cdot\mathbf{r}-3\mathbf{v}_b\cdot\mathbf{r}\right)\mathbf{v}_a^i\mathbf{r}^j\\
&\left.+r^2\left(-4\mathbf{v}_a^i\mathbf{v}_a^j-3\mathbf{v}_a^i\mathbf{v}_b^j-4\mathbf{v}_b^i\mathbf{v}_b^j-4\mathbf{a}^i\mathbf{r}^j+6\mathbf{a}_a^i\mathbf{r}^j\right)\right]\Big\}+O\left(\mathbf{k}^3\right)+..., \qquad (3.35a)
\end{aligned}
$$

$$
\begin{aligned}
T^{ll}_{Fig8b}\left(t,\mathbf{k}\right)=&\sum_{a\neq b}\frac{Gm_am_b}{r}e^{-i\mathbf{k}\cdot\mathbf{x}_a}\left\{\frac{1}{4}\left(\mathbf{v}_a^2+\mathbf{v}_b^2\right)-i\mathbf{v}_a^2\mathbf{k}^i\mathbf{r}^i-\mathbf{k}^i\mathbf{k}^j\left(\mathbf{r}^2\mathbf{v}_a^i\mathbf{v}_a^j-\frac{1}{2}\mathbf{v}_a^2\mathbf{r}^i\mathbf{r}^j\right)\right\}\\
&+O\left(\mathbf{k}^3\right)+..., \qquad (3.36)
\end{aligned}
$$

$$
\begin{aligned}
T^{ll}_{Fig8c}\left(t,\mathbf{k}\right)=\sum_{a\neq b}\frac{Gm_am_b}{2r}e^{-i\mathbf{k}\cdot\mathbf{x}_a}&\left[-4\mathbf{v}_a\cdot\mathbf{v}_b-i\mathbf{k}^i\left(2\mathbf{v}_a\cdot\mathbf{v}_b\mathbf{r}^i+4\mathbf{v}_a\cdot\mathbf{r}\mathbf{v}_b^i-4\mathbf{v}_b\cdot\mathbf{r}\mathbf{v}_a^i\right)\right.\\
&\left.+\mathbf{k}^i\mathbf{k}^j\left(2\mathbf{r}^2\mathbf{v}_a^i\mathbf{v}_b^j+\mathbf{v}_a\cdot\mathbf{v}_b\mathbf{r}^i\mathbf{r}^j-2\mathbf{v}_b\cdot\mathbf{r}\mathbf{v}_a^i\mathbf{r}^j+2\mathbf{v}_a\cdot\mathbf{r}\mathbf{v}_b^i\mathbf{r}^j\right)\right]+O\left(\mathbf{k}^3\right)+..., \qquad (3.37)
\end{aligned}
$$

$$
\begin{aligned}
T^{ll}_{Fig8d}\left(t,\mathbf{k}\right)=\sum_{a\neq b}\frac{Gm_am_b}{r}e^{-i\mathbf{k}\cdot\mathbf{x_a}}&\left\{-4\left(\mathbf{v}\cdot\mathbf{v}_a+\mathbf{a}_a\cdot\mathbf{r}-\frac{1}{r^2}\mathbf{v}\cdot\mathbf{r}\mathbf{v}_a\cdot\mathbf{r}\right)\right.\\
&-2i\mathbf{k}^i\left[\mathbf{r}^i\left(\mathbf{v}\cdot\mathbf{v}_a+\mathbf{a}_a\cdot\mathbf{r}-\frac{\dot{r}}{r}\mathbf{v}_a\cdot\mathbf{r}\right)+\mathbf{v}_a\cdot\mathbf{r}\left(\mathbf{v}^i-2\mathbf{v}_a^i\right)\right]\\
&+\frac{1}{3}\mathbf{k}^i\mathbf{k}^j\left[\mathbf{r}^2\left(\mathbf{v}^i\mathbf{v}_a^j+\mathbf{a}_a\mathbf{r}^i\right)+2\mathbf{r}^i\mathbf{r}^j\left(\mathbf{v}\cdot\mathbf{v}_a+\mathbf{a}_a\cdot\mathbf{r}\right)\right.\\
&\left.\left.+r\dot{r}\mathbf{v}_a^i\mathbf{r}^j+2\mathbf{v}_a\cdot\mathbf{r}\left(2\mathbf{v}^i\mathbf{r}^j-3\mathbf{v}_a^i\mathbf{r}^j\right)-2\frac{\dot{r}}{r}\mathbf{v}_a\cdot\mathbf{r}\mathbf{r}^i\mathbf{r}^j\right]\right\}+O\left(\mathbf{k}^3\right)+..., \qquad (3.38)
\end{aligned}
$$

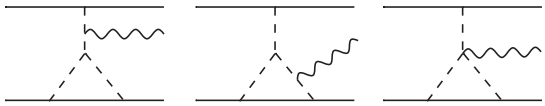

(a) (b) (d)

Figure 3.9: Three-potential-graviton exchange with $\bar{h}^{ii}$ external momentum.

$$
\begin{aligned}
T^{ll}_{Fig8e}(t,\mathbf{k}) = -\sum_{a\neq b}\frac{Gm_am_b}{4r}e^{-i\mathbf{k}\cdot\mathbf{x}_a}\Big\{&2\left(-\mathbf{a}_b\cdot\mathbf{r}+\mathbf{v}_b^2-(\mathbf{v}_b\cdot\mathbf{n})^2\right)\\
&-\frac{i}{2}\mathbf{k}^i\left[\left(\mathbf{a}_b\cdot\mathbf{r}-\mathbf{v}_b^2+(\mathbf{v}_b\cdot\mathbf{n})^2\right)\mathbf{r}^i-2\mathbf{v}_b\cdot\mathbf{r}\mathbf{v}_b^i+\mathbf{r}^2\mathbf{a}_b^i\right]\\
&+\frac{i^2}{6}\mathbf{k}^i\mathbf{k}^j\left[\left(-\mathbf{a}_b\cdot\mathbf{r}+\mathbf{v}_b^2-(\mathbf{v}_b\cdot\mathbf{n})^2\right)\mathbf{r}^i\mathbf{r}^j+4\mathbf{v}_b\cdot\mathbf{r}\mathbf{v}_b^i\mathbf{r}^j-2\mathbf{r}^2\mathbf{a}_b^i\mathbf{r}^j+2\mathbf{r}^2\mathbf{v}_b^i\mathbf{v}_b^j\right]\Big\}\\
&+O\left(\mathbf{k}^3\right)+...,
\end{aligned}
\tag{3.39}
$$

which provides us with

$$
\begin{aligned}
\int d^3\mathbf{x}T^{ll}_{Fig8a-8e}\left[\mathbf{x}^i\mathbf{x}^j\right]_{TF} = \sum_{a\neq b}\frac{Gm_am_b}{12r}\Big\{&\left(10\mathbf{v}_a^2-17\mathbf{v}_b^2-10\mathbf{v}_a\cdot\mathbf{v}_b\right.\\
&\left.+5\left(\mathbf{v}_a\cdot\mathbf{n}\right)^2+2\mathbf{v}_a\cdot\mathbf{n}\mathbf{v}_b\cdot\mathbf{n}-8\left(\mathbf{v}_b\cdot\mathbf{n}\right)^2-5\mathbf{a}_a\cdot\mathbf{r}+8\mathbf{a}_b\cdot\mathbf{r}\right)\mathbf{x}_a^i\mathbf{x}_a^j\\
&+\left(-5\mathbf{v}_a^2+7\mathbf{v}_a\cdot\mathbf{v}_b+5\left(\mathbf{v}_a\cdot\mathbf{n}\right)^2-7\mathbf{v}_a\cdot\mathbf{n}\mathbf{v}_b\cdot\mathbf{n}-5\mathbf{a}_a\cdot\mathbf{r}\right)\mathbf{x}_a^i\mathbf{x}_b^j\\
&+\left(4\mathbf{v}_a\cdot\mathbf{r}-44\mathbf{v}_b\cdot\mathbf{r}\right)\mathbf{v}_a^i\mathbf{x}_a^j+\left(14\mathbf{v}_a\cdot\mathbf{r}-58\mathbf{v}_b\cdot\mathbf{r}\right)\mathbf{v}_a^i\mathbf{x}_b^j\\
&+r^2\left(38\mathbf{v}_a^i\mathbf{v}_a^j-7\mathbf{v}_a^i\mathbf{v}_b^j+14\mathbf{a}_a^i\mathbf{x}_a^j+19\mathbf{a}_a^i\mathbf{x}_b^j\right)\Big\}_{STF}.
\end{aligned}
\tag{3.40}
$$

Finally, the diagrams containing a three-potential-graviton exchange shown in Fig. 3.9 which involve (A.1), (A.31) and (A.34) give

$$
T^{ll}_{Fig9a}(t,\mathbf{k}) = \sum_{a\neq b}\frac{G^2m_a^2m_b}{r^2}e^{-i\mathbf{k}\cdot\mathbf{x}_a}\left(-\frac{5}{2}+\frac{7}{2}i\mathbf{k}^i\mathbf{r}^i-\frac{4}{3}\mathbf{k}^i\mathbf{k}^j\mathbf{r}^i\mathbf{r}^j\right)+O\left(\mathbf{k}^3\right)+... \tag{3.41a}
$$

$$
T^{ll}_{Fig9b}(t,\mathbf{k}) = \sum_{a\neq b}\frac{G^2m_a^2m_b}{r^2}e^{-i\mathbf{k}\cdot\mathbf{x}_a}\left(1-6i\mathbf{k}^i\mathbf{r}^i+\frac{7}{3}\mathbf{k}^i\mathbf{k}^j\mathbf{r}^i\mathbf{r}^j\right)+O\left(\mathbf{k}^3\right)+... \tag{3.41b}
$$

$$
T^{ll}_{Fig9c}(t,\mathbf{k}) = \sum_{a\neq b}\frac{7G^2m_am_b^2}{2r^2}e^{-i\mathbf{k}\cdot\mathbf{x}_a}, \tag{3.41c}
$$

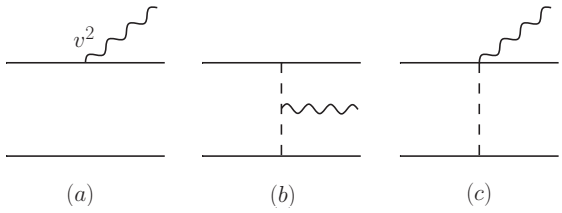

Figure 3.10: Diagrams (a) and (b) contribute to T^{ij}_{0PN} when the external leg is $\bar{h}^{ij}(x)$, while diagrams (a), (b) and (c) contribute to T^{00}_{1PN} when we consider $\bar{h}^{00}(x)$ as the external leg.

which leads to

$$\int d^3\mathbf{x} T^{ll}_{Fig9a-9c}\left[\mathbf{x}^i\mathbf{x}^j\right]_{TF} = \sum_{a\neq b}\frac{G^2 m_a m_b}{r^2}\left[\frac{3}{2}m\mathbf{x}^i_a\mathbf{x}^j_a - m_a\mathbf{x}^i_a\mathbf{x}^j_b\right]_{STF}. \tag{3.42}$$

With this, we now write the total contribution of T^{ll}_{1PN} to the mass quadrupole,

$$\begin{aligned}
&\int d^3\mathbf{x} T^{ll}_{1PN}\left[\mathbf{x}^i\mathbf{x}^j\right]_{TF} \\
&= \sum_a \frac{m_a}{2}\mathbf{v}^4_a\left[\mathbf{x}^i_a\mathbf{x}^j_a\right]_{TF} + \sum_{a\neq b}\frac{Gm_a m_b}{12r}\Big\{\big(22\mathbf{v}^2_a - 17\mathbf{v}^2_b - 10\mathbf{v}_a\cdot\mathbf{v}_b \\
&\quad +5\left(\mathbf{v}_a\cdot\mathbf{n}\right)^2 + 2\mathbf{v}_a\cdot\mathbf{n}\mathbf{v}_b\cdot\mathbf{n} - 8\left(\mathbf{v}_b\cdot\mathbf{n}\right)^2 - 5\mathbf{a}_a\cdot\mathbf{r} + 8\mathbf{a}_b\cdot\mathbf{r} + 12\frac{Gm}{r}\Big)\mathbf{x}^i_a\mathbf{x}^j_a \\
&\quad + \left(-5\mathbf{v}^2_a + 7\mathbf{v}_a\cdot\mathbf{v}_b + 5\left(\mathbf{v}_a\cdot\mathbf{n}\right)^2 - 7\mathbf{v}_a\cdot\mathbf{n}\mathbf{v}_b\cdot\mathbf{n} - 5\mathbf{a}_a\cdot\mathbf{r} - 12\frac{Gm_a}{r}\right)\mathbf{x}^i_a\mathbf{x}^j_b \\
&\quad + \left(4\mathbf{v}_a\cdot\mathbf{r} - 44\mathbf{v}_b\cdot\mathbf{r}\right)\mathbf{v}^i_a\mathbf{x}^j_a + \left(14\mathbf{v}_a\cdot\mathbf{r} - 58\mathbf{v}_b\cdot\mathbf{r}\right)\mathbf{v}^i_a\mathbf{x}^j_b \\
&\quad + r^2\left(38\mathbf{v}^i_a\mathbf{v}^j_a - 7\mathbf{v}^i_a\mathbf{v}^j_b + 14\mathbf{a}^i_a\mathbf{x}^j_a + 19\mathbf{a}^i_a\mathbf{x}^j_b\right)\Big\}_{STF}.
\end{aligned} \tag{3.43}$$

3.3 Lower Order Stress-energy Tensors

Although T^{ij}_{0PN}, T^{ii}_{0PN} and T^{00}_{1PN} have been computed before in [20], to write an expression for the mass quadrupole moment at 2PN order, we need to expand them in the radiation momentum to higher order and terms depending on $\mathbf{k}^2$ must be kept.

To obtain the sixth term of (3.6) we need diagrams in Fig. 3.10a-b. This gives us an expression for the leading order T^{ij}, as shown below:

$$
\begin{aligned}
&T^{kl}_{0PN}(t,\mathbf{k}) \\
&= \sum_a m_a \mathbf{v}_a^k \mathbf{v}_a^l e^{-i\mathbf{k}\cdot\mathbf{x}_a} + \sum_{a\neq b} \frac{G m_a m_b}{2r} e^{-i\mathbf{k}\cdot\mathbf{x}_a} \left\{ -\frac{1}{r^2}\mathbf{r}^k\mathbf{r}^l - \frac{i}{2}\mathbf{k}^i \frac{1}{r^2}\mathbf{r}^i\mathbf{r}^k\mathbf{r}^l \right. \\
&+ \frac{1}{12}\mathbf{k}^i\mathbf{k}^j \left[10\mathbf{r}^2\left(\delta^{kl}\delta^{ij} - \delta^{ik}\delta^{jl}\right) + \delta^{kl}\mathbf{r}^i\mathbf{r}^j + \delta^{ij}\mathbf{r}^k\mathbf{r}^l - 2\delta^{ik}\mathbf{r}^j\mathbf{r}^l + \frac{1}{r^2}2\mathbf{r}^i\mathbf{r}^j\mathbf{r}^k\mathbf{r}^l \right] \\
&- \frac{i}{24}\mathbf{k}^i\mathbf{k}^j\mathbf{k}^m \left[\mathbf{r}^2\mathbf{r}^m\left(10\delta^{ik}\delta^{jl} - 10\delta^{kl}\delta^{ij}\right) - \delta^{ij}\mathbf{r}^m\mathbf{r}^k\mathbf{r}^l + \mathbf{r}^i\mathbf{r}^j\left(2\delta^{mk}\mathbf{r}^l - \delta^{kl}\mathbf{r}^m - \frac{1}{r^2}\mathbf{r}^m\mathbf{r}^k\mathbf{r}^l\right)\right] \\
&+ \frac{1}{240}\mathbf{k}^i\mathbf{k}^j\mathbf{k}^m\mathbf{k}^n \left[\frac{16}{3}\mathbf{r}^4\delta^{mn}\left(\delta^{kl}\delta^{ij} - \delta^{ik}\delta^{jl}\right) + \mathbf{r}^2\delta^{ij}\delta^{mn}\mathbf{r}^k\mathbf{r}^l - 2\mathbf{r}^2\delta^{mn}\delta^{ik}\mathbf{r}^j\mathbf{r}^l \right. \\
&\left. \left. + \mathbf{r}^m\mathbf{r}^n\left(34\mathbf{r}^2\delta^{ik}\delta^{jl} - 33\mathbf{r}^2\delta^{kl}\delta^{ij} - 3\delta^{kl}\mathbf{r}^i\mathbf{r}^j + 6\delta^{ik}\mathbf{r}^j\mathbf{r}^l - 3\delta^{ij}\mathbf{r}^k\mathbf{r}^l - \frac{2}{r^2}\mathbf{r}^i\mathbf{r}^j\mathbf{r}^k\mathbf{r}^l\right)\right]\right\} \\
&+ O\left(\mathbf{k}^5\right) + ...
\end{aligned}
\tag{3.44}
$$

The first term in the expression above is related to Fig.3.10a, which comes from the simple source action term $-\sum \frac{m_a}{2m_{pl}} \int dt_a \mathbf{v}_a^i \mathbf{v}_a^j \overline{h}^{ij}(x_a)$. The other terms come from Fig. 3.10b, which is composed of (A.1) and (A.17) by considering,

$$
F^{\langle H^{00}H^{00}\rangle}\left[q,k,\bar{h}^{ij}\right] = \bar{h}^{ij}\left[-\frac{1}{2}\mathbf{q}^i\mathbf{q}^j - \frac{1}{2}\mathbf{q}^i\mathbf{k}^j - \frac{1}{2}\mathbf{k}^i\mathbf{k}^j + \delta^{ij}\left(\frac{1}{4}\mathbf{q}^2 + \frac{1}{4}\mathbf{k}\cdot\mathbf{q} + \frac{1}{2}\mathbf{k}^2\right)\right]. \tag{3.45}
$$

where $F^{\langle H^{00}H^{00}\rangle}$ is defined in (A.22).

Now, expanding the exponentials up to the fourth order in the radiation momentum, we extract the contribution

$$
\begin{aligned}
&\int d^3\mathbf{x}\partial_0^2 T^{kl}_{0PN}\mathbf{x}^k\mathbf{x}^l\left[\mathbf{x}^i\mathbf{x}^j\right]_{TF} \\
&= \frac{d^2}{dt^2}\left[\sum_a m_a\left(\mathbf{v}_a\cdot\mathbf{x}_a\right)^2\mathbf{x}_a^i\mathbf{x}_a^j\right]_{TF} \\
&\quad + \frac{d^2}{dt^2}\left\{\sum_{a\neq b}\frac{G m_a m_b}{6r}\left[\left(27\mathbf{r}^2 + \mathbf{x}_a^2 - 2\mathbf{x}_a\cdot\mathbf{x}_b - \frac{2}{r^2}\mathbf{r}\cdot\mathbf{x}_a\mathbf{r}\cdot\mathbf{x}_b\right)\mathbf{x}_a^i\mathbf{x}_a^j\right.\right. \\
&\quad \left.\left. + \left(\frac{27}{2}\mathbf{r}^2 + \mathbf{x}_a^2 - \frac{1}{r^2}\left(\mathbf{r}\cdot\mathbf{x}_a\right)^2\right)\mathbf{x}_a^i\mathbf{x}_b^j\right]\right\}_{STF}.
\end{aligned}
\tag{3.46}
$$

Taking the trace of (3.44), we get

$$T^{ll}_{0PN}(t,\mathbf{k}) = \sum_a m_a \mathbf{v}_a^2 e^{-i\mathbf{k}\cdot\mathbf{x}_a} + \sum_{a\neq b} \frac{Gm_a m_b}{2r} e^{-i\mathbf{k}\cdot\mathbf{x}_a} \left[-1 - \frac{i}{2}\mathbf{k}^i\mathbf{r}^i + \frac{1}{4}\mathbf{k}^i\mathbf{k}^j \left(7\mathbf{r}^2\delta^{ij} + \mathbf{r}^i\mathbf{r}^j\right) \right.$$
$$+ \frac{i}{24}\mathbf{k}^i\mathbf{k}^j\mathbf{k}^m \left(21\mathbf{r}^2\delta^{ij}\mathbf{r}^m + 2\mathbf{r}^i\mathbf{r}^j\mathbf{r}^m\right)$$
$$\left. + \frac{1}{144}\mathbf{k}^i\mathbf{k}^j\mathbf{k}^m\mathbf{k}^n \left(7\mathbf{r}^4\delta^{ij}\delta^{mn} - 42\mathbf{r}^2\delta^{ij}\mathbf{r}^m\mathbf{r}^n - 3\mathbf{r}^i\mathbf{r}^j\mathbf{r}^m\mathbf{r}^n\right) \right] + O\left(\mathbf{k}^5\right) + ..., \quad (3.47)$$

which contributes to the quadrupole in the form below:

$$\int d^3\mathbf{x}\partial_0^2 T^{ll}_{0PN}\mathbf{x}^2 \left[\mathbf{x}^i\mathbf{x}^j\right]_{TF}$$
$$= \frac{d^2}{dt^2}\left[\sum_a m_a \mathbf{v}_a^2 \mathbf{x}_a^2 \mathbf{x}_a^i \mathbf{x}_a^j\right]_{TF}$$
$$+ \frac{d^2}{dt^2}\left\{\sum_{a\neq b}\frac{Gm_a m_b}{12r}\left[\left(-104\mathbf{x}_a^2 + 196\mathbf{x}_a\cdot\mathbf{x}_b - 98\mathbf{x}_b^2\right)\mathbf{x}_a^i\mathbf{x}_a^j - 49\mathbf{r}^2\mathbf{x}_a^i\mathbf{x}_b^j\right]\right\}_{STF}. \quad (3.48)$$

To be able to compute the seventh contribution in (3.6), we need an expression for T^{00}_{1PN} up to the fourth order in the radiation momentum. We regard the source action term $-\sum \frac{m_a}{4m_{pl}} \int dt_a \mathbf{v}_a^2 \overline{h}^{00}(x_a)$ and also (A.15), (A.1), (A.4) and (A.18) to solve the diagrams at Fig. 3.10a-c. With this, we get an expression for T^{00}_{1PN} and its contribution to the mass quadrupole at 2PN, respectively:

$$T^{00}_{1PN}(t,\mathbf{k}) = \sum_a \frac{1}{2} m_a \mathbf{v}_a^2 e^{-i\mathbf{k}\cdot\mathbf{x}_a} + \sum_{a\neq b}\frac{Gm_a m_b}{r} e^{-i\mathbf{k}\cdot\mathbf{x}_a}\left[-\frac{1}{2}\right.$$
$$\left. -\frac{3}{8}\mathbf{k}^2 r^2\left(1 + \frac{i}{2}\mathbf{k}^i\mathbf{r}^i - \frac{1}{6}\mathbf{k}^i\mathbf{k}^j\mathbf{r}^i\mathbf{r}^j + \frac{r^2}{36}\mathbf{k}^i\mathbf{k}^j\delta^{ij}\right)\right] + O\left(\mathbf{k}^5\right) + ..., \quad (3.49)$$

$$\int d^3\mathbf{x}\partial_0^2 T^{00}_{1PN}\mathbf{x}^2\left[\mathbf{x}^i\mathbf{x}^j\right]_{TF} = \frac{d^2}{dt^2}\left\{\sum_a \frac{1}{2}m_a\mathbf{v}_a^2\mathbf{x}_a^2\left[\mathbf{x}_a^i\mathbf{x}_a^j\right]_{TF}\right\}$$
$$+ \frac{d^2}{dt^2}\left\{\sum_{a\neq b}\frac{Gm_a m_b}{r}\left[\frac{7}{4}\mathbf{r}^2\left(2\mathbf{x}_a^i\mathbf{x}_a^j + \mathbf{x}_a^i\mathbf{x}_b^j\right) - \frac{1}{2}\mathbf{x}_a^2\mathbf{x}_a^i\mathbf{x}_a^j\right]_{STF}\right\}. \quad (3.50)$$

Moreover, considering the expansion up to the fifth and sixth orders in the radiation momentum at (3.26) and (3.8), respectively, in addition to taking time derivatives, we get

$$\int d^3\mathbf{x}\partial_0^3 T_{0PN}^{0l}\mathbf{x}^2\mathbf{x}^l\left[\mathbf{x}^i\mathbf{x}^j\right]_{TF} = \frac{d^3}{dt^3}\left[\sum_a m_a\mathbf{v}_a\cdot\mathbf{x}_a\mathbf{x}_a^2\mathbf{x}_a^i\mathbf{x}_a^j\right]_{TF}, \tag{3.51}$$

$$\int d^3\mathbf{x}\partial_0^4 T_{0PN}^{00}\mathbf{x}^4\left[\mathbf{x}^i\mathbf{x}^j\right]_{TF} = \frac{d^4}{dt^4}\left[\sum_a m_a\mathbf{x}_a^4\mathbf{x}_a^i\mathbf{x}_a^j\right]_{TF}. \tag{3.52}$$

Before writing the final expression for the 2PN correction to the mass quadrupole moment, we still need to write the contribution of $I_{1PN}^{ij}(\mathbf{a}_{1PN})$, which is given by the two terms

$$\left[\int d^3\mathbf{x}\partial_0 T_{0PN}^{0l}\mathbf{x}^l\mathbf{x}^i\mathbf{x}^j\right]_{TF} \xrightarrow{2PN} \sum_a m_a\mathbf{a}_{1PNa}\cdot\mathbf{x}_a\left[\mathbf{x}_a^i\mathbf{x}_a^j\right]_{TF}, \tag{3.53a}$$

$$\left[\int d^3\mathbf{x}\partial_0^2 T_{0PN}^{00}\mathbf{x}^2\mathbf{x}^i\mathbf{x}^j\right]_{TF} \xrightarrow{2PN} \sum_a 2m_a\left[\mathbf{x}_a^2\mathbf{a}_{1PNa}^i\mathbf{x}_a^j + \mathbf{a}_{1PNa}\cdot\mathbf{x}_a\mathbf{x}_a^i\mathbf{x}_a^j\right]_{STF}, \tag{3.53b}$$

where the 1PN correction to the acceleration, for instance obtained in [40] using the EFT framework, is given by

$$\begin{aligned}\mathbf{a}_{1PN(1)}^i &= \frac{Gm_2}{2r^2}\left\{\mathbf{n}^i\left[\frac{2Gm}{r} - 3\left(\mathbf{v}_1^2+\mathbf{v}_2^2\right) + 7\left(\mathbf{v}_1\cdot\mathbf{v}_2\right) + 3\left(\mathbf{v}_1\cdot\mathbf{n}\right)\left(\mathbf{v}_2\cdot\mathbf{n}\right)\right]\right.\\
&\quad -\mathbf{v}_1^i\left(\mathbf{v}_2\cdot\mathbf{n}\right) - \left(\mathbf{v}_1\cdot\mathbf{n}\right)\mathbf{v}_2^i + \dot{r}\left(6\mathbf{v}_1^i - 7\mathbf{v}_2^i - \mathbf{n}^i\left(\mathbf{v}_2\cdot\mathbf{n}\right)\right)\\
&\quad \left.-6r\mathbf{a}_1^i + 7r\mathbf{a}_2^i + \left(\mathbf{v}^i - \mathbf{n}^i\dot{r}\right)\left(\mathbf{v}_2\cdot\mathbf{n}\right) + r\mathbf{n}^i\left(\mathbf{a}_2\cdot\mathbf{n}\right) + \mathbf{n}^i\left(\mathbf{v}_2\cdot\left(\mathbf{v}-\mathbf{n}\dot{r}\right)\right)\right\}\\
&\quad -\frac{1}{2}\mathbf{a}_1^i\mathbf{v}_1^2 - \mathbf{v}_1^i\left(\mathbf{v}_1\cdot\mathbf{a}_1\right).\end{aligned} \tag{3.54}$$

3.4 Consistency Tests

Here we check the expressions for the components T_{2PN}^{00}, T_{1PN}^{0i} and T_{1PN}^{ll}, which were obtained here for the first time in EFT approach with previous results derived using different methods.

The results presented in section 3.2.1 allow us to write down an expression for the temporal component of the pseudotensor up to 2PN order[2],

$$
\begin{aligned}
&T^{00}\left(t,\mathbf{k}\right)= \\
&e^{-i\mathbf{k}\cdot\mathbf{x}_a}\left\{\sum_a m_a\left(1+\frac{1}{2}\mathbf{v}_a^2+\frac{3}{8}\mathbf{v}_a^4\right)+\sum_{a\neq b}\frac{Gm_am_b}{2r}\left\{-1+\mathbf{v}^2+\frac{7}{2}\mathbf{v}_a^2-\frac{5}{2}\mathbf{v}_b^2+\frac{5}{2}\mathbf{v}_a\cdot\mathbf{v}_b\right.\right. \\
&-\frac{5}{2}\mathbf{v}_a\cdot\mathbf{n}\mathbf{v}_b\cdot\mathbf{n}+2\left(\mathbf{v}_b\cdot\mathbf{n}\right)^2-\dot{r}^2+\mathbf{a}\cdot\mathbf{r}+2\mathbf{a}_b\cdot\mathbf{r}+\frac{G}{r}\left(4m_a-3m_b\right) \\
&+\frac{1}{2}i\mathbf{k}^i\left[\left(\mathbf{v}^2+\frac{1}{2}\mathbf{v}_b^2+\frac{5}{2}\mathbf{v}_a\cdot\mathbf{v}_b-\dot{r}^2-\frac{5}{2}\mathbf{v}_a\cdot\mathbf{n}\mathbf{v}_b\cdot\mathbf{n}+\frac{3}{2}\left(\mathbf{v}_b\cdot\mathbf{n}\right)^2+\mathbf{a}\cdot\mathbf{r}+\frac{3}{2}\mathbf{a}_b\cdot\mathbf{r}\right)\mathbf{r}^i\right. \\
&\left.\left.\left.+\left(8\mathbf{v}_a\cdot\mathbf{r}+\frac{11}{2}\mathbf{v}_b\cdot\mathbf{r}-2r\dot{r}\right)\mathbf{v}_a^i+\left(\frac{9}{2}\mathbf{v}_b\cdot\mathbf{r}+\frac{1}{2}r\dot{r}\right)\mathbf{v}_b^i+r^2\left(7\mathbf{a}_a^i-2\mathbf{a}_b^i\right)+\frac{6Gm}{r}\right]\right\}+O\left(\mathbf{k}^2\right)\right\}
\end{aligned}
\tag{3.55}
$$

We can use (3.7) to read off different contributions of T^{00} to the dynamics of the binary system. For instance, at zeroth order in the radiation momentum, we can read off the mechanical energy of the system. It is straightforward to see in (3.55) that the leading order terms in the PN approximation reproduce the total mass of the two-body system, while the next-to-leading order terms provide us with the Newtonian energy. The terms that account for the next-to-next-to-leading order (2PN) correction to this pseudotensor, which were calculated in the section 3.2.1 of this chapter, give us the following contribution to the conserved energy,

$$
\begin{aligned}
E_{1PN}&=\int d^3\mathbf{x}T_{2PN}^{00}\left(x\right) \\
&=\frac{3}{8}\sum_a m_a\mathbf{v}_a^4+\sum_{a\neq b}\frac{Gm_am_b}{4r}\left[6\mathbf{v}_a^2-7\left(\mathbf{v}_a\cdot\mathbf{v}_b\right)-\left(\mathbf{v}_a\cdot\mathbf{n}\right)\left(\mathbf{v}_b\cdot\mathbf{n}\right)+\frac{Gm}{r}\right].
\end{aligned}
\tag{3.56}
$$

This result is equal to the first correction to the Newtonian energy presented in Eq. (205) of [41] and can also be calculated computing the Hamiltonian function using the Lagrangian obtained by Einstein, Infeld and Hoffman in [42].

[2]To have an expression for T^{00} containing terms of second order in the radiation momentum, we would have to include $\mathbf{k}^2$ terms, but we discarded those terms since they are not needed to extract the contribution of T_{2PN}^{00} to the mass quadrupole moment. Nevertheless, it is enough to consider terms up the first order in the radiation momentum to perform the consistency tests on T_{2PN}^{00} in this section.

Regarding the 2PN terms in Eq. (3.55), we can read off the correction to the center of mass position

$$\begin{aligned}\mathbf{G}_{2PN} &= \int d^3\mathbf{x} T^{00}_{2PN}(x)\,\mathbf{x} \\ &= \frac{3}{8}\sum_a m_a \mathbf{v}_a^4 \mathbf{x}_a + \sum_{a\neq b}\frac{Gm_am_b}{4r}\left\{\left[\frac{19}{2}\mathbf{v}_a^2 - 7\mathbf{v}_a\cdot\mathbf{v}_b - \frac{7}{2}\mathbf{v}_b^2 - \mathbf{v}_a\cdot\mathbf{n}\mathbf{v}_b\cdot\mathbf{n}\right.\right. \\ &\left.\left. -\frac{1}{2}(\mathbf{v}_a\cdot\mathbf{n})^2 + \frac{1}{2}(\mathbf{v}_b\cdot\mathbf{n})^2 - 5\frac{Gm_a}{r} + 7\frac{Gm_b}{r}\right]\mathbf{x}_a - 7(\mathbf{v}_a\cdot\mathbf{r} + \mathbf{v}_b\cdot\mathbf{r})\mathbf{v}_a\right\}, \end{aligned} \tag{3.57}$$

which agrees with the result presented in Eq. (B2c) of [43], where $\frac{d\mathbf{G}}{dt} = \mathbf{P}$, the total conserved linear momentum, such that the center of mass frame is defined by $\mathbf{G} = 0$. By solving this equation iteratively, using the equations of motion to reduce the second time derivatives of the position, we get the 2PN correction to the center of mass frame,

$$\begin{aligned}\delta\mathbf{r}_{2PN} = \frac{\nu\delta m}{m}\left\{\mathbf{r}\left[\left(\frac{3}{8} - \frac{3\nu}{2}\right)\mathbf{v}^4 + \frac{Gm}{r}\left(\left(\frac{19}{8} + \frac{3\nu}{2}\right)\mathbf{v}^2\right)\right.\right. \\ \left.\left. + \left(-\frac{1}{8} + \frac{3\nu}{4}\right)\dot{r}^2 + \left(\frac{7}{4} - \frac{\nu}{2}\right)\frac{Gm}{r}\right] - \mathbf{v}\left[\frac{7}{4}Gm\dot{r}\right]\right\}, \end{aligned} \tag{3.58}$$

which agrees with (B4a), (B4b) and (B5b) of [43].

Let us now consider the results obtained in section 3.2.2 to write down an expression for T^{0l} up to 1PN order,

$$\begin{aligned}&T^{0l}(t,\mathbf{k}) = \\ &e^{-i\mathbf{k}\cdot\mathbf{x}_a}\left\{\sum_a m_a\mathbf{v}_a^l\left(1 + \frac{1}{2}\mathbf{v}_a^2\right) + \sum_{a\neq b}\frac{Gm_am_b}{4r}\left[-3\mathbf{v}_a^l + \mathbf{v}_b^l - \frac{1}{r^2}(\mathbf{v}_a + \mathbf{v}_b)\cdot\mathbf{r}\mathbf{r}^l\right.\right. \\ &\left.\left. -\frac{i}{2}\mathbf{k}^i\left(\mathbf{v}^i\mathbf{r}^l - 16\mathbf{v}_a^i\mathbf{r}^l + 15\mathbf{r}^i\mathbf{v}_a^l - \mathbf{r}^i\mathbf{v}_b^l + 3r\dot{r}\delta^{il} + \frac{1}{r^2}(\mathbf{v}_a + \mathbf{v}_b)\cdot\mathbf{r}\mathbf{r}^i\mathbf{r}^l\right)\right] + O\left(\mathbf{k}^2\right) + ...\right\} \end{aligned} \tag{3.59}$$

Taking into account only terms of order zero in the radiation momentum, we obtain the 1PN correction to the linear momentum of the binary system,

$$\mathbf{P}_{1PN} = \int d^3\mathbf{x} T^{0l}_{1PN}(x) = -\left[\frac{Gm_1m_2}{2r^3}(\mathbf{v}_1 + \mathbf{v}_2)\cdot\mathbf{r}\right]\mathbf{x}_1^l + \left[\frac{m_1}{2}\mathbf{v}_1^2 - \frac{Gm_1m_2}{2r}\right]\mathbf{v}_1^l + 1 \leftrightarrow 2. \tag{3.60}$$

The result above agrees with Eq. (B1) and Eq. (B2b) of reference [43]. Considering all linear terms in the radiation momentum in (3.59), we are able to obtain the 1PN correction to the angular momentum of the binary system,

$$\mathbf{L}^i_{1PN} = -\frac{1}{2}\epsilon^{ilk}\int d^3\mathbf{x}\left(T^{0l}_{1PN}\mathbf{x}^k - T^{0k}_{1PN}\mathbf{x}^l\right) = \frac{1}{2}\nu m\left(\mathbf{r}\times\mathbf{v}\right)^i\left[\left(1-3\nu\right)\mathbf{v}^2 + \frac{Gm}{r}\left(6+2\nu\right)\right], \tag{3.61}$$

which agrees with Eq. (2.9b) of reference [44].

Furthermore, considering the result obtained in section 3.2.3, we provide an expression for $T^{ll}\left(t,\mathbf{k}\right)$ up to 1PN order:

$$\begin{aligned} T^{ll}\left(t,\mathbf{k}\right) = e^{-i\mathbf{k}\cdot\mathbf{x}_a}\Bigg\{&\sum_a m_a\mathbf{v}_a^2\left(1+\frac{1}{2}\mathbf{v}_a^2\right) + \sum_{a\neq b}\frac{Gm_am_b}{4r}\Big\{-2-5\mathbf{v}_a^2+5\mathbf{v}_b^2-\mathbf{v}_a\cdot\mathbf{v}_b-6\dot{r}^2 \\ &-3\mathbf{v}_a\cdot\mathbf{n}\mathbf{v}_b\cdot\mathbf{n}+2\left(\mathbf{v}_b\cdot\mathbf{n}\right)^2+16\dot{r}\mathbf{v}_a\cdot\mathbf{n}-10\mathbf{a}_a\cdot\mathbf{r}-4\mathbf{a}_b\cdot\mathbf{r}+\frac{G}{r}\left(-8m_a+12m_b\right) \\ &+i\mathbf{k}^i\Bigg[\mathbf{r}^i\left(-9\mathbf{v}_a^2+\frac{5}{2}\mathbf{v}_b^2-\frac{1}{2}\mathbf{v}_a\cdot\mathbf{v}_b-\frac{3}{2}\mathbf{v}_a\cdot\mathbf{n}\mathbf{v}_b\cdot\mathbf{n}+\frac{1}{2}\left(\mathbf{v}_b\cdot\mathbf{n}\right)^2\right. \\ &\left.-3\dot{r}^2+8\dot{r}\mathbf{v}_a\cdot\mathbf{n}-5\mathbf{a}_a\cdot\mathbf{r}-\frac{5}{2}\mathbf{a}_b\cdot\mathbf{r}-\frac{10Gm_a}{r}\right)+\left(2\mathbf{v}_a\cdot\mathbf{r}+\frac{25}{2}\mathbf{v}_b\cdot\mathbf{r}\right)\mathbf{v}_a^i \\ &+\left(-\frac{9}{2}\mathbf{v}_a\cdot\mathbf{r}+5\mathbf{v}_b\cdot\mathbf{r}\right)\mathbf{v}_b^i-\mathbf{r}^2\left(3\mathbf{a}_a^i+\frac{5}{2}\mathbf{a}_b^i\right)\Bigg]\Big\}+O\left(\mathbf{k}^2\right)+...\Bigg\}. \end{aligned} \tag{3.62}$$

We can use the moment relation

$$\int d^3\mathbf{x}T^{ll} = \frac{1}{2}\frac{d^2}{dt^2}\int d^3\mathbf{x}T^{00}\mathbf{x}^2. \tag{3.63}$$

to prove the self-consistency of our results. At leading order in the PN expansion, it is trivial to prove that this relation holds using (3.55) and (3.62), while at next-to-leading order more computation is required. From (3.62) we can read off up to 1PN,

$$\begin{aligned} \int d^3\mathbf{x}T^{ll} =& \sum_a m_a\mathbf{v}_a^2\left(1+\frac{1}{2}\mathbf{v}_a^2\right) \\ &+\sum_{a\neq b}\frac{Gm_am_b}{r}\left[-\frac{1}{2}-\frac{1}{4}\mathbf{v}_a\cdot\mathbf{v}_b+\frac{3}{2}\left(\mathbf{v}_a\cdot\mathbf{n}\right)^2-\frac{7}{4}\mathbf{v}_a\cdot\mathbf{n}\mathbf{v}_b\cdot\mathbf{n}+\frac{5}{2}\frac{Gm_a}{r}\right]. \end{aligned} \tag{3.64}$$

To check if the result above satisfies (3.63), we need a complete expression for $T^{00}\left(t,\mathbf{k}\right)$ up to 1PN order and which contains all terms up to the quadratic order in the radiation momentum. In other words, we cannot discard terms proportional to $\mathbf{k}^2$ as we did in section 3.2.1, where

we drppped these terms that would not contribute to the trace-free quadrupole moment. Therefore, the expression that we need for $T^{00}(t,\mathbf{k})$ is the sum of (3.8) with (3.49), which provides us with the following result up to 1PN order:

$$\frac{1}{2}\frac{d^2}{dt^2}\int d^3\mathbf{x}T^{00}\mathbf{x}^2=\frac{1}{2}\frac{d^2}{dt^2}\left[\sum_a m_a\left(1+\frac{1}{2}\mathbf{v}_a^2\right)\mathbf{x}_a^2+\sum_{a\neq b}\frac{Gm_am_b}{r}\left(-\frac{1}{2}\mathbf{x}_a^2+\frac{9}{4}r^2\right)\right]. \quad (3.65)$$

At this point, it is straightforward to show that, after taking the second order time derivative and imposing the leading and next-to-leading order equations of motion that (3.63) holds, as we expected.

3.5 Mass Quadrupole Moment At 2PN Order

We are now ready to sum the contributions (3.25), (3.31), (3.43), (3.46), (3.48), (3.50), (3.51), (3.52) and to write down the expression for the 2PN correction to the mass quadrupole moment in a general orbit,

$$\begin{aligned}I_{2PN}^{ij}=&\sum_a m_a f_{1(a)}^{ij}+\sum_{a\neq b}\frac{Gm_am_b}{r}f_{2(a,b)}^{ij}+\frac{d}{dt}\left[\sum_a m_a f_{3(a)}^{ij}+\sum_{a\neq b}\frac{Gm_am_b}{r}f_{4(a,b)}^{ij}\right]\\&+\frac{d^2}{dt^2}\left[\sum_a m_a f_{5(a)}^{ij}+\sum_{a\neq b}\frac{Gm_am_b}{r}f_{6(a,b)}^{ij}\right]+\frac{d^3}{dt^3}\left[\sum_a m_a f_{7(a)}^{ij}\right]+\frac{d^4}{dt^4}\left[\sum_a m_a f_{8(a)}^{ij}\right],\end{aligned} \quad (3.66)$$

where we have defined the following quantities for convenience:

$$f_{1(a)}^{ij}\equiv\left[\frac{7}{8}\mathbf{v}_a^4\mathbf{x}_a^i\mathbf{x}_a^j+\frac{11}{21}\mathbf{x}_a^2\mathbf{a}_{1PNa}^i\mathbf{x}_a^j-\frac{17}{21}\mathbf{a}_{1PNa}\cdot\mathbf{x}_a\mathbf{x}_a^i\mathbf{x}_a^j\right]_{STF}, \quad (3.67)$$

$$\begin{aligned}f_{2(a,b)}^{ij}\equiv&\frac{1}{12}\Big[\Big(50\mathbf{v}_a^2-28\mathbf{v}_b^2-32\mathbf{v}_a\cdot\mathbf{v}_b-4\dot{r}^2-24\mathbf{v}_a\cdot\mathbf{n}\mathbf{v}_b\cdot\mathbf{n}\\&+8\left(\mathbf{v}_a\cdot\mathbf{n}\right)^2+14\left(\mathbf{v}_b\cdot\mathbf{n}\right)^2-4\mathbf{a}_a\cdot\mathbf{r}+10\mathbf{a}_b\cdot\mathbf{r}+24\frac{Gm_a}{r}+18\frac{Gm_b}{r}\Big)\mathbf{x}_a^i\mathbf{x}_a^j\\&+\left(-4\mathbf{v}_a^2+8\mathbf{v}_a\cdot\mathbf{v}_b-12\mathbf{v}_a\cdot\mathbf{n}\mathbf{v}_b\cdot\mathbf{n}+8\left(\mathbf{v}_a\cdot\mathbf{n}\right)^2-2\dot{r}^2-4\mathbf{a}_a\cdot\mathbf{r}-24\frac{Gm_1}{r}\right)\mathbf{x}_a^i\mathbf{x}_b^j\\&+\mathbf{v}_a^i\mathbf{x}_a^j\left(-16\mathbf{v}_a\cdot\mathbf{r}-64\mathbf{v}_b\cdot\mathbf{r}\right)+\mathbf{v}_a^i\mathbf{x}_b^j\left(40\mathbf{v}_a\cdot\mathbf{r}-32\mathbf{v}_b\cdot\mathbf{r}\right)\end{aligned}$$

$$+\mathbf{r}^2\left(40\mathbf{v}_a^i\mathbf{v}_a^j-8\mathbf{v}_a^i\mathbf{v}_b^j-8\mathbf{a}_a^i\mathbf{x}_a^j-4\mathbf{a}_a^i\mathbf{x}_b^j\right)\Big]_{STF}, \tag{3.68}$$

$$f_{3(a)}^{ij}\equiv-\frac{2}{3}\mathbf{v}_a^2\mathbf{v}_a\cdot\mathbf{x}_a\left[\mathbf{x}_a^i\mathbf{x}_a^j\right]_{TF}, \tag{3.69}$$

$$\begin{aligned}f_{4(a,b)}^{ij}\equiv-\frac{1}{9}\Big[&\left(8\mathbf{r}^2-20\mathbf{r}\cdot\mathbf{x}_b\right)\mathbf{v}_a^i\mathbf{x}_a^j+\left(20\mathbf{r}^2-22\mathbf{r}\cdot\mathbf{x}_b\right)\mathbf{v}_a^i\mathbf{x}_b^j\\&+\left(22\mathbf{v}_a\cdot\mathbf{x}_a-30\mathbf{v}_b\cdot\mathbf{x}_a-8\mathbf{v}_a\cdot\mathbf{x}_b+8\mathbf{v}_b\cdot\mathbf{x}_b-\frac{2}{r^2}\left(\mathbf{v}_a+\mathbf{v}_b\right)\cdot\mathbf{r}\mathbf{r}\cdot\mathbf{x}_b\right)\mathbf{x}_a^i\mathbf{x}_a^j\\&+\left(9\mathbf{v}_a\cdot\mathbf{x}_a-7\mathbf{v}_a\cdot\mathbf{x}_b-\frac{1}{r^2}\left(\mathbf{v}_a+\mathbf{v}_b\right)\cdot\mathbf{r}\mathbf{r}\cdot\mathbf{x}_b\right)\mathbf{x}_a^i\mathbf{x}_b^j\Big]_{STF},\end{aligned} \tag{3.70}$$

$$f_{5(a)}^{ij}\equiv\left(\frac{1}{6}\left(\mathbf{v}_a\cdot\mathbf{x}_a\right)^2+\frac{19}{84}\mathbf{v}_a^2\mathbf{x}_a^2\right)\left[\mathbf{x}_a^i\mathbf{x}_a^j\right]_{TF}, \tag{3.71}$$

$$\begin{aligned}f_{6(a,b)}^{ij}\equiv\Bigg[&\left(\frac{31}{42}\mathbf{x}_a^2-\frac{11}{6}\mathbf{x}_a\cdot\mathbf{x}_b+\frac{8}{9}\mathbf{x}_b^2-\frac{1}{18}\frac{1}{r^2}\mathbf{r}\cdot\mathbf{x}_a\mathbf{r}\cdot\mathbf{x}_b\right)\mathbf{x}_a^i\mathbf{x}_a^j\\&+\left(\frac{4}{9}\mathbf{r}^2+\frac{1}{36}\mathbf{x}_a^2-\frac{1}{36}\frac{1}{r^2}\left(\mathbf{r}\cdot\mathbf{x}_a\right)^2\right)\mathbf{x}_a^i\mathbf{x}_b^j\Bigg]_{STF},\end{aligned} \tag{3.72}$$

$$f_{7(a)}^{ij}\equiv-\frac{1}{7}\mathbf{v}_a\cdot\mathbf{x}_a\mathbf{x}_a^2\left[\mathbf{x}_a^i\mathbf{x}_a^j\right]_{TF}, \tag{3.73}$$

$$f_{8(a)}^{ij}\equiv\frac{23}{1512}\mathbf{x}_a^4\left[\mathbf{x}_a^i\mathbf{x}_a^j\right]_{TF}. \tag{3.74}$$

With the exception of the accelerations in (3.67) which are of 1PN order, all other accelerations in I_{2PN}^{ij} should be taken as the Newtonian acceleration.

In order to write the 2PN correction of the mass quadrupole moment in the center of mass frame, we must have in mind that the positions of the compact bodies in this frame are given by

$$\mathbf{x}_1=\frac{m_2}{m}\mathbf{r}+\delta\mathbf{r}_{1PN}+..., \tag{3.75}$$

$$\mathbf{x}_2=-\frac{m_1}{m}\mathbf{r}+\delta\mathbf{r}_{1PN}+..., \tag{3.76}$$

where $\delta\mathbf{r}_{1PN}$ accounts for the 1PN correction to the center of mass frame, which can be obtained following the procedure presented through (3.57) and (3.58) but this time using

(3.49). Thus, the corrections to the center of frame necessary to write the 2PN mass quadrupole are

$$\delta\mathbf{r}_{1PN} = \frac{\nu\delta m}{2m}\mathbf{r}\left(\mathbf{v}^2 - \frac{Gm}{r}\right), \tag{3.77}$$

$$\begin{aligned}\delta\mathbf{r}_{2PN} = \frac{\nu\delta m}{2m}\Bigg\{\mathbf{r}\Bigg[\left(\frac{3}{4}-3\nu\right)\mathbf{v}^4 + \frac{Gm}{r}\left(\left(\frac{19}{4}+3\nu\right)\mathbf{v}^2\right) \\ + \left(-\frac{1}{4}+\frac{3\nu}{2}\right)\dot{r}^2 + \left(\frac{7}{2}-\nu\right)\frac{Gm}{r}\Bigg] - \mathbf{v}\left[\frac{7}{2}Gm\dot{r}\right]\Bigg\}.\end{aligned} \tag{3.78}$$

Applying (3.75) and (3.76) to (3.4) and (3.5), we obtain the following contributions at 2PN order:

$$I^{ij}_{0PN+2PN} = \frac{\nu^2\delta m^2}{4m}\left(\mathbf{v}^4 - 2\mathbf{v}^2\frac{Gm}{r} + \frac{G^2m^2}{r^2}\right)\left[\mathbf{r}^i\mathbf{r}^j\right]_{TF}, \tag{3.79}$$

$$\begin{aligned}I^{ij}_{1PN+1PN} = \frac{\nu^2\delta m^2}{21m}\Bigg\{\left[-29\mathbf{v}^4 + \frac{Gm}{r}\left(41\mathbf{v}^2 + \frac{17}{2}\dot{r}^2 - 12\frac{Gm}{r}\right)\right]\mathbf{r}^i\mathbf{r}^j \\ + \left(24\mathbf{v}^2 - 19\frac{Gm}{r}\right)r\dot{r}\mathbf{v}^i\mathbf{r}^j + \left(-22\mathbf{v}^2 + 22\frac{Gm}{r}\right)r^2\mathbf{v}^i\mathbf{v}^j\Bigg\}_{STF}.\end{aligned} \tag{3.80}$$

Adding these two contributions to (3.66) after applying (3.75) and (3.76), we finally obtain the expression for the 2PN correction to the mass quadrupole moment in the center of mass frame,

$$\begin{aligned}I^{ij}_{2PN} = m\nu\Bigg\{\mathbf{r}^i\mathbf{r}^j\Bigg[\frac{1}{252}\left(653-1906\nu+337\nu^2\right)\frac{G^2m^2}{r^2} + \frac{1}{756}\left(2021-5947\nu-4883\nu^2\right)\frac{Gm}{r}v^2 \\ - \frac{1}{756}\left(131-907\nu+1273\nu^2\right)\frac{Gm}{r}\dot{r}^2 + \frac{1}{504}\left(253-1835\nu+3545\nu^2\right)v^4 \\ - r\dot{r}\mathbf{r}^i\mathbf{v}^j\left[\frac{1}{378}\left(1085-4057\nu-1463\nu^2\right)\frac{Gm}{r} + \frac{1}{63}\left(26-202\nu+418\nu^2\right)v^2\right] \\ + \mathbf{v}^i\mathbf{v}^j\left[\frac{1}{189}\left(742-335\nu-985\nu^2\right)\frac{Gm}{r} + \frac{1}{126}\left(41-337\nu+733\nu^2\right)v^2\right. \\ \left. + \frac{5}{63}\left(1-5\nu+5\nu^2\right)\dot{r}^2\right]\Bigg\}_{STF}.\end{aligned} \tag{3.81}$$

We can use the result above to compute, for instance, the 2PN correction to the power loss, whose expression in terms of the multipole moments is given by [38]

$$P = -\frac{G}{5}\left\{I^{(3)}_{ij}I^{(3)}_{ij} - \frac{5}{189}I^{(4)}_{ijk}I^{(4)}_{ijk} + \frac{5}{9072}I^{(5)}_{ijkl}I^{(5)}_{ijkl} + \frac{16}{9}J^{(3)}_{ij}J^{(3)}_{ij} - \frac{5}{84}J^{(4)}_{ijk}J^{(4)}_{ijk} + ...\right\}. \tag{3.82}$$

The expressions for these multipole moments below 2PN order are known and can be found for instance in [45]. Considering all terms which contribute to the power loss at 2PN order in the expression above, making use of (3.81) and the 2PN acceleration (B.10) obtained in the appendix B, we get

$$
\begin{aligned}
&P_{EFT}^{2PN} = \\
&-\frac{8}{15}\frac{G^3m^4\nu^2}{r^4}\left\{\frac{2}{3}\left(-253+1026\nu-56\nu^2\right)\frac{G^3m^3}{r^3}+\left[\frac{1}{756}\left(245185+81828\nu+4368\nu^2\right)v^2\right.\right.\\
&\left.-\frac{1}{252}\left(97247+9798\nu+5376\nu^2\right)\dot{r}^2\right]\frac{G^2m^2}{r^2}+\left[\frac{1}{21}\left(-4446+5237\nu-1393\nu^2\right)v^4\right.\\
&+\frac{1}{7}\left(4987-8513\nu+2165\nu^2\right)v^2\dot{r}^2-\left.\frac{1}{63}\left(33510-60971\nu+14290\nu^2\right)\right]\frac{Gm}{r}\\
&+\frac{1}{42}\left(1692-5497\nu+4430\nu^2\right)v^6-\frac{1}{14}\left(1719-10278\nu+6292\nu^2\right)v^4\dot{r}^2\\
&\left.+\frac{1}{14}\left(2018-15207\nu+7572\nu^2\right)v^2\dot{r}^4-\frac{1}{42}\left(2501-20234\nu+8404\nu^2\right)\dot{r}^6\right\}. \qquad (3.83)
\end{aligned}
$$

At this point we can see that (3.81) and (3.83) seem to be in disagreement with the results presented at [46] and [47] where the Epstein-Wagoner formalism and multipolar post-Minkowskian approach of Blanchet, Damour, and Iyer (BDI) were used, respectively. For instance, the mass quadrupole moment presented in this chapter and ones in the mentioned references differ by a factor of $-\frac{4G^2m^2}{r^2}\left[m\nu\mathbf{r}^i\mathbf{r}^j\right]_{TF}$. The power loss shown above and the energy fluxes at (6.13d) in [46] and at (3.5d) in [47] differ by a global minus sign, as well as by the numerical factors on terms depending on $\frac{G^5m^6\nu^2v^2}{r^6}$ and $\frac{G^5m^6\nu^2\dot{r}^2}{r^6}$. The difference in the global sign comes from the relation $P=-\frac{dE}{dt}$, which is actually a matter of convention on how the energy flux is defined. For this reason, we consider instead $|P|=\left|\frac{dE}{dt}\right|$ and compare the result for the power loss obtained here against the ones in the literature, and we find the following difference

$$
P_{EFT}-\bar{P}=\frac{32}{5}\frac{G^5m^6\nu^2}{r^6}\left(4v^2-3\dot{r}^2\right), \qquad (3.84)
$$

where $\bar{P}$ is the modulus of the energy flux computed via the Epstein-Wagoner and BDI approaches [3].

Furthermore, the 2PN acceleration obtained in the appendix B is also different from the one presented in [47], which was computed via the BDI formalism. It turns out that

[3] If the power is expressed in terms of the gauge invariant frequency of a circular orbit $P=\bar{P}$.

these differences should not be a surprise since the gauge choice adopted here and in other formalisms are not the same: in the BDI and in the Epstein-Wagoner approaches the harmonic gauge is used, while in the EFT approach we use the linearized harmonic gauge (2.8), which depends on the background field metric. The different gauge choices for fixing the gravity action imply different coordinate systems. In fact, the difference between the mass quadrupole moments suggests a coordinate transformation of the form

$$\mathbf{r}_{EFT} \to \bar{\mathbf{r}} - \frac{2G^2m^2}{r^2}\bar{\mathbf{r}}, \tag{3.85}$$

where $\bar{\mathbf{r}}$ is the coordinate used in the BDI and Epstein-Wagoner approaches. When this transformation is applied to the power loss (3.83), we can verify that

$$P_{EFT}\left(\bar{\mathbf{r}}\right) = \bar{P}. \tag{3.86}$$

An analogous comparison holds for the mass quadrupole moment and the 2PN acceleration, showing the agreement between our results and the literature. It should also be noticed that this coordinate transformation was already brought to attention in [48] when the authors used NRGR to calculate the spacetime metric generated by a point mass at rest.

4.0 Analytic Solutions to the Binary Equations of Motion

The adiabatic approximation is often used to find the analytic solutions to the motion, including inspiral radiation reaction effects [49–51]. Using the PN expansions of the conserved energy E and flux $\mathcal{F}$, the adiabatic waveforms are obtained by solving the energy balance equation $\mathrm{d}E/\mathrm{d}t = \mathcal{F}$. The balance equation leads to the secular evolutions of the orbital angular frequency $\omega(t)$, from which one can derive the accumulated phase of gravitational waves $\phi(t) = 2\int \mathrm{d}\tau\omega(\tau)$. An implicit assumption in the energy balance equation is that E does not change much over an orbital timescale. In other words, the adiabatic solutions are orbit-averaged and thus remove some of the orbital detail. The adiabatic approximation fails to account for secular evolution of some of the orbital elements, which can lead to measurable phasing effects [52].

When considering spinning black holes, which adds 6 additional degrees of freedom, the binary motions become more complicated. The convention of the PN order counting of the spin here is defined as $|\boldsymbol{S}| = \chi m^2$, where m is the mass of the object and χ a dimensionless spin parameter. For a maximally rotating compact BHs, $\chi \sim 1$. The leading contributions from spin-orbit effects enter into the motion at 1.5PN and spin-spin at 2PN, before the leading order radiation reaction force. The major effect of the presence of the spin on the orbital evolution is that a spin component perpendicular to the orbital angular momentum causes the orbital plane to precess. This means the orbital plane will change its orientation when it is not perpendicular to the spin vector. Thus the observed waveform, depending on the orbital orientation with respect to the detector, will modulate due to spin-induced orbital precession. The secular evolutions of the spins themselves are given by the spin precession equations [53, 54]. With the spin precession equations, it is possible to determine the angular momentum transfer between orbital and spin angular momenta and the total angular momentum loss during the inspiral regime. One of the recent works to construct analytic spin-precessing inspirals is through multiple scale analysis [55, 56]. This method gives orbit-averaged and precession-averaged closed form solutions by making a clean separation among the orbital time, precession time, and radiation reaction time scales and treating the

physical parameters by averaging over the longer time scales to solve for the shorter ones. However, any averaging procedure results in the loss of some of the orbital dynamics.

In order to find analytic solutions to the spinning binary equations of motion and spin precession equations without any averaging procedures, we follow the Dynamical Renormalization Group (DRG) formalism proposed by Galley and Rothstein in [15]. The idea of the DRG method is based on renormalization group theory and the resummation of the singularities for perturbative ordinary differential equation problems [57]. The DRG method applied to binary inspirals starts by treating some of the higher PN order radiation reaction terms as a perturbation to a conservative background orbit. The secular growths of the perturbations are then resummed to preserve the correct power counting of the perturbations. In their work, Galley and Rothstein calculated the resummed solution for a non-spinning binary with leading order radiation up to the second-order corrections and included the PN corrections to the radiation reaction force. In this chapter we incorporate spin-orbit effects and the leading-order radiation reaction, using the DRG method to obtain real-time solutions to the generic precessing compact binaries.

4.1 Leading Order Spin-Orbit Equations of Motion And Spin Precessions

The equations of motion of the compact binaries in the center-of-mass frame, including the Newtonian order, the leading-order spin-orbit contributions at 1.5PN in covariant spin supplementary condition (SSC), and the Burke-Thorne term due to the radiation-reaction force at 2.5PN, are given by [9, 14, 58]

$$\boldsymbol{a} = \boldsymbol{a}_{\rm N} + \boldsymbol{a}_{\rm SO} + \boldsymbol{a}_{\rm RR}, \tag{4.1}$$

where the terms in the post-Newtonian hierarchy are

$$\boldsymbol{a}_{\rm N} = -\frac{M}{r^2}\hat{\boldsymbol{n}}, \tag{4.2}$$

$$\boldsymbol{a}_{\rm SO} = \frac{1}{r^3}\Big\{6\hat{\boldsymbol{n}}\Big[(\hat{\boldsymbol{n}}\times\boldsymbol{v})\cdot\Big(2\boldsymbol{S}+\Delta\boldsymbol{\Sigma}\Big)\Big] - \Big[\boldsymbol{v}\times\Big(7\boldsymbol{S}+3\Delta\boldsymbol{\Sigma}\Big)\Big] + 3\dot{r}\Big[\hat{\boldsymbol{n}}\times\Big(3\boldsymbol{S}+\Delta\boldsymbol{\Sigma}\Big)\Big]\Big\}, \tag{4.3}$$

$$\boldsymbol{a}_{\rm RR} = \frac{M^2\nu}{15r^4}\dot{r}\Big(\frac{136M}{r} + 72\boldsymbol{v}^2\Big)\boldsymbol{r} - \frac{8M^2\nu}{5r^3}\Big(\frac{3M}{r} + \boldsymbol{v}^2\Big)\boldsymbol{v}. \tag{4.4}$$

In the expressions above, $\boldsymbol{r}$ and $\boldsymbol{v}$ are the binary relative center-of-mass separation and velocity, $\hat{\boldsymbol{n}} \equiv \boldsymbol{r}/r$ and $\dot{r} = {\rm d}r/{\rm d}t = \hat{\boldsymbol{n}} \cdot \boldsymbol{v}$. The binary masses are denoted as $m_{1,2}$, the total binary mass $M = m_1 + m_2$, $\nu \equiv m_1 m_2/M^2$ and $\Delta \equiv (m_1 - m_2)/M$. The combinations of the individual spins are written as

$$\boldsymbol{S} = \boldsymbol{S}_1 + \boldsymbol{S}_2, \qquad \boldsymbol{\Sigma} = \frac{\boldsymbol{S}_2}{X_2} - \frac{\boldsymbol{S}_1}{X_1}, \tag{4.5}$$

with $X_a = m_a/M$. The spin vectors precess due to spin-orbit coupling following the relation of [10, 14]

$$\dot{\boldsymbol{S}}_a = \frac{1}{r^3}\big(\boldsymbol{L}_N \times \boldsymbol{S}_a\big)\left(2 + \frac{3}{2}\frac{m_b}{m_a}\right), \tag{4.6}$$

where $\{a, b\}$ are the binary labels $\{1, 2\}$, and $\boldsymbol{L}_N = \nu M(\boldsymbol{r} \times \boldsymbol{v})$ is the Newtonian orbital angular momentum.

In order to obtain the analytic solutions to the inspiral equations of motions and the spin precession equations (4.1)-(4.6), we adopt a coordinate frame $\{\boldsymbol{n}, \boldsymbol{\lambda}, \boldsymbol{l}\}$, moving along with the center-of-mass and the orientation of its motion [58–60], where $\boldsymbol{l} = \boldsymbol{n} \times \boldsymbol{v}/|\boldsymbol{n} \times \boldsymbol{v}|$ and $\boldsymbol{\lambda} = \boldsymbol{l} \times \boldsymbol{n}$ to complete an orthonormal basis triad. In this moving basis, the relative velocity can be expressed as

$$\boldsymbol{v} = \dot{r}\boldsymbol{n} + r\omega\boldsymbol{\lambda} \tag{4.7}$$

where ω is the orbital angular frequency of the binary. The relative acceleration $\boldsymbol{a} = {\rm d}\boldsymbol{v}/{\rm d}t$ in the moving basis is

$$\boldsymbol{a} = (\ddot{r} - r\omega^2)\boldsymbol{n} + (r\dot{\omega} + 2\dot{r}\omega)\boldsymbol{\lambda} + r\varpi\omega\boldsymbol{l}, \tag{4.8}$$

where the orbital plane precession ϖ of the orbit is defined as $\varpi \equiv -\boldsymbol{\lambda} \cdot {\rm d}\boldsymbol{l}/{\rm d}t$.

In terms of the moving basis components, the equations of motions (4.1) are

$$\ddot{r} - r\omega^2 = -\frac{M}{r^2} + \frac{64M^3\nu}{15r^4}\dot{r} + \frac{16M^2\nu}{5r^3}\dot{r}^3 + \frac{16M^2\nu}{5r}\dot{r}\omega^2 + \frac{\omega}{r^2}\big(5S_l + 3\Delta\Sigma_l\big), \tag{4.9}$$

$$r\dot{\omega} + 2\dot{r}\omega = -\frac{24M^3\nu}{5r^3}\omega - \frac{8M^2\nu}{5r^2}\dot{r}^2\omega - \frac{8M^2\nu}{5}\omega^3 - \frac{2\dot{r}}{r^3}S_l, \tag{4.10}$$

$$\varpi = \frac{2\dot{r}}{r^4\omega} S_\lambda + \frac{7}{r^3} S_n + \frac{3\Delta}{r^3}\Sigma_n, \tag{4.11}$$

where we decompose the spin $\boldsymbol{S} = S_n \boldsymbol{n} + S_\lambda \boldsymbol{\lambda} + S_l \boldsymbol{l}$, and similarly for $\boldsymbol{\Sigma}$. The spin precession equations (4.6) become

$$\frac{\mathrm{d}S_n^a}{\mathrm{d}t} = \Big(\omega - \Omega_a\Big) S_\lambda^a, \tag{4.12}$$

$$\frac{\mathrm{d}S_\lambda^a}{\mathrm{d}t} = -\Big(\omega - \Omega_a\Big) S_n^a + \varpi S_l^a, \tag{4.13}$$

$$\frac{\mathrm{d}S_l^a}{\mathrm{d}t} = -\varpi S_\lambda^a, \tag{4.14}$$

where we denote

$$\Omega_a \equiv \frac{\nu M \omega}{r}\left(2 + \frac{3}{2}\frac{m_b}{m_a}\right), \tag{4.15}$$

which is the norm of the precession vector of the a-th spin. The precession frequency ϖ, explicitly given by (4.11), is of order $\mathcal{O}(S)$. At linear order in spin, the precession equations become

$$\frac{\mathrm{d}S_n^a}{\mathrm{d}t} = \Big(\omega - \Omega_a\Big) S_\lambda^a, \tag{4.16a}$$

$$\frac{\mathrm{d}S_\lambda^a}{\mathrm{d}t} = -\Big(\omega - \Omega_a\Big) S_n^a + \mathcal{O}(S^2), \tag{4.16b}$$

$$\frac{\mathrm{d}S_l^a}{\mathrm{d}t} = \mathcal{O}(S^2). \tag{4.16c}$$

Thus at order $\mathcal{O}(S)$, the l-component of the spin vectors are invariant, which are also the only components that appears in the orbital equations of motion in (4.9) and (4.10). In solving these two equations by the DRG method, we then are able to treat S_l and Σ_l as time-independent constants. Following Ref [15], here we ignore the 1PN and 2PN conservative forces, as well as the next-to-leading order spin-orbit effects, which is the same order in the Post-Newtonian expansion as the 2.5PN radiation reaction terms. Instead, we focus on the leading order radiation reaction effects on spinning objects. In order to obtain gravitational wave templates, to be consistent we would need to include at least the 1PN conservative forces.

4.2 DRG Solutions to Dynamics and Spin Precession

The background quasi-circular orbit of a conserved binary with Newtonian and leading spin-orbit effects can be described by

$$\Omega_B^2 = \frac{M}{R_B^3} - \frac{\Omega_B}{R_B^3}\big(5S_l + 3\Delta\Sigma_l\big), \tag{4.17}$$

with constant radius R_B and constant angular frequency Ω_B. To include the radiation reaction as perturbative effects, we write the orbital solutions as

$$r(t) = R_B + \delta r(t) + \delta r_S(t), \qquad \omega(t) = \Omega_B + \delta\omega(t) + \delta\omega_S(t), \tag{4.18}$$

where the first time-dependent terms $\delta r(t)$ and $\delta\omega(t)$ are the perturbation due to the 2.5PN radiation reaction force without the spin at a given time t. The $\delta r_S(t)$ and $\delta\omega_S(t)$ represent the perturbations due to the interaction of 1.5PN spin effects and the 2.5PN radiation reaction. The power counting at the initial time t_0 for each perturbation is given by

$$\delta r \sim v^5 R_B, \qquad \delta\omega \sim v^6/R_B, \qquad \delta r_S \sim Sv^4/R_B, \qquad \delta\omega_S \sim Sv^5/R_B^3 \tag{4.19}$$

where we keep the spin as a placeholder expansion parameter instead of converting to PN orders for generality. Substituting the perturbed orbital radius and frequency into the equations of motion (4.9) and (4.10), we find the solutions to the perturbation

$$\begin{aligned}\delta r_S(t) =& -\Big(\frac{144}{5}S_l + 48\Delta\Sigma_l\Big)\nu R_B^3\Omega_B^5(t-t_0) + A_B^S\cos\left(\Omega_B(t-t_0)+\Phi_B\right)\\ &+\frac{\big(7S_l+3\Delta\Sigma_l\big)}{2\Omega_B R_B^3}A_B\Big[2\Omega_B(t-t_0)\cos\left(\Omega_B(t-t_0)+\Phi_B\right)-\sin\left(\Omega_B(t-t_0)+\Phi_B\right)\Big],\end{aligned} \tag{4.20a}$$

$$\begin{aligned}\delta\omega_S(t) =& \Big(-\frac{24}{5}S_l+\frac{216}{5}\Delta\Sigma_l\Big)\nu R_B^2\Omega_B^6(t-t_0)+\big(5S_l+3\Delta\Sigma_l\big)\frac{A_B}{R_B^4}\sin\left(\Omega_B(t-t_0)+\Phi_B\right)\\ &-\big(14S_l+6\Delta\Sigma_l\big)\frac{A_B}{R_B^4}\Omega_B(t-t_0)\cos\left(\Omega_B(t-t_0)+\Phi_B\right)\\ &-\frac{2A_B^S\Omega_B}{R_B}\cos\left(\Omega_B(t-t_0)+\Phi_B\right).\end{aligned} \tag{4.20b}$$

and also the time integration of $\delta\omega_S(t)$, $\delta\Phi_S(t)$, which is the perturbation of the orbital phase $\phi(t)$,

$$\begin{aligned}\delta\Phi_S(t) =&\Big(-\frac{12}{5}S_l - \frac{2A_B^S}{R_B}\sin\left(\Omega_B(t-t_0)+\Phi_B\right)\\ &+\frac{108}{5}\Delta\Sigma_l\Big)\nu R_B^2\Omega_B^6(t-t_0)^2 - \Big(19S_l+9\Delta\Sigma_l\Big)\frac{A_B}{\Omega_B R_B^4}\cos\left(\Omega_B(t-t_0)+\Phi_B\right)\\ &-\Big(14S_l+6\Delta\Sigma_l\Big)\frac{A_B}{R_B^4}(t-t_0)\sin\left(\Omega_B(t-t_0)+\Phi_B\right),\end{aligned} \tag{4.20c}$$

where Φ_B, A_B, and A_B^S are integration constants. $\{R_B, \Omega_B, \Phi_B, A_B, A_B^S\}$ forms a set of bare parameters to be determined by initial conditions. While $e_B = A_B/R_B$ is the small orbital eccentricity of order $\mathcal{O}(v^5)$ induced by the radiation reaction force, the interaction between the spin and radiation reaction lead to a smaller eccentricity $e_B^S = A_B^S/R_B \sim \mathcal{O}(Sv^4)$. The spin-radiation eccentricity deforms the circular orbit out-of-phase compared to the radiation eccentricity, although with a fixed phase difference.

To maintain the power countings of the perturbations, the secularly growing terms in (4.20) are absorbed into the bare parameters through the relations

$$R_B(t_0) = R_R(\tau) + \delta_R^{v^5}(\tau, t_0) + \delta_R^S(\tau, t_0), \tag{4.21a}$$

$$\Omega_B(t_0) = \Omega_R(\tau) + \delta_\Omega^{v^5}(\tau, t_0) + \delta_\Omega^S(\tau, t_0), \tag{4.21b}$$

$$\Phi_B(t_0) = \Phi_R(\tau) + \delta_\Phi^{v^5}(\tau, t_0) + \delta_\Phi^S(\tau, t_0), \tag{4.21c}$$

$$A_B^S(t_0) = A_R^S(\tau) + \delta_A^S(\tau, t_0), \tag{4.21d}$$

where $\{R_R, \Omega_R, \Phi_R, A_R^S\}$ are the "renormalized" parameters depending on an arbitrary renormalization scale τ. The quantities $\{\delta_R^{v^5}, \delta_R^S, \delta_\Omega^{v^5}, \delta_\Omega^S, ...\}$ are counter-terms, to be determined by renormalizing the perturbation expansions. Introducing the renormalization scale into the perturbation solutions (4.20) by writing $t - t_0 = (t-\tau) + (\tau - t_0)$ and using the counter-terms to cancel all the secular $(\tau - t_0)$ terms, we find that

$$r(t) = R_R(t) + \left(1 - \frac{\left(7S_l + 3\Delta\Sigma_l\right)}{2\Omega_R(t)R_R^3(t)}\right)A_R(t)\sin\Phi_R(t) + A_R^S(t)\cos\Phi_R(t), \tag{4.22a}$$

$$\omega(t) = \Omega_R(t) - \frac{2\Omega_R(t)A_R(t)}{R_R(t)}\left(1 - \frac{\left(5S_l + 3\Delta\Sigma_l\right)}{2\Omega_R(t)R_R^3(t)}\right)\sin\Phi_R(t) - \frac{2A_R^S\Omega_R(t)}{R_R(t)}\cos\Phi_R(t), \tag{4.22b}$$

$$\phi(t) = \Phi_R(t) + \frac{2A_R(t)}{R_R(t)}\left(1 - \frac{\big(19S_l + 9\Delta\Sigma_l\big)}{2\Omega_R(t)R_R^3(t)}\right)\cos\Phi_R(t) - \frac{2A_R^S(t)}{R_R(t)}\sin\Phi_R(t), \tag{4.22c}$$

where $r(t)$ and $\omega(t)$ are the orbital radius and frequency defined in the previous section, and $\phi(t)$ is the time integral of $\omega(t)$ representing the orbital phase of the binary inspiral. The renormalized parameters are determined at arbitrary time via the renomalization group equations, determined using the fact that the corresponding bare parameters are independent of the choice of τ. The "beta-functions" of the RG equations are determined by the counter-terms, leading to the first-order equations satisfied by the renormalized parameters. We give the RG solutions in the form of invariance in time as

$$\frac{64\nu M^3}{5}t + \frac{2\mathscr{S}}{5M^{1/2}}R_R(t)^{5/2} + \frac{\mathscr{S}^2}{M}R_R(t) + \frac{2\mathscr{S}^{8/3}}{\sqrt{3}M^{4/3}}\tan^{-1}\left(\frac{1}{\sqrt{3}} + \frac{2M^{1/6}R_R(t)^{1/2}}{\sqrt{3}\mathscr{S}^{1/3}}\right) + \frac{\mathscr{S}^{8/3}}{3M^{4/3}}\ln\left(\frac{\Big(\mathscr{S}^{1/3} - M^{1/6}R_R(t)^{1/2}\Big)^2}{\mathscr{S}^{2/3} + \mathscr{S}^{1/3}M^{1/6}R_R(t)^{1/2} + M^{1/3}R_R(t)}\right) = \text{constant}, \tag{4.23a}$$

$$\Omega_R^2(t)R_R^3(t) + \Omega_R(t)\big(5S_l + 3\Delta\Sigma_l\big) = M, \tag{4.23b}$$

$$\Phi_R(t) + \frac{R_R^{5/2}(t)}{32M^{5/2}\nu} - \frac{5\Big(41S_l + 15\Delta\Sigma_l\Big)}{256\nu M^2\mathscr{S}^2}\Big(\frac{64\nu M^3}{5}t + \frac{1}{4}R_R^4(t) + \frac{2\mathscr{S}}{5M^{1/2}}R_R^{5/2}(t)\Big) = \text{constant}, \tag{4.23c}$$

$$A_R(t) = \text{constant}, \tag{4.23d}$$

$$A_R^S(t) - \frac{5A_R\Big(7S_l + 3\Delta\Sigma_l\Big)}{64\nu M^2\mathscr{S}^2}\left(\frac{64\nu M^3}{5}t + \frac{1}{4}R_R^4(t) + \frac{2\mathscr{S}}{5M^{1/2}}R_R^{5/2}(t)\right) = \text{constant}, \tag{4.23e}$$

where for convenience we have defined $\mathscr{S} \equiv (51 + 21\Delta\Sigma_l)/4$. Remember, at this order the l-component of the spin vectors are constant. The constants in the equations above can be further determined using the initial conditions by solving (4.22) at a given time instant. The expressions in (4.22) combined with (4.23) give the resummed solution to the 0PN spinning inspiral dynamics valid up to times $(t - t_0)$ of order $1/(\nu v^5(t)\Omega_R(t))$. To improve the accuracy,

we need to calculate higher order perturbations in the same formalism or include higher PN conservative corrections to the motions.

The background solution to the conserved spin precessions has a constant precession frequency. We renormalize the precession frequency perturbed by the radiation reaction using the same DRG procedure. The resummed solutions to the spin precession equations (4.6) are

$$S^a_+(t) = \mathcal{S}^a_{+R}(t) \exp\left\{ i\left[\frac{2A^S_R(t)}{R_R(t)} - \frac{3\nu_a}{\nu} A^S_R(t)\Omega_R(t)^2 R_R(t)\right]\sin\Phi_R(t) \right.$$
$$- i\left[\frac{2A_R(t)}{R_R(t)} - \Big(19S_l + 9\Delta\Sigma_l\Big)\frac{A_R(t)}{R_R(t)^4\Omega_R(t)} - \frac{3\nu_a}{\nu}\Omega_R(t)^2 A_R(t) R_R(t)\right.$$
$$\left.\left. + \frac{\nu_a}{\nu}\Big(\frac{29}{2}S_l + \frac{9}{2}\Delta\Sigma_l\Big)\frac{A_R(t)\Omega_R(t)}{R_R(t)^2}\right]\cos\Phi_R(t)\right\}, \tag{4.24}$$

where $\nu_a \equiv (2 + \frac{3m_b}{2m_a})\nu^2$ and $S^a_+ \equiv S^a_n + iS^a_\lambda$ contains the two precessing components of the spin vector in the moving triad $\{\boldsymbol{n}, \boldsymbol{\lambda}, \boldsymbol{l}\}$ coordinate system. The exponential preserves the magnitudes of the spin vectors, which is conserved as can easily be seen from Eq. (4.6). The renormalized parameter $\mathcal{S}^a_{+R}(t)$ can be written in terms of invariance over time and other parameters as

$$i\ln\mathcal{S}^a_{+R}(t) - \Phi_R(t) - \frac{5\nu_a R^{3/2}_R(t)}{96M^{3/2}\nu^2} - \frac{5\Big(41S_l + 15\Delta\Sigma_l\Big)\nu_a}{384M^2\nu^2}\ln\left(M^{1/2}R^{3/2}_R(t) - \mathscr{S}\right) = \text{constant}. \tag{4.25}$$

We include the more detailed calculations and renormalization procedures in the appendices for interested readers.

4.3 Numerical Solution Comparison

To compare our analytic solutions to the orbital equations of motion and the spin precession equations, we solve the sets of equations numerically and compare with the DRG solution solved with the same initial conditions. We choose to compare compact binary systems of total mass $M = 1$. The initial conditions for the physical parameters are related

to the renormalized parameters through the renormalized solutions (C.12) and (C.35) at $t_i = 0$. We choose for our initial conditions

$$\begin{aligned}
&\begin{cases}
\Omega_R(0) &= 10^{-2}/M \\
R_R(0) &= \left(\dfrac{M}{\Omega_R(0)^2} - \dfrac{5S_l + 3\Delta\Sigma_l}{\Omega_R(0)}\right)^{1/3} \\
\Phi_R(0) &= 0 \\
A_R^S(0) &= 0 \\
A_R(0) &= \dfrac{\dfrac{64\nu}{5}R_R(0)^6\Omega_R(0)^5 + \dfrac{\nu}{5}R_R(0)^3\Omega_R(0)^4(144S_l + 240\Delta\Sigma_l)}{\left(1 + \dfrac{7S_l + 3\Delta\Sigma_l}{2R_R(0)^3\Omega_R(0)}\right)}
\end{cases} \\
\Longrightarrow \quad &\begin{cases}
r(0) &= R_R(0) \\
\dot{r}(0) &= 0 \\
\omega(0) &= \Omega_R(0) \\
\phi(0) &= \dfrac{2A_R(0)}{R_R(0)}\left(1 - \dfrac{19S_l + 9\Delta\Sigma_l}{2R_R(0)^3\Omega_R(0)}\right)
\end{cases}
\end{aligned} \tag{4.26}$$

where the expression for $A_R(0)$ comes from

$$\begin{aligned}
\dot{r}(t_i) =& A_R(t_i)\Omega_R(t_i)\cos\Phi_R(t_i)\left(1 + \frac{7S_l + 3\Delta\Sigma_l}{2R_R(t_i)^3\Omega_R(t_i)}\right) - \frac{64\nu}{5}R_R(t_i)^6\Omega_R(t_i)^6 \\
&- \frac{1}{5}\nu R_R(t_i)^3\Omega_R(t_i)^5(144S_l + 240\Delta\Sigma_l) - A_R^S(t_i)\Omega_R(t_i)\sin\Phi_R(t_i).
\end{aligned} \tag{4.27}$$

and $\dot{r}(0)$ is taken to be zero for quasi-circular motion. Meanwhile, we impose a small non-vanishing $\mathcal{O}(v^5)$ eccentricity $e_R = A_R/R_R(t)$, and a spin-induced eccentricity $e_R^S = A_R^S(0)/R_R(0)$ at $\mathcal{O}(v^4 S)$ that runs starting from zero.

For initial spin vectors we consider the compact components maximally rotating, meaning the dimensionless spin parameter $\chi \sim 1$ where for each spin $|\boldsymbol{S}_a| = \chi_a m_a^2$, with $\chi_{\max} = 1$ for black holes. In Fig. 4.1 we compare the resummed solutions to the orbital equations of motion with the numerical and adiabatic solutions [61] for two different choices of mass ratio and spins. For the left column, we choose an equal mass binary and anti-aligned spin initial configuration:

$$\frac{\boldsymbol{S}_1(0)}{m_1^2} = \cos 70^\circ \hat{\boldsymbol{n}} + \cos 60^\circ \hat{\boldsymbol{\lambda}} + \cos 140^\circ \hat{\boldsymbol{l}},$$

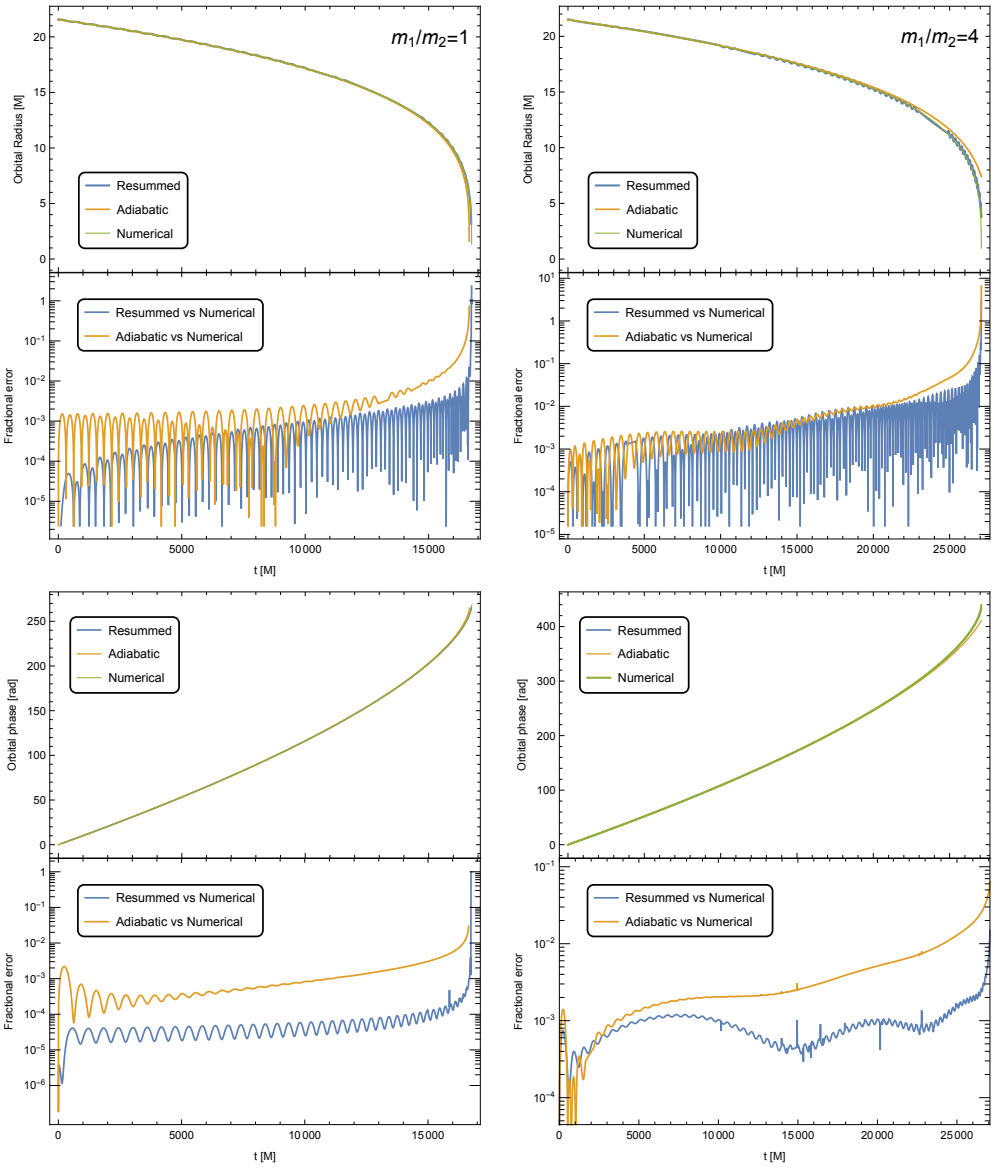

Figure 4.1: **Left Column**: Compact binary with equal component mass and anti-aligned initial spin vectors. **Right Column**: Compact binary with component mass ratio $m_1 : m_2 = 4$ and misaligned initial spin vectors. The initial spin configurations are given by (4.28) and (4.29), respectively. The first and third rows are the plots for physical values: the orbital radius and phase versus time with initial data given in (4.26), respectively. The analytical renormalization group resummed solutions are plotted in **blue**, the adiabatic solutions are in **orange**, and the numerical solutions to the leading order spin-radiation equations of motion are in **green**. Below each physical plot the fractional errors are shown, comparing the numerical solutions with analytical resummed solutions in **blue** and the adiabatic solutions in **orange**.

$$\frac{\boldsymbol{S}_2(0)}{m_2^2} = \frac{\cos 70^\circ \cos 50^\circ}{\cos 140^\circ}\hat{\boldsymbol{n}} + \frac{\cos 60^\circ \cos 50^\circ}{\cos 140^\circ}\hat{\boldsymbol{\lambda}} + \cos 50^\circ \hat{\boldsymbol{l}}. \tag{4.28a}$$

The physical interpretation for the angle of 140° and 50° is the angle between the spin vectors and the orbital angular momentum $\boldsymbol{L}$. (At linear order in spin, equal mass systems satisfy the spin-orbit resonance orientations [62].) In the right column, we choose a moderate mass ratio ($m_1 : m_2 = 4$), with a randomly chosen initial spin configuration:

$$\frac{\boldsymbol{S}_1(0)}{m_1^2} = 0.4\hat{\boldsymbol{n}} - 0.7\hat{\boldsymbol{\lambda}} + 0.5\hat{\boldsymbol{l}}, \qquad \frac{\boldsymbol{S}_2(0)}{m_2^2} = 0.9\hat{\boldsymbol{n}} + 0.1\hat{\boldsymbol{\lambda}} - 0.4\hat{\boldsymbol{l}}. \tag{4.29}$$

Specifically, the plots show the orbital radius $r(t)$ and orbital phase $\phi(t)$ for resummed, adiabatic, and numerical solutions to the binary equations of motion. Below each plot of the physical solutions are the fractional errors comparing the numerical results to resummed and adiabatic ones. From these plots, we can see the DRG methods are more accurate compared to the adiabatic solutions, with roughly an order of magnitude improvement in calculating the accumulated orbital phase over most of the inspiral.

We can see the importance of using the DRG method increases as we include higher-order corrections by comparing Fig. 4.1 to the results in Ref. [15]. In that chapter, the authors included the 0PN (i.e. Newtonian) contribution and the leading order radiation reaction term. As can be seen by looking at Fig. 1 of that chapter, the DRG and adiabatic results give the same order relative errors.[1] When including the 1.5PN spin contribution as we did here, there is an order of magnitude improvement, as shown in Fig. 4.1.

We compare the resummed solutions of the spin precession equations with the numerical solutions to (4.16) in Fig. 4.2. The two columns have the same choices for mass ratio and spin configurations as in Fig. 4.1. In the top two panels, we plot the resummed solutions to the $\boldsymbol{n}$- and $\boldsymbol{\lambda}$-components, respectively, for the total spin vector (in blue) and the difference between the resummed and numerical solution (in red). We also include an inset plot of the spin precession for the last quarter of the inspiral to illustrate the phase difference. That the error accumulated from the resummed results of the spin precession becomes significant is

[1] Note that the authors of Ref. [15] show how to obtain the result including 1PN contributions, but did not provide any numerical results. They also did the "two-loop" contribution, which includes $\mathcal{O}(v^{10})$ corrections. Including these, the DRG method shows roughly an order of magnitude improvement compared to the adiabatic solution, as can be seen in Fig. 2 of that chapter.

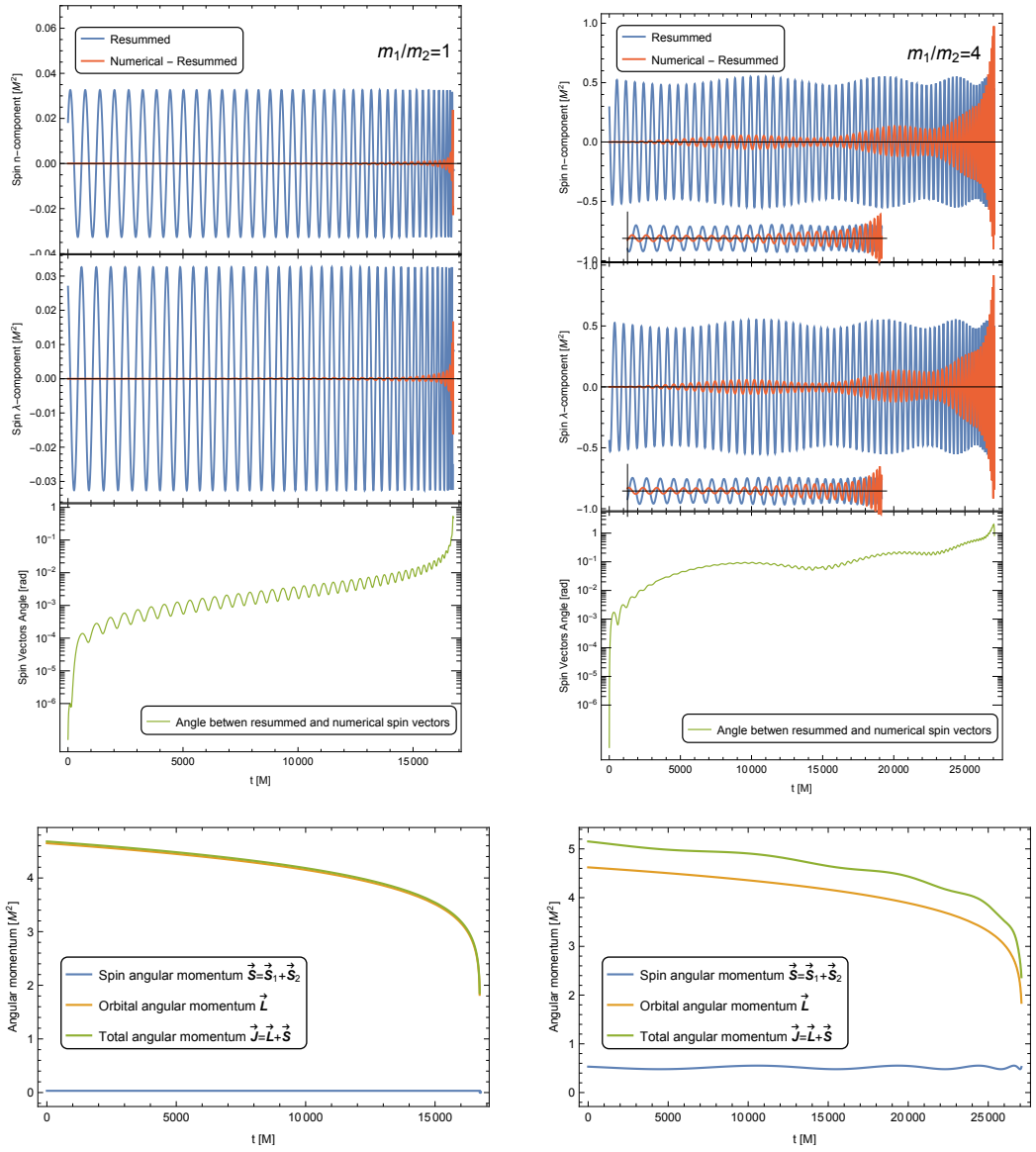

Figure 4.2: **Left Column**: Compact binary with equal component mass and anti-aligned initial spin vectors. **Right Column**: Compact binary with component mass ratio $m_1 : m_2 = 4$ and misaligned initial spin vectors. The initial spin configurations are given by (4.28) and (4.29), respectively. In the first two rows from top down, the resummed solutions are in **blue**, for the corresponding spin vectors in n-component and λ-component. The difference of the resummed results from the numerical ones is shown in **red**. The lower inset on the right zooms in on the spin precession for the last 1/4 part of the inspiral. The third row shows the angle between the spin vector derived from the resummed solutions and the numerical solutions. In the last row, the instantaneous change of spin, orbital, and total angular momenta are shown.

the consequence of the Post-Newtonian method breaking down for large velocities during the later portion of the inspiral. We expect better accuracy when spin-spin effects and higher PN order terms are incorporated. In the third panel, we plot the angle between the spin vector results from the resummed and numerical solutions.

With the inclusion of radiation reaction, the total angular momentum changes direction and magnitude. In the bottom row of Fig. 4.2, we show the angular momenta changing throughout the inspiral. The equal mass binary shown in the left panel has a fixed total spin magnitude due to the symmetric form in (4.6). Both binaries exhibit a rapid loss of orbital and total angular momenta at the end of the inspiral in sync with the drop of the orbital radius in Fig 4.1.

In Fig. 4.3 we give a rough comparison of the computational runtime improvement of the DRG methods. The numerical solution for the equations of motion and spin precession was calculated in C++ implementing the ODEINT library [63]. We adopt the Dormand-Prince algorithm at fifth order with adaptive step sizes and control the tolerance error to be consistent with the theoretical resummed solution errors. Fig. 4.3 shows the runtime of the numerical and DRG methods solving the same sets of initial conditions, changing the binary mass ratio Count times in each run. In order to try to have a meaningful comparison, we manipulate the average steps taken per run for the DRG methods to have similar output lengths (i.e., number of time steps for the solution) with the numerical integration. For example, in a total of 50 runs, the numerical integration takes 10 seconds and averagely 11235 steps per run, while the DRG method takes about 1 second and averagely 11438 steps per run. As can be seen, the DRG method is an order of magnitude faster than the numerical solution.

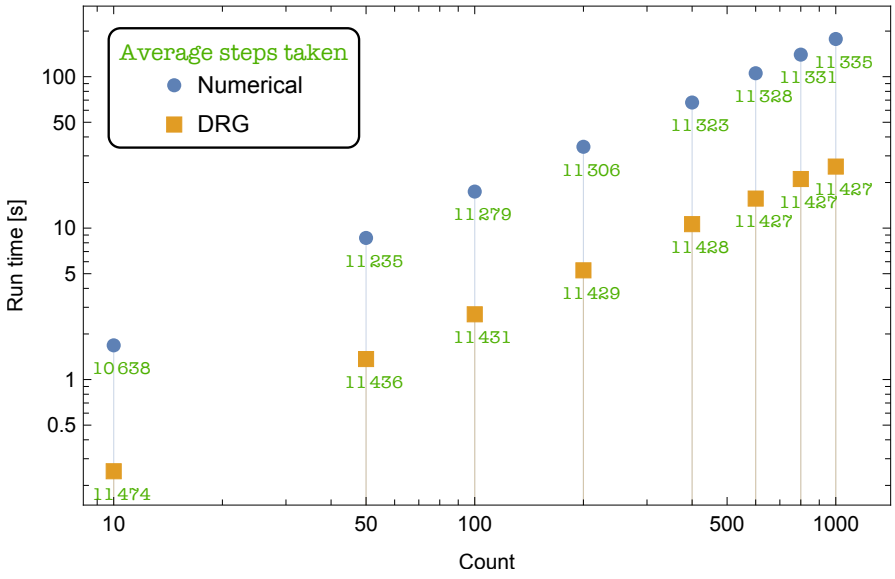

Figure 4.3: C++ runtime comparison between numerical integration and DRG resummed substitution. The count in the x-axis stands for the total choices of initial conditions in a particular run, and green numbers below the plot points are the average steps taken per run. The blue dots show the total computation time for the numerical integration solutions and the orange squares shows the time for the DRG resummed results substitutions.

5.0 Conclusion

To conclude, we summarize the results of the studies discussed in previous chapters, detailed features of the each analysis can be found in the corresponding sections.

In Chapter 3, we provided an independent computation of the 2PN correction to the mass quadrupole moment of a binary system of compact bodies moving in general orbits, using the EFT approach in the linearized harmonic gauge. We calculated high order corrections to the components of the pseudo-stress-energy tensor, which were used to obtain the mass quadrupole moment correction as well as the 1PN correction to the conserved energy and to the linear and angular momenta of the system and the 2PN correction to the center of mass frame. We used these quantities to perform tests that confirmed the consistency of our results within the EFT formalism itself and with results presented in the literature computed using different formalisms. Therefore, we not only extracted the contributions of the stress-energy pseudotensor to the 2PN correction to the mass quadrupole, but we provided the expressions for the components of the pseudotensor with higher order corrections that will be useful for future calculations on the dynamics of compact binary system.

We also calculated the 2PN correction to the equation of motion in the linearized harmonic gauge that was used, together with the mass quadrupole moment obtained in this chapter, to write down the power loss due to the emission of gravitational waves. We thus compared our results against the literature and we showed that the 2PN correction to the mass quadrupole moment, to the relative acceleration of the two-body system and to the power loss obtained in this chapter are in agreement with the results computed via the BDI and in the Epstein-Wagoner formalisms once a coordinate transformation is performed.

Although the 2PN correction to the mass quadrupole and to the equation of motion of compact binary systems obtained here were known in the literature, this derivation establishes the ground work for higher order calculations in the EFT formalism. Finally, these are the final missing ingredients necessary for the analysis of the radiation reaction of the binary system at the next-to-next-to-leading order in the EFT approach, which will be presented in the future.

In Chapter 4 we have solved the spinning binary dynamics including the 2.5PN radiation reaction and the leading order spin-orbit effects throughout the inspiral using the dynamical renormalization group formalism,. The solution is obtained by the resummation of the secularly growing perturbations to the physical parameters including orbital radius, angular frequency, orbital phase, and spin precession phases. We solved the resummed solutions to the equations of motion and spin precession equations in a moving triad frame at any time instant. Renormalized parameters defined to describe the resummed solutions are determined using the renormalization group equations and can be written in terms of conserved identities.

The solutions are applicable to arbitrary initial configurations and do not dependent on any specific spin orientations. The comparison of numerical solutions and our analytic solutions shows greater accuracy than the adiabatic solutions and a sizable improvement in computation time compared to the numerical solutions. The use of the DRG method is more important for spinning BHs than for the non-spinning case. However, there is further improvements that can be made. The spin component comparison is not ideal, as shown in Fig. 4.2 with increasing phase differences. When initial spins are relatively large compare to orbital angular momentum, the discrepancy grows very fast in the early part of the inspiral. This is due to the beginning of the breakdown of the PN expansion. We hope to fix this issue and enhance the accuracy by the inclusion of spin-spin effects and higher-order PN terms into the formulation in the future works.

Appendix A Gravity EFT Feynman Rules and Useful Integrals

In this appendix we show the ingredients used to compute the components of the pseudotensor. We used the package xAct [64] from Mathematica for the extraction of the vertices from the action.

A.1 Source Terms

The source action terms needed to compute the contributions to T^{00}_{2PN} are given below:

$$S^{\mathbf{v}^0} = -\sum_a \frac{m_a}{2m_{Pl}} \int dt_a H^{00}(x_a), \tag{A.1}$$

$$S^{\mathbf{v}^1} = \sum_a \frac{m_a}{m_{Pl}} \int dt_a \mathbf{v}_a^i H^{0i}(x_a), \tag{A.2}$$

$$S^{\mathbf{v}^2} = -\sum_a \frac{m_a}{2m_{Pl}} \int dt_a \left(\frac{\mathbf{v}_a^2}{2} H^{00}(x_a) + \mathbf{v}_a^i \mathbf{v}_a^j H^{ij}(x_a) \right), \tag{A.3}$$

$$S^{\mathbf{v}^0}_{\bar{h}^{00}} = \sum_a \frac{m_a}{4m_{Pl}^2} \int dt_a H^{00}(x_a) \bar{h}^{00}(x_a), \tag{A.4}$$

$$S^{\mathbf{v}^1}_{\bar{h}^{00}} = -\sum_a \frac{m_a}{2m_{Pl}^2} \int dt_a \mathbf{v}_a^i H^{0i}(x_a) \bar{h}^{00}(x_a), \tag{A.5}$$

$$S^{\mathbf{v}^2}_{\bar{h}^{00}} = \sum_a \frac{m_a}{8m_{Pl}^2} \int dt_a \left(3\mathbf{v}_a^2 H^{00}(x_a) + 2\mathbf{v}_a^i \mathbf{v}_a^j H^{ij}(x_a) \right) \bar{h}^{00}(x_a), \tag{A.6}$$

$$S^{\mathbf{v}^4}_{\bar{h}^{00}} = -\sum_a \frac{3m_a}{16m_{Pl}} \int dt_a \mathbf{v}_a^4 \bar{h}^{00}(x_a), \tag{A.7}$$

$$S^{\mathbf{v}^0}_{H^2} = \sum_a \frac{m_a}{8m_{Pl}^2} \int dt_a H^{00}(x_a) H^{00}(x_a), \tag{A.8}$$

$$S^{\mathbf{v}^0}_{H^2\bar{h}^{00}} = -\sum_a \frac{3m_a}{16m_{Pl}^3} \int dt_a H^{00}(x_a) H^{00}(x_a) \bar{h}^{00}(x_a). \tag{A.9}$$

In addition, to write down the contributions for T^{0i}_{1PN} we must to consider

$$S^{\mathbf{v}^1}_{\bar{h}^{0i}} = -\sum_a \frac{m_a}{2m_{Pl}^2} \int dt_a \mathbf{v}_a^i H^{00}(x_a) \bar{h}^{0i}(x_a), \tag{A.10}$$

$$S^{\mathbf{v}^3}_{\bar{h}^{0i}} = \sum_a \frac{m_a}{2m_{Pl}} \int dt \mathbf{v}_a^2 \mathbf{v}_a^i \bar{h}^{0i}\left(x_a\right), \tag{A.11}$$

whereas for T^{ll}_{1PN} the following terms are also necessary,

$$S^{\mathbf{v}^2}_{\bar{h}^{ij}} = \sum_a \frac{m_a}{4m_{pl}^2} \int dt_a \mathbf{v}_a^i \mathbf{v}_a^j H^{00}\left(x_a\right) \overline{h}^{ij}\left(x_a\right), \tag{A.12}$$

$$S^{\mathbf{v}^4}_{\bar{h}^{ij}} = -\sum_a \frac{m_a}{4m_{pl}} \int dt_a \mathbf{v}_a^2 \mathbf{v}_a^i \mathbf{v}_a^j \overline{h}^{ij}\left(x_a\right). \tag{A.13}$$

Although all the sources terms above are conveniently expressed in position space, effectively we perform the partial Fourier transform[1]

$$H^{\mu\nu}\left(t,\mathbf{q}\right) = \int d^3x H^{\mu\nu}\left(t,\mathbf{x}\right) e^{-i\mathbf{q}\cdot\mathbf{x}}, \tag{A.14}$$

to carry out the Feynman diagrams in momentum space.

A.2 Vertices

From the EH action expanded in the radiation and potential fields and fixed with the background gauge, we obtain the propagator

$$\left\langle H_{\mu\nu}\left(t,\mathbf{q}\right) H_{\alpha\beta}\left(t',\mathbf{q}'\right)\right\rangle = -i\left(2\pi\right)^3 P_{\mu\nu\alpha\beta}\delta\left(t-t'\right)\delta^3\left(\mathbf{q}+\mathbf{q}'\right)\frac{1}{\mathbf{q}^2}, \tag{A.15}$$

as well as its correction

$$\left\langle H_{\mu\nu}\left(t,\mathbf{q}\right) H_{\alpha\beta}\left(t',\mathbf{q}'\right)\right\rangle_{v^2} = -i\left(2\pi\right)^3 P_{\mu\nu\alpha\beta}\frac{d^2}{dtdt'}\delta\left(t-t'\right)\delta^3\left(\mathbf{q}+\mathbf{q}'\right)\frac{1}{\mathbf{q}^4}. \tag{A.16}$$

The two-potential-one-radiation vertex regarded inside the momentum integrals of the internal potential momenta coupled to the particles has the form

$$\int \frac{d^3\mathbf{q}}{\left(2\pi\right)^3}\int \frac{d^3\mathbf{q}'}{\left(2\pi\right)^3} e^{-i\mathbf{q}\cdot\mathbf{x}_1} e^{-i\mathbf{q}'\cdot\mathbf{x}_2}\left\langle iS_{\bar{h}H^2}\right\rangle = -\frac{i}{m_{Pl}}\delta\left(t-t'\right)\int \frac{d^3\mathbf{q}}{\left(2\pi\right)^3} e^{-i\mathbf{q}\cdot\mathbf{x}}\frac{F\left[q,k,\bar{h}\right]}{\mathbf{q}^2\left(\mathbf{q}+\mathbf{k}\right)^2}, \tag{A.17}$$

[1] We consider the partial Fourier transform for the radiation field as well.

for which the different contractions necessary to write down the contributions to T^{00}_{2PN} are

$$F^{\left\langle H^{00}H^{00}\right\rangle}\left[q,k,\bar{h}^{00}\right]=\bar{h}^{00}\left[\frac{3}{4}\left(\mathbf{q}^2+\mathbf{k}\cdot\mathbf{q}\right)-\frac{5}{4}q_0^2-\frac{5}{4}k_0q_0-\frac{1}{2}k_0^2\right], \tag{A.18}$$

$$F^{\left\langle \mathbf{v}_1^kH^{0k}H^{00}\right\rangle}\left[q,k,\bar{h}^{00}\right]=\bar{h}^{00}\mathbf{v}_1^k\left[-\mathbf{q}^k\left(q_0+\frac{1}{2}k_0\right)\right], \tag{A.19}$$

$$F^{\left\langle \mathbf{v}_1^k\mathbf{v}_1^lH^{kl}H^{00}\right\rangle}\left[q,k,\bar{h}^{00}\right]=\bar{h}^{00}\mathbf{v}_1^k\mathbf{v}_1^l\left[\frac{1}{4}\delta^{kl}\left(\mathbf{q}^2+3\mathbf{k}\cdot\mathbf{q}\right)-\frac{1}{2}\mathbf{k}^k\mathbf{k}^l\right], \tag{A.20}$$

$$F^{\left\langle \mathbf{v}_1^kH^{0k}H^{0l}\mathbf{v}_2^l\right\rangle}\left[q,k,\bar{h}^{00}\right]=\bar{h}^{00}\mathbf{v}_1^k\mathbf{v}_2^l\left[-\frac{1}{4}\delta^{kl}\left(\mathbf{q}^2+\mathbf{k}\cdot\mathbf{q}\right)+\frac{1}{4}\mathbf{k}^k\mathbf{k}^l\right]. \tag{A.21}$$

On the other hand, to compute the contributions to T^{0i}_{1PN}, the contractions required are

$$F^{\left\langle H^{00}H^{00}\right\rangle}\left[q,k,\bar{h}^{0i}\right]=\bar{h}^{0i}\left[q_0\left(\mathbf{q}^i+\frac{1}{2}\mathbf{k}^i\right)+k_0\left(\frac{1}{2}\mathbf{q}^i+\mathbf{k}^i\right)\right], \tag{A.22}$$

$$F^{\left\langle \mathbf{v}_1^kH^{0k}H^{00}\right\rangle}\left[q,k,\bar{h}^{0i}\right]=\bar{h}^{0i}\mathbf{v}_1^k\left[-\delta^{ik}\left(\frac{1}{2}\mathbf{q}^2+\mathbf{k}\cdot\mathbf{q}\right)+\mathbf{q}^i\mathbf{k}^k+\frac{1}{2}\mathbf{k}^i\mathbf{k}^k\right], \tag{A.23}$$

whereas for T^{ll}_{1PN} we need

$$F^{\left\langle H^{00}H^{00}\right\rangle}\left[q,k,\bar{h}^{ll}\right]=\bar{h}^{ll}\left[\frac{1}{4}\mathbf{q}^2+\frac{1}{4}\mathbf{k}\cdot\mathbf{q}-\frac{3}{4}\left(q_0^2+k_0q_0+2k_0^2\right)\right], \tag{A.24}$$

$$F^{\left\langle \mathbf{v}_1^kH^{0k}H^{00}\right\rangle}\left[q,k,\bar{h}^{ll}\right]=\bar{h}^{ll}\mathbf{v}_1^k\left[-k_0\left(\mathbf{q}^k+\frac{1}{2}\mathbf{k}^k\right)\right], \tag{A.25}$$

$$F^{\left\langle \mathbf{v}_1^k\mathbf{v}_1^lH^{kl}H^{00}\right\rangle}\left[q,k,\bar{h}^{ll}\right]=\bar{h}^{ll}\mathbf{v}_1^k\mathbf{v}_1^l\left[\delta^{kl}\left(-\frac{1}{4}\mathbf{q}^2+\frac{1}{4}\mathbf{k}\cdot\mathbf{q}\right)-\frac{1}{2}\mathbf{k}^k\mathbf{k}^l\right], \tag{A.26}$$

$$F^{\left\langle \mathbf{v}_1^kH^{0k}H^{0l}\mathbf{v}_2^l\right\rangle}\left[q,k,\bar{h}^{ll}\right]=\bar{h}^{ll}\mathbf{v}_1^k\mathbf{v}_2^l\left[\frac{1}{4}\delta^{kl}\left(\mathbf{q}^2+\mathbf{k}\cdot\mathbf{q}\right)-\frac{1}{2}\mathbf{q}^l\mathbf{k}^k+\frac{1}{2}\mathbf{q}^k\mathbf{k}^l+\frac{1}{4}\mathbf{k}^k\mathbf{k}^l\right]. \tag{A.27}$$

The three-graviton vertex, in turn, comes naturally in a simple form even not integrated on the internal momenta:

$$\left\langle H^{00}_{\mathbf{q}_1}H^{00}_{\mathbf{q}_2}H^{00}_{\mathbf{q}_3}\right\rangle=-\frac{(2\pi)^3}{4m_{Pl}}\delta\left(t_2-t_1\right)\delta\left(t_3-t_1\right)\delta^3\left(\boldsymbol{q}_1+\boldsymbol{q}_2+\boldsymbol{q}_3\right)\frac{\left(\boldsymbol{q}_1^2+\boldsymbol{q}_2^2+\boldsymbol{q}_3^2\right)}{\boldsymbol{q}_1^2\boldsymbol{q}_2^2\boldsymbol{q}_3^2}. \tag{A.28}$$

The composition of the three-potential-graviton vertex with two-potential-one-radiation-graviton vertex, after integrating in the third momentum, the integrand takes the form

$$\frac{F\left[\mathbf{q}_1,\mathbf{q}_2,\mathbf{k},\bar{h}\right]}{\mathbf{q}_1^2\mathbf{q}_2^2\left(\mathbf{q}_1+\mathbf{k}\right)^2\left(\mathbf{q}_1+\mathbf{q}_2+\mathbf{k}\right)^2}, \tag{A.29}$$

in which the numerators for the contractions needed to compute the contributions for T^{00}_{2PN} and T^{ll}_{1PN} are, respectively,

$$F^{\langle H^{00}H^{00}H^{00}\rangle}\left[\mathbf{q}_1,\mathbf{q}_2,\mathbf{k},\bar{h}^{00}\right] = \frac{1}{4}\bar{h}_{00}\left[\mathbf{q}_1^4+\frac{5}{2}\mathbf{q}_1^2\left(\mathbf{q}_1\cdot\mathbf{q}_2\right)+\frac{5}{2}\mathbf{q}_1^2\mathbf{q}_2^2+\left(\mathbf{q}_1+\mathbf{q}_2\right)^2\left(\mathbf{q}_1\cdot\mathbf{k}\right)\right.$$
$$\left.+\frac{5}{2}\mathbf{q}_1^2\left(\mathbf{q}_2\cdot\mathbf{k}\right)+3\left(\mathbf{q}_1\cdot\mathbf{k}\right)\left(\mathbf{q}_2\cdot\mathbf{k}\right)-\left(\mathbf{q}_1\cdot\mathbf{k}\right)^2+\left(\mathbf{q}_2\cdot\mathbf{k}\right)^2\right], \tag{A.30}$$

$$F^{\langle H^{00}H^{00}H^{00}\rangle}\left[\mathbf{q}_1,\mathbf{q}_2,\mathbf{k},\bar{h}^{ll}\right] = -\frac{\bar{h}^{ll}}{8}\left[2\mathbf{q}_1^4-\mathbf{q}_1^2\mathbf{q}_1\cdot\mathbf{q}_2+10\mathbf{q}_1^2\mathbf{q}_1\cdot\mathbf{k}+10\left(\mathbf{q}_1\cdot\mathbf{k}\right)^2-\mathbf{q}_1^2\mathbf{q}_2^2\right.$$
$$\left.-\mathbf{q}_1^2\mathbf{q}_2\cdot\mathbf{k}-2\left(\mathbf{q}_1\cdot\mathbf{k}\right)\left(\mathbf{q}_2\cdot\mathbf{k}\right)-2\left(\mathbf{q}_2\cdot\mathbf{k}\right)^2\right]. \tag{A.31}$$

The three-potential-one-radiation-graviton vertex integrated in the internal momenta can be expressed in this way:

$$\prod_{i=1}^{3}\int\frac{d^3\mathbf{q}_i}{\left(2\pi\right)^9}e^{i\mathbf{q}_i\cdot\mathbf{x}_i}\left\langle iS_{\bar{h}H^3}\right\rangle$$
$$=-\frac{1}{m_{Pl}^2}\delta\left(t_2-t_1\right)\delta\left(t_3-t_1\right)\int\frac{d^3\mathbf{q}_2}{\left(2\pi\right)^3}\int\frac{d^3\mathbf{q}_3}{\left(2\pi\right)^3}\frac{e^{i\left(\mathbf{q}_2+\mathbf{q}_3\right)\cdot\mathbf{x}}F\left[\mathbf{q}_2,\mathbf{q}_3,\mathbf{k},\bar{h}\right]}{\mathbf{q}_2^2\mathbf{q}_3^2\left(\mathbf{q}_2+\mathbf{q}_3+\mathbf{k}\right)^2}, \tag{A.32}$$

where we have chosen to integrate on $\mathbf{q}_1$, for instance coupled to particle 1, and leaving the momenta $\mathbf{q}_2$ and $\mathbf{q}_3$, both coupled to particle 2, to be integrated in the process of solving the diagrams. For this case, the contractions required to write down the contribution for T^{00}_{2PN} and T^{ll}_{1PN}, respectively, are given by

$$F^{\langle H^{00}H^{00}H^{00}\rangle}\left[\mathbf{q}_2,\mathbf{q}_3,\mathbf{k},\bar{h}^{00}\right] = -\frac{1}{8}\bar{h}^{00}\left(\mathbf{q}_2^2+\mathbf{q}_3^2+\mathbf{q}_2\cdot\mathbf{q}_3+\mathbf{q}_2\cdot\mathbf{k}+\mathbf{q}_3\cdot\mathbf{k}\right), \tag{A.33}$$

$$F^{\langle H^{00}H^{00}H^{00}\rangle}\left[\mathbf{q}_2,\mathbf{q}_3,\mathbf{k},\bar{h}^{ll}\right] = -\frac{7}{8}\bar{h}^{ll}\left(\mathbf{q}_2^2+\mathbf{q}_3^2+\mathbf{q}_2\cdot\mathbf{q}_3+\mathbf{q}_2\cdot\mathbf{k}+\mathbf{q}_3\cdot\mathbf{k}\right). \tag{A.34}$$

A.2.1 Integrals

To solve integrals in the momentum space, it is helpful to use some general relations that can be obtained by using Feynman parameters [65]. If we consider a spacetime of d dimensions, then for $D = d - 1$ we have

$$\int \frac{d^D\mathbf{k}}{(2\pi)^D}\frac{e^{-i\mathbf{k}\cdot\mathbf{r}}}{(\mathbf{k}^2)^a} = \frac{1}{(4\pi)^{\frac{D}{2}}}\frac{\Gamma\left(\frac{D}{2}-a\right)}{\Gamma(a)}\left(\frac{r^2}{4}\right)^{a-\frac{D}{2}}, \tag{A.35a}$$

$$\int \frac{d^D\mathbf{k}}{(2\pi)^D}\frac{1}{[\mathbf{k}^2]^a\left[(\mathbf{k}-\mathbf{p})^2\right]^b} = \frac{(\mathbf{p}^2)^{\frac{D}{2}-a-b}}{(4\pi)^{\frac{D}{2}}}\frac{\Gamma\left(a+b-\frac{D}{2}\right)}{\Gamma(a)\,\Gamma(b)}\frac{\Gamma\left(\frac{D}{2}-a\right)\Gamma\left(\frac{D}{2}-b\right)}{\Gamma(D-a-b)}, \tag{A.35b}$$

$$\int \frac{d^D\mathbf{k}}{(2\pi)^D}\frac{\mathbf{k}^i}{[\mathbf{k}^2]^a\left[(\mathbf{k}-\mathbf{p})^2\right]^b} = \frac{\mathbf{p}^i\,(\mathbf{p}^2)^{\frac{D}{2}-a-b}}{(4\pi)^{\frac{D}{2}}}\frac{\Gamma\left(a+b-\frac{D}{2}\right)}{\Gamma(a)\,\Gamma(b)}\frac{\Gamma\left(\frac{D}{2}-a+1\right)\Gamma\left(\frac{D}{2}-b\right)}{\Gamma(D-a-b+1)}, \tag{A.35c}$$

$$\begin{aligned}\int \frac{d^D\mathbf{k}}{(2\pi)^D}\frac{\mathbf{k}^i\mathbf{k}^j}{[\mathbf{k}^2]^a\left[(\mathbf{k}-\mathbf{p})^2\right]^b} &= \frac{1}{(4\pi)^{\frac{D}{2}}}\frac{(\mathbf{p}^2)^{\frac{D}{2}-a-b}}{\Gamma(a)\,\Gamma(b)\,\Gamma(D-a-b+2)}\\ &\times\left\{\frac{g^{ij}\mathbf{p}^2}{2}\Gamma\left(a+b-1-\frac{D}{2}\right)\Gamma\left(\frac{D}{2}-a+1\right)\Gamma\left(\frac{D}{2}-b+1\right)\right.\\ &\left.+\mathbf{p}^i\mathbf{p}^j\Gamma\left(a+b-\frac{D}{2}\right)\Gamma\left(\frac{D}{2}-b\right)\Gamma\left(\frac{D}{2}-a+2\right)\right\}.\end{aligned} \tag{A.35d}$$

These integrals are especially important to solve diagrams that has a composition of the three-potential-graviton vertex with the two-potential-one-radiation vertex, where an analysis of the integrals in an arbitrary dimension D is required to handle divergences.

Appendix B Acceleration at 2PN

In this appendix we present the result for the 2PN acceleration computed via the EFT approach in the linearized harmonic gauge.

To write down the equation of motion of the binary system at 2PN order, we need to obtain the Lagrangian by integrating out the potential modes of the gravitational fields in the action. Below the diagrams which contribute to the dynamics at 2PN order are presented.

The simplest contribution to the 2PN Lagrangian comes from the diagram show in Fig. B.1, which gives the following contribution:

$$L_{FigB1} = \sum_a \frac{1}{16} m_a \mathbf{v}_a^6. \tag{B.1}$$

Next, we have the diagrams with one-graviton exchange illustrated in Fig. B.2. Summing those diagrams together yields

$$\begin{aligned} L_{FigB2} = \sum_{a\neq b} \frac{G m_a m_b}{16 r^3} \Big\{ & 15 r^4 \mathbf{a}_a \cdot \mathbf{a}_b + r^2 \left[14 \mathbf{v}_a^2 - 20 \mathbf{v}_a^2 \mathbf{v}_a \cdot \mathbf{v}_b + 2 \left(\mathbf{v}_a \cdot \mathbf{v}_b \right)^2 \right. \\ & \left. + 3 \mathbf{v}_a^2 \mathbf{v}_b^2 + 2 \mathbf{v}_b^2 \mathbf{a}_a \cdot \mathbf{r} - \mathbf{a}_a \cdot \mathbf{r} \mathbf{a}_b \cdot \mathbf{r} + 28 \mathbf{a}_b \cdot \mathbf{v}_a \mathbf{v}_a \cdot \mathbf{r} + 24 \mathbf{a}_a \cdot \mathbf{v}_a \mathbf{v}_b \cdot \mathbf{r} \right] \\ & + 2 \left(\mathbf{a}_b \cdot \mathbf{r} - \mathbf{v}_b^2 \right) \left(\mathbf{v}_a \cdot \mathbf{r} \right)^2 + 12 \left(\mathbf{v}_a \cdot \mathbf{v}_b - \mathbf{v}_a^2 \right) \mathbf{v}_a \cdot \mathbf{r} \mathbf{v}_b \cdot \mathbf{r} + \frac{3}{r^2} \left(\mathbf{v}_a \cdot \mathbf{r} \right)^2 \left(\mathbf{v}_b \cdot \mathbf{r} \right)^2 \Big\}. \end{aligned} \tag{B.2}$$

v^6

Figure B.1: Diagram with no graviton exchange.

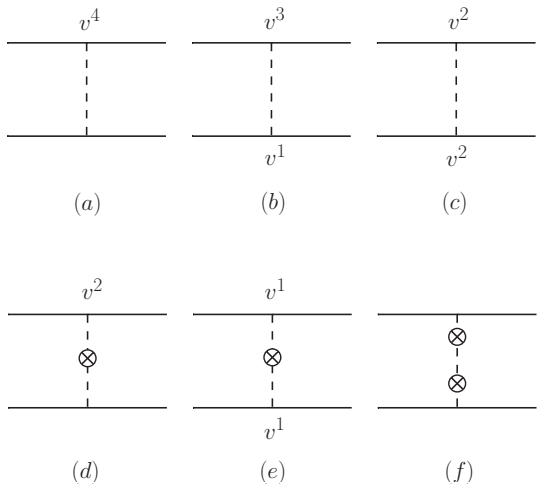

Figure B.2: Diagrams with one-graviton exchange.

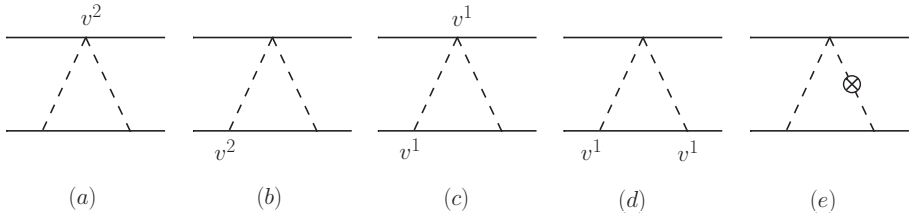

Figure B.3: Diagrams with two-graviton exchange.

In Fig. B.3 we show all diagrams with two-graviton exchange that enter at the second PN order. The sum of those diagrams is

$$L_{FigB3} = \sum_{a\neq b} \frac{G^2 m_a^2 m_b}{4r^4} \left(6r^2\mathbf{v}_a^2 + 7r^2\mathbf{v}_b^2 - 14r^2\mathbf{v}_a\cdot\mathbf{v}_b + 2\dot{r}\mathbf{v}_a\cdot\mathbf{r} - 2\mathbf{v}_a\cdot\mathbf{r}\mathbf{v}_b\cdot\mathbf{r}\right). \qquad \text{(B.3)}$$

There is also the diagram with a three-graviton source term as well as other two diagrams with combinations of the two-graviton source, as shown in Fig. B.4. Their contribution to the Lagrangian is

$$L_{FigB4} = -\sum_{a\neq b} \frac{G^3 m_a^2 m_b}{2r^3} \left(m_a + 3m_b\right). \qquad \text{(B.4)}$$

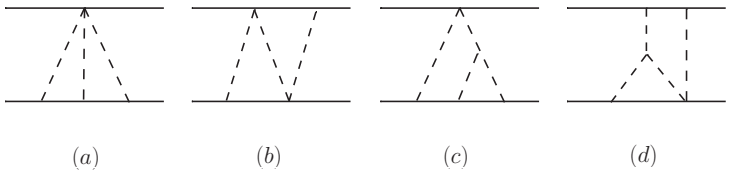

Figure B.4: (a) three-graviton emission from one of the bodies; (b) symmetric three-graviton exchange; (c) composition of a three-graviton vertex with a two-graviton vertex in the source term.

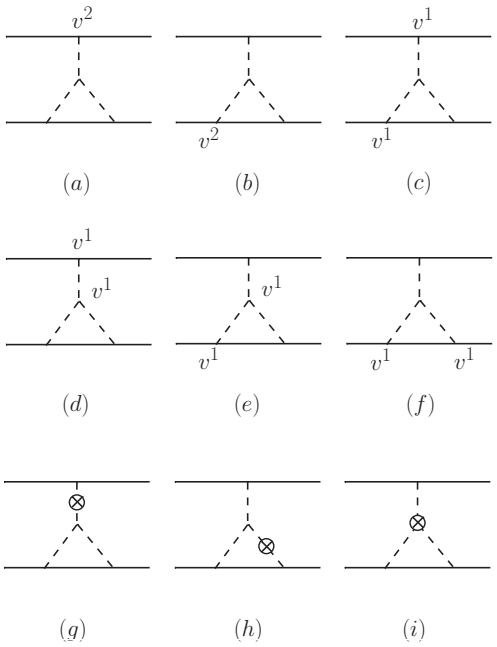

Figure B.5: Diagrams with three-graviton exchange.

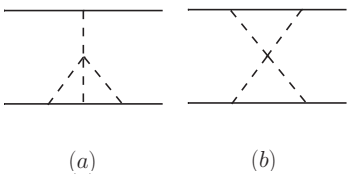

Figure B.6: Diagrams with four-graviton vertex.

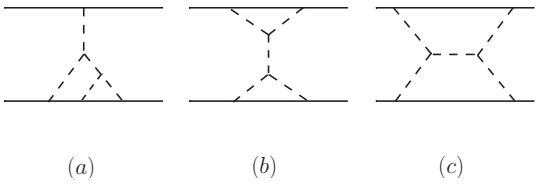

Figure B.7: Diagrams with five propagators.

The diagrams which contain three-graviton vertices are illustrated in Fig. B.5 and give

$$L_{FigB5} = \sum_{a\neq b} \frac{G^2 m_a^2 m_b}{2r^4} \left[r^2 \left(5\mathbf{v}_a^2 - 6\mathbf{v}_a \cdot \mathbf{v}_b + 2\mathbf{v}_b^2 + 2\mathbf{a}_b \cdot \mathbf{r} \right) - 9 \left(\mathbf{v}_a \cdot \mathbf{r} \right)^2 \right.$$
$$\left. + 14 \mathbf{v}_a \cdot \mathbf{r} \mathbf{v}_b \cdot \mathbf{r} - 3 \left(\mathbf{v}_b \cdot \mathbf{r} \right)^2 \right]. \tag{B.5}$$

In Fig. B.6, we show diagrams with a four-graviton vertex that enter at the 2PN order and, together, yield the result

$$L_{FigB6} = \sum_{a\neq b} \frac{G^3 m_a^3 m_b}{r^3}. \tag{B.6}$$

Lastly, the diagrams with five propagators are shown in Fig. B.7 and provide us with the following result:

$$L_{FigB7} = \sum_{a\neq b} \frac{G^3 m_a^2 m_b}{r^3} \left(m_b - 2m_a \right). \tag{B.7}$$

Summing up all contributions from Fig. B.1 to Fig. B.7, we write down the Lagrangian at 2PN order in the linearized harmonic gauge:

$$L_{2PN} = \frac{1}{16} m_1 \mathbf{v}_1^6 - \frac{G^3 m_1 m_2}{2r^3} \left(3m_1^2 + m_1 m_2 \right) + \frac{G^2 m_1 m_2}{4r^2} \left[\left(16 m_1 + 11 m_2 \right) \mathbf{v}_1^2 \right.$$

$$
\begin{aligned}
&-13m\mathbf{v}_1\cdot\mathbf{v}_2-4m_2\mathbf{a}_1\cdot\mathbf{r}-\frac{2}{r^2}\left(8m_1+3m_2\right)\left(\mathbf{v}_1\cdot\mathbf{r}\right)^2+\frac{12}{r^2}m\mathbf{v}_1\cdot\mathbf{r}\mathbf{v}_2\cdot\mathbf{r}\Bigg]\\
&+\frac{Gm_1m_2}{8r}\Bigg[\frac{15}{2}r^2\mathbf{a}_1\cdot\mathbf{a}_2+7\mathbf{v}_1^4-10\mathbf{v}_1^2\mathbf{v}_1\cdot\mathbf{v}_2+\left(\mathbf{v}_1\cdot\mathbf{v}_2\right)^2+\frac{3}{2}\mathbf{v}_1^2\mathbf{v}_2^2\\
&+\mathbf{a}_1\cdot\mathbf{r}\mathbf{v}_2^2-14\mathbf{a}_1\cdot\mathbf{v}_2\mathbf{v}_2\cdot\mathbf{r}+12\mathbf{a}_1\cdot\mathbf{v}_1\mathbf{v}_2\cdot\mathbf{r}-\frac{1}{2}\mathbf{a}_1\cdot\mathbf{r}\mathbf{a}_2\cdot\mathbf{r}-\frac{1}{r^2}\mathbf{a}_1\cdot\mathbf{r}\left(\mathbf{v}_2\cdot\mathbf{r}\right)^2\\
&+\frac{1}{r^2}\left(6\mathbf{v}_1\cdot\mathbf{r}\mathbf{v}_2\cdot\mathbf{r}\mathbf{v}_1\cdot\mathbf{v}_2-\left(\mathbf{v}_1\cdot\mathbf{r}\right)^2\mathbf{v}_2^2-6\mathbf{v}_1\cdot\mathbf{r}\mathbf{v}_2\cdot\mathbf{r}\mathbf{v}_2^2+\frac{3}{2r^2}\left(\mathbf{v}_1\cdot\mathbf{r}\right)^2\left(\mathbf{v}_2\cdot\mathbf{r}\right)^2\right)\Bigg]\\
&+1\leftrightarrow 2. \qquad \text{(B.8)}
\end{aligned}
$$

We use the Lagrangian above to determine the equations of motion of the two-body system at the second PN order. Below we show the acceleration for one of the objects in the binary:

$$
\begin{aligned}
\mathbf{a}_1^{2PN}=&\frac{1}{8}\frac{Gm_2}{r^3}\mathbf{r}\Bigg\{\frac{G^2}{r^2}\left(-2m_1^2-20m_1m_2+16m_2^2\right)+\frac{G}{r}\Big[\left(18m_1+56m_2\right)\mathbf{v}_1^2\\
&-\left(84m_1+128m_2\right)\mathbf{v}_1\cdot\mathbf{v}_2+\left(58m_1+64m_2\right)\mathbf{v}_2^2+30m_1\mathbf{a}_1\cdot\mathbf{r}-12m\mathbf{a}_2\cdot\mathbf{r}\\
&+\frac{28}{r^2}\left(m_1-4m_2\right)\mathbf{v}_1\cdot\mathbf{r}\left(\mathbf{v}_1\cdot\mathbf{r}-2\mathbf{v}_2\cdot\mathbf{r}\right)-\frac{1}{r^2}\left(56m_1+176m_2\right)\left(\mathbf{v}_2\cdot\mathbf{r}\right)^2\Big]\\
&+2\mathbf{v}_1^4-16\left(\mathbf{v}_1\cdot\mathbf{v}_2\right)^2-16\mathbf{v}_2^4+32\mathbf{v}_1\cdot\mathbf{v}_2\mathbf{v}_2^2-2\mathbf{v}_1^2\mathbf{a}_2\cdot\mathbf{r}-2\mathbf{v}_2^2\mathbf{a}_2\cdot\mathbf{r}\\
&-4\mathbf{a}_2\cdot\mathbf{v}_2\mathbf{v}_2\cdot\mathbf{r}+\frac{\left(\mathbf{v}_2\cdot\mathbf{r}\right)^2}{r^2}\left(12\mathbf{v}_1^2-48\mathbf{v}_1\cdot\mathbf{v}_2+36\mathbf{v}_2^2\right)-15\frac{\left(\mathbf{v}_2\cdot\mathbf{r}\right)^4}{r^4}\Bigg\}\\
&+\frac{1}{4}\frac{Gm_2}{r^3}\mathbf{v}_1\Bigg\{\frac{G}{r}\left[\left(48m_2-15m_1\right)\mathbf{v}_1\cdot\mathbf{r}+\left(23m_1-40m_2\right)\mathbf{v}_2\cdot\mathbf{r}\right]\\
&+\mathbf{v}_2\cdot\mathbf{r}\left(4\mathbf{v}_1^2+16\mathbf{v}_1\cdot\mathbf{v}_2-20\mathbf{v}_2^2\right)-24\frac{\mathbf{v}_1\cdot\mathbf{r}\left(\mathbf{v}_2\cdot\mathbf{r}\right)^2}{r^2}+18\frac{\left(\mathbf{v}_2\cdot\mathbf{r}\right)^3}{r^2}\\
&+\mathbf{v}_1\cdot\mathbf{r}\left(8\mathbf{v}_1^2-16\mathbf{v}_1\cdot\mathbf{v}_2+16\mathbf{v}_2^2-2\mathbf{a}_2\cdot\mathbf{r}\right)+2r^2\left(12\mathbf{a}_1-7\mathbf{a}_2\right)\cdot\mathbf{v}_1\Big\}\\
&+2\mathbf{a}_1\cdot\mathbf{v}_1\mathbf{v}_1^2\mathbf{v}_1+\frac{1}{4}\mathbf{a}_1\left(49\frac{G^2m_1m_2}{r^2}+36\frac{G^2m_2^2}{r^2}+12\frac{Gm_2}{r}\mathbf{v}_1^2+\mathbf{v}_1^4\right)\\
&+\frac{1}{4}\frac{Gm_2}{r^3}\mathbf{v}_2\Bigg\{\frac{G}{r}\left[\left(31m_1-24m_2\right)\mathbf{v}_1\cdot\mathbf{r}+\left(40m_2-9m_1\right)\mathbf{v}_2\cdot\mathbf{r}\right]\\
&+\mathbf{v}_2\cdot\mathbf{r}\left(-4\mathbf{v}_1^2-16\mathbf{v}_1\cdot\mathbf{v}_2+20\mathbf{v}_2^2\right)+24\frac{\mathbf{v}_1\cdot\mathbf{r}\left(\mathbf{v}_2\cdot\mathbf{r}\right)^2}{r^2}-18\frac{\left(\mathbf{v}_2\cdot\mathbf{r}\right)^3}{r^2}\\
&+\mathbf{v}_1\cdot\mathbf{r}\left(16\mathbf{v}_1\cdot\mathbf{v}_2-16\mathbf{v}_2^2\right)-14r^2\mathbf{a}_2\cdot\mathbf{v}_2\Big\}\\
&-\frac{7}{4}\frac{Gm_2}{r}\mathbf{a}_2\left(6\frac{Gm}{r}+\mathbf{v}_1^2+\mathbf{v}_2^2\right). \qquad \text{(B.9)}
\end{aligned}
$$

All accelerations in the right hand side of the equality above should be regarded as Newtonian accelerations if we want the entire expression to be of definite 2PN order. To write the acceleration in the center of mass frame, we have to consider, in addition to (B.9), the reduced contribution from applying the equation of motion inside the (3.54) as well as the PN corrections to the center of mass frame (3.75) and (3.76). Adding these contributions together, we finally obtain the expression for the relative acceleration of the two-body system in the center of mass frame, at the second PN order, in the linearized harmonic gauge:

$$
\begin{aligned}
&\mathbf{a}_{2PN} \\
=&-\frac{Gm}{8r^3}\left\{\mathbf{r}\left[(56+174\nu)\frac{G^2m^2}{r^2}-\left(32+52\nu-16\nu^2\right)\frac{Gm}{r}v^2+\left(112-200\nu-16\nu^2\right)\frac{Gm}{r}\dot{r}^2\right.\right. \\
&+\left(24\nu-32\nu^2\right)v^4-\left(36\nu-48\nu^2\right)v^2\dot{r}^2+\left(15\nu-45\nu^2\right)\dot{r}^4\Big] \\
&\left.+4r\dot{r}\mathbf{v}\left[\left(-12+41\nu+8\nu^2\right)\frac{Gm}{r}-\left(15\nu+4\nu^2\right)v^2+\left(9\nu+6\nu^2\right)\dot{r}^2\right]\right\}. \qquad \text{(B.10)}
\end{aligned}
$$

The differences between our 2PN Lagrangian result with Gilmore and Ross' is

$$
\begin{aligned}
&\delta L \\
=&\frac{2m_1^3m_2}{r^3}+\frac{4m_1^2m_2^2}{r^3}+\frac{2m_1m_2^3}{r^3}-\frac{2m_1^2m_2\boldsymbol{v}_1^2}{r^2}-\frac{2m_1m_2^2\boldsymbol{v}_1^2}{r^2}-\frac{2m_1^2m_2\boldsymbol{v}_2^2}{r^2}-\frac{2m_1m_2^2\boldsymbol{v}_2^2}{r^2} \\
&+\frac{4m_1^2m_2(\boldsymbol{n}\cdot\boldsymbol{v_1})^2}{r^2}+\frac{4m_1m_2^2(\boldsymbol{n}\cdot\boldsymbol{v_1})^2}{r^2}+\frac{4m_1^2m_2(\boldsymbol{n}\cdot\boldsymbol{v}_2)^2}{r^2}+\frac{4m_1m_2^2(\boldsymbol{n}\cdot\boldsymbol{v}_2)^2}{r^2} \\
&-\frac{8m_1^2m_2(\boldsymbol{n}\cdot\boldsymbol{v_1})(\boldsymbol{n}\cdot\boldsymbol{v_2})}{r^2}-\frac{8m_1m_2^2(\boldsymbol{n}\cdot\boldsymbol{v_1})(\boldsymbol{n}\cdot\boldsymbol{v_2})}{r^2}+\frac{4m_1^2m_2(\boldsymbol{v}_1\cdot\boldsymbol{v}_2)}{r^2}+\frac{4m_1m_2^2(\boldsymbol{v}_1\cdot\boldsymbol{v}_2)}{r^2}, \qquad \text{(B.11)}
\end{aligned}
$$

which is a total time derivative

$$
\begin{aligned}
&\frac{\mathrm{d}}{\mathrm{d}t}\left(-\frac{2m_1^2m_2(\boldsymbol{n}\cdot\boldsymbol{v_1})}{r^2}-\frac{2m_1m_2^2(\boldsymbol{n}\cdot\boldsymbol{v_1})}{r^2}+\frac{2m_1^2m_2(\boldsymbol{n}\cdot\boldsymbol{v_2})}{r^2}+\frac{2m_1m_2^2(\boldsymbol{n}\cdot\boldsymbol{v_2})}{r^2}\right) \\
=&-\frac{2m_1^2m_2(\boldsymbol{n}\cdot\boldsymbol{a}_1)}{r}-\frac{2m_1m_2^2(\boldsymbol{n}\cdot\boldsymbol{a}_1)}{r}+\frac{2m_1^2m_2(\boldsymbol{n}\cdot\boldsymbol{a}_2)}{r}+\frac{2m_1m_2^2(\boldsymbol{n}\cdot\boldsymbol{a}_2)}{r}-\frac{2m_1^2m_2\boldsymbol{v}_1^2}{r^2} \\
&-\frac{2m_1m_2^2\boldsymbol{v}_1^2}{r^2}-\frac{2m_1^2m_2\boldsymbol{v}_2^2}{r^2}-\frac{2m_1m_2^2\boldsymbol{v}_2^2}{r^2}+\frac{4m_1^2m_2(\boldsymbol{n}\cdot\boldsymbol{v_1})^2}{r^2}+\frac{4m_1m_2^2(\boldsymbol{n}\cdot\boldsymbol{v_1})^2}{r^2} \\
&+\frac{4m_1^2m_2(\boldsymbol{n}\cdot\boldsymbol{v}_2)^2}{r^2}+\frac{4m_1m_2^2(\boldsymbol{n}\cdot\boldsymbol{v}_2)^2}{r^2}-\frac{8m_1^2m_2(\boldsymbol{n}\cdot\boldsymbol{v_1})(\boldsymbol{n}\cdot\boldsymbol{v_2})}{r^2}-\frac{8m_1m_2^2(\boldsymbol{n}\cdot\boldsymbol{v_1})(\boldsymbol{n}\cdot\boldsymbol{v_2})}{r^2} \\
&+\frac{4m_1^2m_2(\boldsymbol{v}_1\cdot\boldsymbol{v}_2)}{r^2}+\frac{4m_1m_2^2(\boldsymbol{v}_1\cdot\boldsymbol{v}_2)}{r^2} \qquad \text{(B.12)}
\end{aligned}
$$

after applying the leading Newtonian EOM. Adding the total time derivative that does not contribute to the EOM, the Lagrangian difference in (B.11) becomes

$$\delta L = \left(\frac{2m_1^2 m_2}{r} + \frac{2m_1 m_2^2}{r}\right)\left(\left((\boldsymbol{n}\cdot\boldsymbol{a}_1) + \frac{m_2}{r^2}\right) - \left((\boldsymbol{n}\cdot\boldsymbol{a}_2) - \frac{m_1}{r^2}\right)\right) \tag{B.13}$$

One cannot substitute EOM into the Lagrangian, and naively expect to get the same equations back out again. It is because when varying with respect to one of the variables, the Euler-Lagrange equation assumes the fixation of the other variables. However, the original equations of motion introduce the explicit relation between the dynamical arguments. The substitution into the Lagrangian, in general, does not give the correct equations of motion again. Since it is not a "double-zero" term, L in (B.13) contributes non-vanishing terms to the EoM.

The two Lagrangians are related by a gauge transformation of

$$\boldsymbol{x}_1 \to \boldsymbol{x}_1 + \frac{2(m_1+m_2)m_2}{r^2}\boldsymbol{x}, \qquad \boldsymbol{x}_2 \to \boldsymbol{x}_2 - \frac{2(m_1+m_2)m_1}{r^2}\boldsymbol{x} \tag{B.14}$$

that results the 2PN differences (B.11) from the Newtonian kinetic and potential energies. The center-of-mass position G^i, derived from

$$\frac{\partial L}{\partial v_i} - \frac{\mathrm{d}}{\mathrm{d}t}\frac{\partial L}{\partial a_i} = \frac{\mathrm{d}}{\mathrm{d}t}G^i, \tag{B.15}$$

and summing the binary index. Both Lagrangians, despite difference gauge fixing, lead to the same G^i that resonates with the results of $\int \mathrm{d}x T^{00} x^i$ from our 2PN mass quadrupole calculations. This is consistent with the gauge transformation (B.14), that the point particles are translated away from each other and leave the center-of-mass unchanged.

Appendix C Orbital Equations of Motion Resummation Solutions

We start by investigating the quasi-circular background orbit solution of the conservative spinning binary. In this case, the radius and the orbital angular frequency are constants apart from small non-secular perturbations induced by the presence of spins. The constant radius R_B and orbital frequency Ω_B satisfy

$$\Omega_B^2 = \frac{M}{R_B^3} - \frac{\Omega_B}{R_B^3}\big(5S_l + 3\Delta\Sigma_l\big) + \mathcal{O}(S^2). \tag{C.1}$$

at linear order in spin. Setting the spins to zero, the relation between R_B and Ω_B reduces to the usual Newtonian circular motion equation. To solve for Ω_B with a given R_B, we can either solve the quadratic equation above or substitute for Ω_B iteratively. The analytic solutions to the dynamics of quasi-circular conservative spinning binary systems have been studied [60, 66].

C.1 Perturbations Of Quasi-circular Orbits

Next we describe the deviation of the quasi-circular background orbit as a result of the leading order radiation reaction and linear spin-orbit effects by isolating the perturbative corrections $r(t) = R_B + \delta r(t) + \delta r_S(t)$ and $\omega(t) = \Omega_B + \delta\omega(t) + \delta\omega_S(t)$. The first time-dependent terms $\delta r(t)$ and $\delta\omega(t)$ are the perturbation that arise due to the 2.5PN radiation reaction force without the spin at a given time t, which are given by [15]

$$\delta r(t) = -\frac{64\nu}{5} R_B^6 \Omega_B^6 (t - t_0) + A_B \sin\left(\Omega_B(t - t_0) + \Phi_B\right), \tag{C.2}$$

$$\delta\omega(t) = \frac{96\nu}{5} R_B^5 \Omega_B^7 (t - t_0) - \frac{2\Omega_B A_B}{R_B} \sin\left(\Omega_B(t - t_0) + \Phi_B\right), \tag{C.3}$$

with bare parameters $\{R_B, \Omega_B, A_B, \Phi_B\}$, and $\delta r \sim v^5 R_B, \delta\omega \sim v^6/R_B$ at the initial time t_0. On the other hand, the terms due to the interaction of 1.5PN spin effects and the 2.5PN

radiation reaction start with the power counting of $\delta r_S \sim Sv^4/R_B$ and $\delta\omega_S \sim Sv^5/R_B^3$. Expanding the equations of motion (4.9) and (4.10) to $\mathcal{O}(Sv^6)$ gives

$$\delta\ddot{r}_S(t) - 2R_B\Omega_B\delta\omega_S(t) - 3\Omega_B^2\delta r_S(t) = \frac{\delta\omega(t)}{R_B^2}(5S_l + 3\Delta\Sigma_l), \tag{C.4}$$

$$R_B\delta\dot{\omega}_S(t) + 2\Omega_B\delta\dot{r}_S(t) = -\left(\frac{2S_l}{R_B^3}\delta\dot{r}(t) + \Big(88S_l + \frac{264}{5}\Delta\Sigma_l\Big)\nu R_B^3\Omega_B^6\right), \tag{C.5}$$

with $\delta r(t)$ and $\delta\omega(t)$ the values given in (C.2) and (C.3). Integrating (C.5) with respect to time, solving for $\delta\omega_S$, and substituting back into (C.4) gives the differential equation for δr_S,

$$\begin{aligned}\delta\ddot{r}_S(t) + \Omega_B^2\delta r_S(t) = &-\Big(\frac{144}{5}S_l + 48\Delta\Sigma_l\Big)\nu R_B^3\Omega_B^7(t-t_0)\\ &-(14S_l + 6\Delta\Sigma_l)\frac{\Omega_B A_B}{R_B^3}\sin\left(\Omega_B(t-t_0)+\Phi_B\right).\end{aligned} \tag{C.6}$$

The differential equation has a solution of the form

$$\begin{aligned}\delta r_S(t) = &-\Big(\frac{144}{5}S_l + 48\Delta\Sigma_l\Big)\nu R_B^3\Omega_B^5(t-t_0)\\ &+\frac{\big(7S_l + 3\Delta\Sigma_l\big)}{2\Omega_B R_B^3}A_B\Big[2\Omega_B(t-t_0)\cos\left(\Omega_B(t-t_0)+\Phi_B\right) - \sin\left(\Omega_B(t-t_0)+\Phi_B\right)\Big]\\ &+A_B^S\cos\left(\Omega_B(t-t_0)+\Phi_B\right),\end{aligned} \tag{C.7a}$$

where $A_B^S \sim Sv^4/R_B$ is a bare parameter in the general solution to the homogeneous equation of (C.6), to be determined by initial conditions. While $e_B = A_B/R_B$ is the small orbital eccentricity of order $\mathcal{O}(v^5)$ induced by the radiation reaction force, the interaction between the spin and radiation reaction lead to a smaller eccentricity $e_B^S = A_B^S/R_B \sim \mathcal{O}(Sv^4)$. The spin-radiation eccentricity deforms the circular orbit out-of-phase relative to the radiation eccentricity, with a fixed phase difference.

As a result, the angular frequency perturbation $\delta\omega_S(t)$ and its time integration $\delta\Phi_S(t)$ are given by

$$\begin{aligned}\delta\omega_S(t) = &\Big(-\frac{24}{5}S_l + \frac{216}{5}\Delta\Sigma_l\Big)\nu R_B^2\Omega_B^6(t-t_0) + \big(5S_l + 3\Delta\Sigma_l\big)\frac{A_B}{R_B^4}\sin\left(\Omega_B(t-t_0)+\Phi_B\right)\\ &-\big(14S_l + 6\Delta\Sigma_l\big)\frac{A_B}{R_B^4}\Omega_B(t-t_0)\cos\left(\Omega_B(t-t_0)+\Phi_B\right)\\ &-\frac{2A_B^S\Omega_B}{R_B}\cos\left(\Omega_B(t-t_0)+\Phi_B\right),\end{aligned} \tag{C.7b}$$

$$\delta\Phi_S(t) = \Big(-\frac{12}{5}S_l + \frac{108}{5}\Delta\Sigma_l \Big)\nu R_B^2 \Omega_B^6 (t-t_0)^2 - \frac{\Big(19S_l + 9\Delta\Sigma_l\Big)A_B}{\Omega_B R_B^4}\cos\left(\Omega_B(t-t_0)+\Phi_B\right)$$
$$- \Big(14S_l + 6\Delta\Sigma_l\Big)\frac{A_B}{R_B^4}(t-t_0)\sin\left(\Omega_B(t-t_0)+\Phi_B\right) - \frac{2A_B^S}{R_B}\sin\left(\Omega_B(t-t_0)+\Phi_B\right). \tag{C.7c}$$

The perturbation $\delta\Phi_S(t)$, of order $\mathcal{O}(Sv^4)$ to the angle $\phi(t)$, is the analog of the orbital phase in planar motion of non-spinning systems. Though it is no longer a physical angle now that the orbital plane precesses due to the spins, it is a combination of the Euler angles, defined in a later section, essential to the time evolution of the moving frame of reference.

We split the perturbation terms into the non-secular terms that remain small permanently, and the secular ones that grows with time. As time progresses, the secular terms gradually become dominant and break down the PN power counting, therefore they need to be resummed.

C.2 Renormalization

The full set of bare solutions to the orbit motion including linear spin-orbit terms and 2.5PN Burke-Thorne terms is given by

$$r(t) = R_B + \delta r(t) + \delta r_S(t), \tag{C.8a}$$
$$\omega(t) = \Omega_B + \delta\omega(t) + \delta\omega_S(t), \tag{C.8b}$$
$$\phi(t) = \Phi_B + \delta\Phi(t) + \delta\Phi_S(t), \tag{C.8c}$$

with the corresponding perturbations in (C.2) and (C.7). We renormalize these terms by removing the t_0 dependence with the introduction of counter-terms for the bare parameters. The $\mathcal{O}(v^5)$ terms were renormalized in Ref. [15]. Thanks to the newly added $\mathcal{O}(Sv^4)$ perturbations, the bare parameters have to include higher order counter-terms, which means

$$R_B(t_0) = R_R(\tau) + \delta_R^{v^5}(\tau, t_0) + \delta_R^S(\tau, t_0), \tag{C.9a}$$
$$\Omega_B(t_0) = \Omega_R(\tau) + \delta_\Omega^{v^5}(\tau, t_0) + \delta_\Omega^S(\tau, t_0), \tag{C.9b}$$

$$\Phi_B(t_0) = \Phi_R(\tau) + \delta^{v^5}_\Phi(\tau, t_0) + \delta^S_\Phi(\tau, t_0), \tag{C.9c}$$

$$A^S_B(t_0) = A^S_R(\tau) + \delta^S_A(\tau, t_0). \tag{C.9d}$$

In terms of the renormalized initial parameters and the renormalization scale $t - t_0 = (t - \tau) + (\tau - t_0)$, the spin-orbit result becomes

$$\begin{aligned}
r(t) =& R_R + \delta^S_R - \frac{64\nu}{5} R_R^6 \Omega_R^6 (t-\tau) + A_R \sin\left(\Omega_R(t-\tau) + \Phi_R\right) \\
&- \left(\frac{144}{5} S_l + 48\Delta\Sigma_l\right) \nu R_R^3 \Omega_R^5 (t-\tau) - \left(\frac{144}{5} S_l + 48\Delta\Sigma_l\right) \nu R_R^3 \Omega_R^5 (\tau - t_0) \\
&+ \frac{\left(7S_l + 3\Delta\Sigma_l\right)}{2\Omega_R R_R^3} A_R \Big[2\Omega_R (t-\tau) \cos\left(\Omega_R(t-\tau) + \Phi_R\right) \\
&\qquad + 2\Omega_R(\tau - t_0) \cos\left(\Omega_R(t-\tau) + \Phi_R\right) - \sin\left(\Omega_R(t-\tau) + \Phi_R\right) \Big] \\
&+ A^S_R \cos\left(\Omega_R(t-\tau) + \Phi_R\right) + \delta^S_A \cos\left(\Omega_R(t-\tau) + \Phi_R\right),
\end{aligned} \tag{C.10a}$$

$$\begin{aligned}
\omega(t) =& \Omega_R + \delta^S_\Omega + \frac{96\nu}{5} R_R^5 \Omega_R^7 (t-\tau) - \frac{2\Omega_R A_R}{R_R} \sin\left(\Omega_R(t-\tau) + \Phi_R\right) \\
&+ \Big(- \frac{24}{5} S_l + \frac{216}{5} \Delta\Sigma_l \Big) \nu R_R^2 \Omega_R^6 (t-\tau) + \Big(- \frac{24}{5} S_l + \frac{216}{5} \Delta\Sigma_l \Big) \nu R_R^2 \Omega_R^6 (\tau - t_0) \\
&+ \Big(5S_l + 3\Delta\Sigma_l\Big) \frac{A_R}{R_R^4} \sin\left(\Omega_R(t-\tau) + \Phi_R\right) \\
&- \Big(14S_l + 6\Delta\Sigma_l\Big) \frac{A_R}{R_R^4} \Omega_R (t-\tau) \cos\left(\Omega_R(t-\tau) + \Phi_R\right) \\
&- \Big(14S_l + 6\Delta\Sigma_l\Big) \frac{A_R}{R_R^4} \Omega_R (\tau - t_0) \cos\left(\Omega_R(t-\tau) + \Phi_R\right) \\
&- \frac{2A^S_R \Omega_R}{R_R} \cos\left(\Omega_R(t-\tau) + \Phi_R\right) - \frac{2\delta^S_A \Omega_R}{R_R} \cos\left(\Omega_R(t-\tau) + \Phi_R\right),
\end{aligned} \tag{C.10b}$$

$$\begin{aligned}
\phi(t) =& \Phi_R + \delta^S_\Phi + (t-\tau)\Omega_R + (t-\tau)\delta^S_\Omega + (\tau - t_0)\delta^S_\Omega + \frac{48\nu}{5} R_R^5 \Omega_R^7 (t-\tau)^2 \\
&+ \frac{2A_R}{R_R} \cos\left(\Omega_R(t-\tau) + \Phi_R\right) - \Big(\frac{12}{5} S_l - \frac{108}{5} \Delta\Sigma_l\Big) \nu R_R^2 \Omega_R^6 (t-\tau)^2 \\
&+ \Big(- \frac{24}{5} S_l + \frac{216}{5} \Delta\Sigma_l \Big) \nu R_R^2 \Omega_R^6 (t-\tau)(\tau - t_0) \\
&+ \Big(- \frac{12}{5} S_l + \frac{108}{5} \Delta\Sigma_l \Big) \nu R_R^2 \Omega_R^6 (\tau - t_0)^2 \\
&- \Big(19S_l + 9\Delta\Sigma_l\Big) \frac{A_R}{\Omega_R R_R^4} \cos\left(\Omega_R(t-\tau) + \Phi_R\right)
\end{aligned}$$

$$
\begin{aligned}
&- \Big(14S_l + 6\Delta\Sigma_l\Big)\frac{A_R}{R_R^4}(t-\tau)\sin\left(\Omega_R(t-\tau)+\Phi_R\right) \\
&- \Big(14S_l + 6\Delta\Sigma_l\Big)\frac{A_R}{R_R^4}(\tau-t_0)\sin\left(\Omega_R(t-\tau)+\Phi_R\right) - \frac{2A_R^S}{R_R}\sin\left(\Omega_R(t-\tau)+\Phi_R\right) \\
&- \frac{2\delta_A^S}{R_R}\sin\left(\Omega_R(t-\tau)+\Phi_R\right). \qquad \text{(C.10c)}
\end{aligned}
$$

By observation we can write down the counter-terms that cancel the $(\tau - t_0)$ terms completely as

$$
\begin{aligned}
\delta_R^S(\tau,t_0) &= \left(\frac{144}{5}S_l + 48\Delta\Sigma_l\right)\nu R_R^3\Omega_R^5(\tau-t_0), && \text{(C.11a)}\\
\delta_\Omega^S(\tau,t_0) &= \Big(\frac{24}{5}S_l - \frac{216}{5}\Delta\Sigma_l\Big)\nu R_R^2\Omega_R^6(\tau-t_0), && \text{(C.11b)}\\
\delta_\Phi^S(\tau,t_0) &= \Big(-\frac{12}{5}S_l + \frac{108}{5}\Delta\Sigma_l\Big)\nu R_R^2\Omega_R^6(\tau-t_0)^2, && \text{(C.11c)}\\
\delta_A^S(\tau,t_0) &= -\Big(7S_l + 3\Delta\Sigma_l\Big)\frac{A_R}{R_R^3}(\tau-t_0). && \text{(C.11d)}
\end{aligned}
$$

Choosing the arbitrary renormalization scale to be $\tau = t_0$, the equations of motion is now described by the renormalized quantities $\{R_R, \Omega_R, \Phi_R, A_R, A_R^S\}$ as

$$
\begin{aligned}
r(t) =& R_R(t) + \left(1 - \frac{\big(7S_l + 3\Delta\Sigma_l\big)}{2\Omega_R(t)R_R^3(t)}\right)A_R(t)\sin\Phi_R(t) + A_R^S(t)\cos\Phi_R(t), && \text{(C.12a)}\\
\omega(t) =& \Omega_R(t) - \frac{2\Omega_R(t)A_R(t)}{R_R(t)}\left(1 - \frac{\big(5S_l + 3\Delta\Sigma_l\big)}{2\Omega_R(t)R_R^3(t)}\right)\sin\Phi_R(t) - \frac{2A_R^S\Omega_R(t)}{R_R(t)}\cos\Phi_R(t), && \text{(C.12b)}\\
\phi(t) =& \Phi_R(t) + \frac{2A_R(t)}{R_R(t)}\left(1 - \frac{\big(19S_l + 9\Delta\Sigma_l\big)}{2\Omega_R(t)R_R^3(t)}\right)\cos\Phi_R(t) - \frac{2A_R^S(t)}{R_R(t)}\sin\Phi_R(t). && \text{(C.12c)}
\end{aligned}
$$

The explicit secular terms have been removed thanks to the choice of τ, and the t_0-dependencies have been absorbed into the counter-terms. The runnings of $\{R_R, \Omega_R, \Phi_R, A_R, A_R^S\}$ and their dependence on the initial conditions are then determined by the renormalization group equations.

C.3 Renormalization Group Solutions

Exploiting the fact that the bare quantities $\{R_B(t_0), \Omega_B(t_0), \Phi_B(t_0), A_B^S(t_0)\}$ are independent of the arbitrary scale τ, we can write down the renormalization group equations for the renormalized quantities $\{R_R(t), \Omega_R(t), \Phi_R(t), A_R^S(t)\}$ as

$$\frac{\mathrm{d}R_R}{\mathrm{d}\tau} = -\frac{64\nu}{5}R_R^6(\tau)\Omega_R^6(\tau) - \left(\frac{144}{5}S_l + 48\Delta\Sigma_l\right)\nu R_R^3(\tau)\Omega_R^5(\tau), \tag{C.13}$$

$$\frac{\mathrm{d}\Omega_R}{\mathrm{d}\tau} = \frac{96\nu}{5}R_R^5(\tau)\Omega_R^7(\tau) - \Big(\frac{24}{5}S_l - \frac{216}{5}\Delta\Sigma_l\Big)\nu R_R^2(\tau)\Omega_R^6(\tau), \tag{C.14}$$

$$\frac{\mathrm{d}\Phi_R}{\mathrm{d}\tau} = \Omega_R(\tau), \tag{C.15}$$

$$\frac{\mathrm{d}A_R^S}{\mathrm{d}\tau} = \Big(7S_l + 3\Delta\Sigma_l\Big)\frac{A_R}{R_R^3}. \tag{C.16}$$

The right-hand sides of the RG equations, which are called beta functions, includes more iterative time-derivative terms that are of higher orders starting from $\mathcal{O}(v^{11})$ and $\mathcal{O}(S^2)$. The RG solutions to Ω_R, Φ_R and A_R^S in terms of R_R and the initial conditions are

$$\Omega_R(t) = \left[\frac{M^{1/2}}{R_R^{3/2}(t)} - \left(\frac{5S_l + 3\Delta\Sigma_l}{2R_R^3(t)}\right)\right] = \left[\frac{M}{R_R^3(t)} - \sqrt{\frac{M}{R_R^3(t)}}\left(\frac{5S_l + 3\Delta\Sigma_l}{R_R^3(t)}\right)\right]^{\frac{1}{2}} + \mathcal{O}(S^2), \tag{C.17a}$$

$$\begin{aligned}\Phi_R(t) =& \Phi_R(t_i) + \frac{1}{32M^{5/2}\nu}\Big[R_R^{5/2}(t_i) - R_R^{5/2}(t)\Big] + \frac{5\Big(41S_l + 15\Delta\Sigma_l\Big)}{256M^3\nu}\Big[R_R(t_i) - R_R(t)\Big] \\ &+ \frac{5\mathscr{S}^{2/3}\Big(41S_l + 15\Delta\Sigma_l\Big)}{128\sqrt{3}\nu M^{10/3}}\left[\tan^{-1}\left(\frac{1}{\sqrt{3}}\Big(1 + \frac{2M^{1/6}R_R(t_i)^{1/2}}{\mathscr{S}^{1/3}}\Big)\right)\right. \\ &\qquad\left. - \tan^{-1}\left(\frac{1}{\sqrt{3}}\Big(1 + \frac{2M^{1/6}R_R(t)^{1/2}}{\mathscr{S}^{1/3}}\Big)\right)\right] \\ &+ \frac{5\mathscr{S}^{2/3}\Big(41S_l + 15\Delta\Sigma_l\Big)}{768\nu M^{10/3}}\left[\ln\left(\frac{\Big(\mathscr{S}^{1/3} - M^{1/6}R_R(t_i)^{1/2}\Big)^2}{\mathscr{S}^{2/3} + \mathscr{S}^{1/3}M^{1/6}R_R(t_i)^{1/2} + M^{1/3}R_R(t_i)}\right)\right. \\ &\qquad\left. - \ln\left(\frac{\Big(\mathscr{S}^{1/3} - M^{1/6}R_R(t)^{1/2}\Big)^2}{\mathscr{S}^{2/3} + \mathscr{S}^{1/3}M^{1/6}R_R(t)^{1/2} + M^{1/3}R_R(t)}\right)\right],\end{aligned} \tag{C.17b}$$

$$
\begin{aligned}
A_R^S(t) =& A_R^S(t_i) + \frac{5A_R}{64\nu M^3}\Big(7S_l + 3\Delta\Sigma_l\Big)\Big[R_R(t_i) - R_R(t)\Big] \\
&+ \frac{5A_R\mathscr{S}^{2/3}\Big(7S_l + 3\Delta\Sigma_l\Big)}{32\sqrt{3}\nu M^{10/3}}\Bigg[\tan^{-1}\left(\frac{1}{\sqrt{3}}\Big(1 + \frac{2M^{1/6}R_R(t_i)^{1/2}}{\mathscr{S}^{1/3}}\Big)\right) \\
&\qquad\qquad - \tan^{-1}\left(\frac{1}{\sqrt{3}}\Big(1 + \frac{2M^{1/6}R_R(t)^{1/2}}{\mathscr{S}^{1/3}}\Big)\right)\Bigg] \\
&+ \frac{5A_R\mathscr{S}^{2/3}\Big(7S_l + 3\Delta\Sigma_l\Big)}{192\nu M^{10/3}}\Bigg[\ln\left(\frac{\Big(\mathscr{S}^{1/3} - M^{1/6}R_R(t_i)^{1/2}\Big)^2}{\mathscr{S}^{2/3} + \mathscr{S}^{1/3}M^{1/6}R_R(t_i)^{1/2} + M^{1/3}R_R(t_i)}\right) \\
&\qquad\qquad - \ln\left(\frac{\Big(\mathscr{S}^{1/3} - M^{1/6}R_R(t)^{1/2}\Big)^2}{\mathscr{S}^{2/3} + \mathscr{S}^{1/3}M^{1/6}R_R(t)^{1/2} + M^{1/3}R_R(t)}\right)\Bigg],
\end{aligned}
\tag{C.17c}
$$

where $\mathscr{S} \equiv (51S_l + 21\Delta\Sigma_l)/4$ is a constant combination of the initial spins, defined for convenience. Substituting in to the radial RG equation, we find

$$
\frac{\mathrm{d}R_R}{\mathrm{d}\tau} = -\frac{64\nu M^3}{5R_R^3} + \frac{16\nu M^{5/2}}{5R_R^{9/2}}(51S_l + 21\Delta\Sigma_l), \tag{C.18}
$$

or, rearranging,

$$
\frac{R_R^{9/2}}{R^{3/2} - M^{-1/2}\mathscr{S}}\mathrm{d}R_R = -\frac{64\nu M^3}{5}\mathrm{d}\tau. \tag{C.19}
$$

Integrating both sides gives the exact but implicit relation,

$$
\begin{aligned}
-\frac{64\nu M^3}{5}(t - t_i) =& \frac{1}{4}\big(R_R(t)^4 - R_R(t_i)^4\big) + \frac{2\mathscr{S}}{5M^{1/2}}\big(R_R(t)^{5/2} - R_R(t_i)^{5/2}\big) \\
&+ \frac{\mathscr{S}^2}{M}\big(R_R(t) - R_R(t_i)\big) + \frac{2\mathscr{S}^{8/3}}{\sqrt{3}M^{4/3}}\Bigg[\tan^{-1}\left(\frac{1}{\sqrt{3}}\Big(1 + \frac{2M^{1/6}R_R(t)^{1/2}}{\mathscr{S}^{1/3}}\Big)\right) \\
&\qquad\qquad - \tan^{-1}\left(\frac{1}{\sqrt{3}}\Big(1 + \frac{2M^{1/6}R_R(t_i)^{1/2}}{\mathscr{S}^{1/3}}\Big)\right)\Bigg] \\
&+ \frac{\mathscr{S}^{8/3}}{3M^{4/3}}\Bigg[\ln\left(\frac{\Big(\mathscr{S}^{1/3} - M^{1/6}R_R(t)^{1/2}\Big)^2}{\mathscr{S}^{2/3} + \mathscr{S}^{1/3}M^{1/6}R_R(t)^{1/2} + M^{1/3}R_R(t)}\right)
\end{aligned}
$$

$$- \ln\left(\frac{\left(\mathscr{S}^{1/3} - M^{1/6}R_R(t_i)^{1/2}\right)^2}{\mathscr{S}^{2/3} + \mathscr{S}^{1/3}M^{1/6}R_R(t_i)^{1/2} + M^{1/3}R_R(t_i)}\right)\Bigg]. \tag{C.20}$$

The parameter A_R is unchanged when the spin is added, and from [15] we learned that A_R has a zero β-function at the order we are working, i.e., A_R is a constant, given by initial conditions, proportional to the initial eccentricity $e_R(0) = A_R(0)/R_R(0) \sim \mathcal{O}(v^5)$.

Using the relation above for $R_R(t)$, we can further simply the expressions of $\Phi_R(t)$ and $A_R^S(t)$ in terms of $R_R(t)$ and time t, eliminating the logarithm and the arctangent terms. Written as an invariant in time, the renormalized quantities with the leading order spin-orbit effect are shown in (4.23)

Note that one constraint appears in the RG equations of $R_R(t)$, (C.13), which indicates the range of effectiveness of the DRG method,

$$\frac{\mathrm{d}R_R}{\mathrm{d}\tau} = -\frac{64\nu M^3}{5R_R^3} + \frac{64\nu M^{5/2}\mathscr{S}}{5R_R^{9/2}} + \mathcal{O}(S^2) = -\frac{64\nu M^{5/2}}{5R_R^{9/2}}\Big(M^{1/2}R_R^{3/2} - \mathscr{S}\Big). \tag{C.21}$$

If $\mathscr{S} = (51S_l + 21\Delta\Sigma_l)/4$ is positive, $R_R(t)$, which is the dominant part of the binary center-of-mass separation $r(t)$, decreases until $R_R(t) = \mathscr{S}^{2/3}M^{-1/3}$. Given a limitation on the smallest value of $R_R(t)$ and combining with (C.20), it is possible to determine an approximate end time of the inspiral phase described by the Post-Newtonian equations of motion (4.1). This could provide useful information to numerical simulations as well.

C.4 Spin Precession Equations

In this section, we aim to obtain the analytic solutions for the spin precession equations at linear order in spin (4.16) by applying DRG methods, with the quasi-circular solutions to the equations of motion from the previous section. For a conservative binary system moving in nearly circular motion, solving equations in the form of

$$\frac{\mathrm{d}S_n^a}{\mathrm{d}t} = (\Omega - \Omega_a)S_\lambda^a, \qquad \frac{\mathrm{d}S_\lambda^a}{\mathrm{d}t} = -(\Omega - \Omega_a)S_n^a, \qquad \text{with} \quad \Omega_a = \frac{\nu M\Omega}{R}\Big(2 + \frac{3}{2}\frac{m_b}{m_a}\Big), \tag{C.22}$$

is fairly straightforward for constant radius R and orbital frequency Ω. The solutions are $S_n^a = S_\parallel^a \sin\Big((\Omega-\Omega_a)(t-t_0)+\Phi\Big)$ and $S_\lambda^a = S_\parallel^a \cos\Big((\Omega-\Omega_a)(t-t_0)+\Phi\Big)$, where $S_\parallel^a$ is determined by the initial spin vectors.

With the inclusion of the radiation reaction force and the resulting time-dependence of $r(t)$ and $\omega(t)$, the spin vectors precess in a way entangled with the orbit motion. Defining $S_+^a \equiv S_n^a + iS_\lambda^a$, the precession equations (4.16) can be combined and written as

$$\frac{\mathrm{d}S_+^a(t)}{\mathrm{d}t} = -i\big(\omega(t)-\Omega_a(t)\big)S_+^a(t). \tag{C.23}$$

A simple integration with respect to time leads to

$$i\Big[\ln S_+^a(t) - \ln S_+^a(t_0)\Big] = \int_{t_0}^{t} \mathrm{d}\tau\big[\omega(t)-\Omega_a(t)\big]. \tag{C.24}$$

To solve for the integral on the right-hand side, we denote $\nu_a \equiv (2+\frac{3m_b}{2m_a})\nu^2$ and recall that $M \sim \Omega_B^2 R_B^3 + \Omega_B(5S_l+3\Delta\Sigma_l)$, such that Ω_a in (4.15) at leading order in spin becomes

$$\begin{aligned}\Omega_a(t) = \frac{\nu_a}{\nu}\Big(\Omega_B^2R_B^3+\Omega_B(5S_l+3\Delta\Sigma_l)\Big)\left[\frac{\Omega_B}{R_B}+\frac{\delta\omega}{R_B}-\frac{\Omega_B\delta r}{R_B^2}\right]+\frac{\nu_a}{\nu}\Omega_B^3R_B^2\left(\frac{\delta\omega_S}{\Omega_B}-\frac{\delta r_S}{R_B}\right)\\ +\mathcal{O}(S^2),\end{aligned} \tag{C.25}$$

with the 2.5PN radiation perturbation $\{\delta r, \delta\omega\}$ from (C.2), and the leading order spin-orbit perturbation $\{\delta r_S, \delta\omega_S\}$ from (C.7).

As a check of self-consistency, notice that we have the choice of substituting M either as a function of the physical values $\{r(t),\omega(t)\}$ using the results from (C.8), or the bare parameters $\{R_B,\Omega_B\}$, which give the same result after summing up the perturbation expansions.

Substituting the corresponding perturbations back into (C.25), we obtain the explicit time-dependence of the precession norm Ω_a,

$$\begin{aligned}\Omega_a(t) = \frac{\nu_a}{\nu}\Bigg[&\Omega_B^3R_B^2+(5S_l+3\Delta\Sigma_l)\frac{\Omega_B^2}{R_B}+32\nu R_B^7\Omega_B^9(t-t_0)\\ &+(184S_l+\frac{936}{5}\Delta\Sigma_l)\nu R_B^4\Omega_B^8(t-t_0)-3A_B\Omega_B^3R_B\sin\left(\Omega_B(t-t_0)+\Phi_B\right)\\ &-\Big(\frac{13}{2}S_l+\frac{9}{2}\Delta\Sigma_l\Big)\frac{A_B\Omega_B^2}{R_B^2}\sin\left(\Omega_B(t-t_0)+\Phi_B\right)\\ &-(21S_l+9\Delta\Sigma_l)\frac{A_B\Omega_B^3}{R_B^2}(t-t_0)\cos\left(\Omega_B(t-t_0)+\Phi_B\right)\end{aligned}$$

$$- 3A_B^S\Omega_B^3 R_B \cos\left(\Omega_B(t-t_0)+\Phi_B\right)\Bigg]. \tag{C.26}$$

Combined with the expression for $\delta\omega(t)$ in terms of the time-independent bare parameters, we can perform the integration in (C.24) to write down

$$\begin{aligned}
&i\Big[\ln S_+^a(t) - \ln S_+^a(t_0)\Big] \\
=&\left(\Omega_B - \frac{\nu_a}{\nu}\Omega_B^3 R_B^2 - \frac{\nu_a}{\nu}(5S_l+3\Delta\Sigma_l)\frac{\Omega_B^2}{R_B}\right)(t-t_0) \\
&+\left(\frac{48\nu}{5}R_B^5\Omega_B^7 - \Big(\frac{12}{5}S_l - \frac{108}{5}\Delta\Sigma_l\Big)\nu R_B^2\Omega_B^6 - 16\nu_a R_B^7\Omega_B^9\right. \\
&\qquad\qquad\left. - (92S_l + \frac{468}{5}\Delta\Sigma_l)\nu_a R_B^4\Omega_B^8\right)(t-t_0)^2 \\
&+\left(\frac{2A_B}{R_B} - \Big(5S_l+3\Delta\Sigma_l\Big)\frac{A_B}{R_B^4\Omega_B} - \frac{3\nu_a}{\nu}\Omega_B^2 A_B R_B\right. \\
&\qquad\left. - \frac{\nu_a}{\nu}\Big(\frac{13}{2}S_l + \frac{9}{2}\Delta\Sigma_l\Big)\frac{A_B\Omega_B}{R_B^2}\right)\Big[\cos\left(\Omega_B(t-t_0)+\Phi_B\right) - \cos\Phi_B\Big] \\
&-\left(\Big(14S_l+6\Delta\Sigma_l\Big)\frac{A_B}{R_B^4\Omega_B} - \frac{\nu_a}{\nu}(21S_l+9\Delta\Sigma_l)\frac{A_B\Omega_B}{R_B^2}\right) \\
&\quad\times\Big[\Omega_B(t-t_0)\sin\Big(\Omega_B(t-t_0)+\Phi_B\Big) + \cos\left(\Omega_B(t-t_0)+\Phi_B\right) - \cos\Phi_B\Big] \\
&-\left(\frac{2A_B^S}{R_B} - \frac{3\nu_a}{\nu}A_B^S\Omega_B^2 R_B\right)\Big[\sin\left(\Omega_B(t-t_0)+\Phi_B\right) - \sin\Phi_B\Big].
\end{aligned} \tag{C.27}$$

The constant terms $\sin\Phi_B$ and $\cos\Phi_B$ can be absorbed by redefining the initial condition $i\ln S_+^a(t_0)$, or via a bare parameter $i\ln\mathcal{S}_{+B}^a$,

$$\begin{aligned}
i\ln S_+^a(t_0) \to i\ln\mathcal{S}_{+B}^a &+ \left(\frac{2A_B}{R_B} - \Big(5S_l+3\Delta\Sigma_l\Big)\frac{A_B}{R_B^4\Omega_B} - \frac{3\nu_a}{\nu}\Omega_B^2 A_B R_B\right. \\
&\qquad\left. - \frac{\nu_a}{\nu}\Big(\frac{13}{2}S_l+\frac{9}{2}\Delta\Sigma_l\Big)\frac{A_B\Omega_B}{R_B^2}\right)\cos\Phi_B \\
&-\left(\Big(14S_l+6\Delta\Sigma_l\Big)\frac{A_B}{R_B^4\Omega_B} - (21S_l+9\Delta\Sigma_l)\frac{\nu_a}{\nu}\frac{A_B\Omega_B}{R_B^2}\right)\cos\Phi_B \\
&-\left(\frac{2A_B^S}{R_B} - \frac{3\nu_a}{\nu}A_B^S\Omega_B^2 R_B\right)\sin\Phi_B.
\end{aligned} \tag{C.28}$$

The logarithm of the spin components then becomes

$$
\begin{aligned}
& i \ln S^a_+(t) \\
& = i \ln \mathcal{S}^a_{+B} + \left(\Omega_B - \frac{\nu_a}{\nu} \Omega_B^3 R_B^2 - \frac{\nu_a}{\nu} (5 S_l + 3 \Delta\Sigma_l) \frac{\Omega_B^2}{R_B} \right) (t - t_0) \\
& + \left(\frac{48\nu}{5} R_B^5 \Omega_B^7 - \Big(\frac{12}{5} S_l - \frac{108}{5} \Delta\Sigma_l \Big) \nu R_B^2 \Omega_B^6 \right. \\
& \qquad \left. - 16 \nu_a R_B^7 \Omega_B^9 - (92 S_l + \frac{468}{5} \Delta\Sigma_l) \nu_a R_B^4 \Omega_B^8 \right) (t - t_0)^2 \\
& + \left(\frac{2 A_B}{R_B} - \Big(19 S_l + 9 \Delta\Sigma_l \Big) \frac{A_B}{R_B^4 \Omega_B} - \frac{3 \nu_a}{\nu} \Omega_B^2 A_B R_B \right. \\
& \qquad \left. + \frac{\nu_a}{\nu} \Big(\frac{29}{2} S_l + \frac{9}{2} \Delta\Sigma_l \Big) \frac{A_B \Omega_B}{R_B^2} \right) \cos\left(\Omega_B (t - t_0) + \Phi_B \right) \\
& - \left(\Big(14 S_l + 6 \Delta\Sigma_l \Big) \frac{A_B}{R_B^4} - \frac{\nu_a}{\nu} (21 S_l + 9 \Delta\Sigma_l) \frac{A_B \Omega_B^2}{R_B^2} \right) (t - t_0) \sin\Big(\Omega_B (t - t_0) + \Phi_B \Big) \\
& - \left(\frac{2 A_B^S}{R_B} - \frac{3 \nu_a}{\nu} A_B^S \Omega_B^2 R_B \right) \sin\left(\Omega_B (t - t_0) + \Phi_B \right). \qquad \text{(C.29)}
\end{aligned}
$$

Given the spin vector expansions in terms of the bare parameters $\{R_B, \Omega_B, \Phi_B, A_B, A_B^S, \mathcal{S}^a_{+B}\}$, the next step is to renormalize the spin components by replacing the bare parameters by the renormalized ones plus counter-terms, and splitting $t - t_0 = (t - \tau) + (\tau - t_0)$ with a choice of an arbitrary renormalization scale τ.

C.5 Spin Renormalization

To begin, the bare parameter $\ln \mathcal{S}^a_{+B}$ is related to the renormalized value $\ln \mathcal{S}^a_{+R}$ through

$$
\ln \mathcal{S}^a_{+B}(t_0) = \ln \mathcal{S}^a_{+R}(\tau) + \delta^a_{\ln S}(\tau, t_0). \qquad \text{(C.30)}
$$

The renormalization treatment is performed for the natural logarithm of the spin components. As a result, $\mathcal{S}^a_{+B} = \mathcal{S}^a_{+R} e^{\delta^a_{\ln S}}$. The exponential implies that it is the phase of the precession

that is renormalized. Dividing the bare parameters into the renormalized parts and the counter-terms and introducing the renormalization scale τ, Eq. (C.29) then becomes

$$
\begin{aligned}
&i\Big[\ln S_+^a(t) - \Big(\ln \mathcal{S}_{+R}^a + \delta_{\ln S}^a\Big)\Big] \\
&= \Bigg(\Omega_R + \delta_\Omega - \frac{\nu_a}{\nu}\Big(\Omega_R^3 R_R^2 + 3\Omega_R^2 R_R^2 \delta_\Omega + 2\Omega_R^3 R_R \delta_R\Big) \\
&\qquad - \frac{\nu_a}{\nu}(5S_l + 3\Delta\Sigma_l)\Big(\frac{\Omega_R^2}{R_R} + \frac{2\Omega_R\delta_\Omega}{R_R} - \frac{\Omega_R^2\delta_R}{R_R^2}\Big)\Bigg) \times \big[(t-\tau) + (\tau - t_0)\big] \\
&+ \left(\frac{48\nu}{5} R_R^5 \Omega_R^7 - \Big(\frac{12}{5}S_l - \frac{108}{5}\Delta\Sigma_l\Big)\nu R_R^2\Omega_R^6 - 16\nu_a R_R^7\Omega_R^9 - (92S_l + \frac{468}{5}\Delta\Sigma_l)\nu_a R_R^4\Omega_R^8\right) \\
&\qquad \times \big[(t-\tau)^2 + 2(t-\tau)(\tau - t_0) + (\tau - t_0)^2\big] \\
&+ \left(\frac{2A_R}{R_R} - \Big(19S_l + 9\Delta\Sigma_l\Big)\frac{A_R}{R_R^4\Omega_R} - \frac{3\nu_a}{\nu}\Omega_R^2 A_R R_R \right. \\
&\qquad \left. + \frac{\nu_a}{\nu}\Big(\frac{29}{2}S_l + \frac{9}{2}\Delta\Sigma_l\Big)\frac{A_R\Omega_R}{R_R^2}\right)\cos\big(\Omega_R(t-\tau) + \Phi_R\big) \\
&- \Big(\Big(14S_l + 6\Delta\Sigma_l\Big)\frac{A_R}{R_R^4} - \frac{\nu_a}{\nu}(21S_l + 9\Delta\Sigma_l)\frac{A_R\Omega_R^2}{R_R^2}\Big)\big[(t-\tau) + (\tau - t_0)\big]\sin\big(\Omega_R(t-\tau) + \Phi_R\big) \\
&- \left(\frac{2A_R^S}{R_R} + \frac{2\delta_A^S}{R_R} - \frac{3\nu_a}{\nu}A_R^S\Omega_R^2 R_R - \frac{3\nu_a}{\nu}\delta_A^S\Omega_R^2 R_R\right)\sin\big(\Omega_R(t-\tau) + \Phi_R\big). \qquad \text{(C.31)}
\end{aligned}
$$

The counter-terms are the combined results in [15] and (C.11a),

$$\delta_R(\tau, t_0) = \frac{64\nu}{5} R_R^6\Omega_R^6(\tau - t_0) + \delta_R^S(\tau, t_0), \qquad \text{(C.32a)}$$

$$\delta_\Omega(\tau, t_0) = -\frac{96\nu}{5} R_R^5\Omega_R^7(\tau - t_0) + \delta_\Omega^S(\tau, t_0), \qquad \text{(C.32b)}$$

$$\delta_\Phi(\tau, t_0) = -\Omega_R(\tau - t_0) + \frac{48\nu}{5} R_R^5\Omega_R^7(\tau - t_0)^2 + \delta_\Phi^S(\tau, t_0). \qquad \text{(C.32c)}$$

After some algebra, (C.31) can be simplified to

$$
\begin{aligned}
&i\Big[\ln S_+^a(t) - \Big(\ln \mathcal{S}_{+R}^a + \delta_{\ln S}^a\Big)\Big] \\
&= \Big(\Omega_R - \frac{\nu_a}{\nu}\Omega_R^3 R_R^2 - \frac{\nu_a}{\nu}(5S_l + 3\Delta\Sigma_l)\frac{\Omega_R^2}{R_R}\Big)(t-\tau) \\
&\quad + \Big(\Omega_R - \frac{\nu_a}{\nu}\Omega_R^3 R_R^2 - \frac{\nu_a}{\nu}(5S_l + 3\Delta\Sigma_l)\frac{\Omega_R^2}{R_R}\Big)(\tau - t_0) \\
&\quad + \left(\frac{48\nu}{5} R_R^5\Omega_R^7 - \Big(\frac{12}{5}S_l - \frac{108}{5}\Delta\Sigma_l\Big)\nu R_R^2\Omega_R^6 - 16\nu_a R_R^7\Omega_R^9\right.
\end{aligned}
$$

$$
\begin{aligned}
&\quad - (92S_l + \frac{468}{5}\Delta\Sigma_l)\nu_a R_R^4\Omega_R^8\Big)\big[(t-\tau)^2 - (\tau-t_0)^2\big] \\
&+ \Bigg(\frac{2A_R}{R_R} - \Big(19S_l + 9\Delta\Sigma_l\Big)\frac{A_R}{R_R^4\Omega_R} - \frac{3\nu_a}{\nu}\Omega_R^2 A_R R_R \\
&\qquad + \frac{\nu_a}{\nu}\Big(\frac{29}{2}S_l + \frac{9}{2}\Delta\Sigma_l\Big)\frac{A_R\Omega_R}{R_R^2}\Bigg)\cos\left(\Omega_R(t-\tau) + \Phi_R\right) \\
&- \Bigg(\Big(14S_l + 6\Delta\Sigma_l\Big)\frac{A_R}{R_R^4} - \frac{\nu_a}{\nu}(21S_l + 9\Delta\Sigma_l)\frac{A_R\Omega_R^2}{R_R^2}\Bigg)(t-\tau)\sin\Big(\Omega_R(t-\tau) + \Phi_R\Big) \\
&- \Bigg(\frac{2A_R^S}{R_R} - \frac{3\nu_a}{\nu}A_R^S\Omega_R^2 R_R\Bigg)\sin\left(\Omega_R(t-\tau) + \Phi_R\right). \qquad \text{(C.33)}
\end{aligned}
$$

Notice that the terms proportional to $(t-\tau)(\tau-t_0)$ are completely canceled, which was emphasized in [15] as an important check of self-consistency. Here the cancellation is due to exactly the same set of substitutions we could use to replace M to obtain (C.25), where the two different choices led to the same expansion result.

To cancel the remaining secular pieces that are proportional to the powers of $(\tau - t_0)$, the counter-term $\delta^a_{\ln S}$ is fixed to be

$$
\begin{aligned}
i\delta^a_{\ln S}(\tau, t_0) = &- \Big(\Omega_R - \frac{\nu_a}{\nu}\Omega_R^3 R_R^2 - \frac{\nu_a}{\nu}(5S_l + 3\Delta\Sigma_l)\frac{\Omega_R^2}{R_R}\Big)(\tau - t_0) \\
&+ \Bigg(\frac{48\nu}{5}R_R^5\Omega_R^7 - \Big(\frac{12}{5}S_l - \frac{108}{5}\Delta\Sigma_l\Big)\nu R_R^2\Omega_R^6 - 16\nu_a R_R^7\Omega_R^9 \\
&\qquad - (92S_l + \frac{468}{5}\Delta\Sigma_l)\nu_a R_R^4\Omega_R^8\Bigg)(\tau - t_0)^2. \qquad \text{(C.34)}
\end{aligned}
$$

Choosing the arbitrary scale τ to equal t, the renormalized solution to $\ln \mathcal{S}^a_+(t)$ becomes

$$
\begin{aligned}
i\ln S^a_+(t) = &i\ln \mathcal{S}^a_{+R} - \Bigg(\frac{2A_R^S}{R_R} - \frac{3\nu_a}{\nu}A_R^S\Omega_R^2 R_R\Bigg)\sin\Phi_R \\
&+ \Bigg(\frac{2A_R}{R_R} - \Big(19S_l + 9\Delta\Sigma_l\Big)\frac{A_R}{R_R^4\Omega_R} - \frac{3\nu_a}{\nu}\Omega_R^2 A_R R_R \\
&\qquad + \frac{\nu_a}{\nu}\Big(\frac{29}{2}S_l + \frac{9}{2}\Delta\Sigma_l\Big)\frac{A_R\Omega_R}{R_R^2}\Bigg)\cos\Phi_R. \qquad \text{(C.35)}
\end{aligned}
$$

or more explicitly in terms of the exponential,

$$S^a_+(t) = \mathcal{S}^a_{+R} \exp\Bigg\{ i\left(\frac{2A^S_R}{R_R} - \frac{3\nu_a}{\nu} A^S_R \Omega^2_R R_R\right) \sin\Phi_R \\ - i\left(\frac{2A_R}{R_R} - \Big(19S_l + 9\Delta\Sigma_l\Big)\frac{A_R}{R^4_R\Omega_R} - \frac{3\nu_a}{\nu}\Omega^2_R A_R R_R \right. \\ \left. + \frac{\nu_a}{\nu}\Big(\frac{29}{2}S_l + \frac{9}{2}\Delta\Sigma_l\Big)\frac{A_R\Omega_R}{R^2_R}\right)\cos\Phi_R \Bigg\}. \tag{C.36}$$

The renormalized quantities as functions of time have runnings obtained from the RG flow in Section C.3, with only the remaining the spin component bare parameter $\mathcal{S}^a_{+R}$ to be done in the next section.

C.6 Spin Component Renormalization Group Solution

The running of the renormalized parameter $\mathcal{S}^a_{+R}$ can be determined using (C.34), which leads to

$$\begin{aligned}
&\frac{\mathrm{d}}{\mathrm{d}\tau} i \ln \mathcal{S}^a_{+R}(\tau) \\
&= \Big(\Omega_R - \frac{\nu_a}{\nu}\Omega^3_R R^2_R - \frac{\nu_a}{\nu}(5S_l + 3\Delta\Sigma_l)\frac{\Omega^2_R}{R_R}\Big) \\
&+ \left[\frac{\mathrm{d}\Omega_R}{\mathrm{d}\tau} - \frac{\nu_a}{\nu}\Omega^3_R R^2_R\left(\frac{3}{\Omega_R}\frac{\mathrm{d}\Omega_R}{\mathrm{d}\tau} + \frac{2}{R_R}\frac{\mathrm{d}R_R}{\mathrm{d}\tau}\right) - \frac{\nu_a}{\nu}(5S_l + 3\Delta\Sigma_l)\frac{\Omega^2_R}{R_R}\left(\frac{2}{\Omega_R}\frac{\mathrm{d}\Omega_R}{\mathrm{d}\tau} - \frac{1}{R_R}\frac{\mathrm{d}R_R}{\mathrm{d}\tau}\right)\right] \\
&\quad \times (\tau - t_0) \\
&+ \left[\frac{96\nu}{5} R^5_B \Omega^7_B - \Big(\frac{24}{5}S_l - \frac{216}{5}\Delta\Sigma_l\Big)\nu R^2_B\Omega^6_B - 32\nu_a R^7_B\Omega^9_B - (184S_l + \frac{936}{5}\Delta\Sigma_l)\nu_a R^4_B\Omega^8_B\right] \\
&\quad \times (\tau - t_0).
\end{aligned} \tag{C.37}$$

It seems to be formally divergent and has the dependence on the cut-off t_0. However, replacing the derivatives of R_R and Ω_R by their RG equations (C.13) and (C.14), we encounter the non-trivial cancellation and obtain a finite β-function,

$$\frac{\mathrm{d}}{\mathrm{d}\tau} i \ln \mathcal{S}^a_{+R}(\tau) = \Omega_R - \frac{\nu_a}{\nu}\frac{M\Omega_R}{R_R}. \tag{C.38}$$

Notice the similarity in form between the RG equation and (C.23), the precession equation we start with.

In order to find a solution to the RG equation of the spin component, we can write the relation between the τ-derivative of $i\ln\mathcal{S}^a_{+R}$ and the derivative with respect to the renormalized parameter R_R as

$$\frac{\mathrm{d}}{\mathrm{d}R_R} i\ln\mathcal{S}^a_{+R}(\tau) = \left(\frac{\mathrm{d}R_R}{\mathrm{d}\tau}\right)^{-1} \frac{\mathrm{d}}{\mathrm{d}\tau} i\ln\mathcal{S}^a_{+R}(\tau). \tag{C.39}$$

Using the RGEs (C.13) and (C.38), we obtain a solution to $\mathcal{S}^a_{+R}(\tau)$ in terms of $R_R(\tau)$ and initial conditions

$$\begin{aligned} i\ln\mathcal{S}^a_{+R}(t) =& i\ln\mathcal{S}^a_{+R}(t_i) + \Big(\Phi_R(t) - \Phi_R(t_i)\Big) + \frac{5\nu_a}{96M^{3/2}\nu^2}\Big[R_R^{3/2}(t) - R_R^{3/2}(t_i)\Big] \\ &+ \frac{5\Big(41S_l + 15\Delta\Sigma_l\Big)\nu_a}{384M^2\nu^2}\Big[\ln\big(M^{1/2}R_R^{3/2}(t) - \mathscr{S}\big) - \ln\big(M^{1/2}R_R^{3/2}(t_i) - \mathscr{S}\big)\Big]. \end{aligned} \tag{C.40}$$

The expressions are not unique in terms of $\Phi_R(t)$ and $R_R(t)$ due to several RG invariants between them. The invariance over time with spin components can be found from the $\mathcal{S}^a_{+R}(\tau)$ solution, which is given by

$$i\ln\mathcal{S}^a_{+R}(t) - \Phi_R(t) - \frac{5\nu_a R_R^{3/2}(t)}{96M^{3/2}\nu^2} - \frac{5\Big(41S_l + 15\Delta\Sigma_l\Big)\nu_a}{384M^2\nu^2}\ln\big(M^{1/2}R_R^{3/2}(t) - \mathscr{S}\big) = \text{constant}. \tag{C.41}$$

Putting all the pieces together, the resummed solution of $S^a_+(t)$ is given by

$$\begin{aligned} S^a_+(t) =& \mathcal{S}^a_{+R}(t_i) \times \left(\frac{M^{1/2}R_R^{3/2}(t_i) - \mathscr{S}}{M^{1/2}R_R^{3/2}(t) - \mathscr{S}}\right)^{\frac{5i(41S_l+15\Delta\Sigma_l)\nu_a}{(384M^2\nu^2)}} \\ &\times \exp\left\{ -i\left[\Big(\Phi_R(t) - \Phi_R(t_i)\Big) + \frac{5\nu_a\Big(R_R^{3/2}(t) - R_R^{3/2}(t_i)\Big)}{96M^{3/2}\nu^2}\right] \right. \\ &+ i\left(\frac{2A^S_R(t)}{R_R(t)} - \frac{3\nu_a}{\nu}A^S_R(t)\Omega_R(t)^2R_R(t)\right)\sin\Phi_R(t) \\ &\left. - i\left[\frac{2A_R(t)}{R_R(t)} - \Big(19S_l + 9\Delta\Sigma_l\Big)\frac{A_R(t)}{R_R(t)^4\Omega_R(t)} - \frac{3\nu_a}{\nu}\Omega_R(t)^2A_R(t)R_R(t)\right.\right. \end{aligned}$$

$$+\frac{\nu_a}{\nu}\Big(\frac{29}{2}S_l+\frac{9}{2}\Delta\Sigma_l\Big)\frac{A_R(t)\Omega_R(t)}{R_R(t)^2}\Bigg]\cos\Phi_R(t)\Bigg\}, \tag{C.42}$$

with $\{R_R(t),\Omega_R(t),\Phi_R(t),A_R(t),A^S_R(t),\mathcal{S}^a_{+R}(t)\}$ given by (C.17), (C.20) and (C.40).

The quantity $\mathcal{S}^a_{+R}(t_i)$ depends on the initial conditions of dynamics and spin vectors. For instance, taking the initial input $S^a_n(t_i)$ and $S^a_\lambda(t_i)$, while getting $A_R(t_i)$, $R_R(t_i)$, $\Omega_R(t_i)$ and $\Phi_R(t_i)$ from numerically solving the initial conditions $r(t_i)$, $\dot{r}(t_i)$, $\omega(t_i)$ and $\phi(t_i)$ from the dynamics, we can determine the value of $\mathcal{S}^a_{+R}(t_i)$ through

$$\begin{aligned}\mathcal{S}^a_{+R}(t_i)=&\big(S^a_n(t_i)+iS^a_\lambda(t_i)\big)\\
&\times\exp\Bigg\{i\Bigg[\frac{2A_R(t_i)}{R_R(t_i)}-\Big(19S_l+9\Delta\Sigma_l\Big)\frac{A_R(t_i)}{R^4_R(t_i)\Omega_R(t_i)}-\frac{3\nu_a}{\nu}\Omega^2_R(t_i)A_R(t_i)R_R(t_i)\\
&\qquad+\frac{\nu_a}{\nu}\Big(\frac{29}{2}S_l+\frac{9}{2}\Delta\Sigma_l\Big)\frac{A_R(t_i)\Omega_R(t_i)}{R^2_R(t_i)}\Bigg)\cos\Phi_R(t_i)\Bigg]\\
&\qquad-i\left(\frac{2A^S_R(t_i)}{R_R(t_i)}-\frac{3\nu_a}{\nu}A^S_R(t_i)\Omega^2_R(t_i)R_R(t_i)\right)\sin\Phi_R(t_i)\Bigg\}.\end{aligned} \tag{C.43}$$

One immediate validation of the formulation is that the length of the spin vector should be a constant. Thus $\big|S^a_+(t)\big|=\sqrt{(S^a_n)^2+(S^a_\lambda)^2}$ should be a constant, since S^a_l does not change with time. From (C.42) and (C.43) we can see that the length is preserved, $\big|S^a_+(t)\big|=\big|S^a_{+R}(t_i)\big|=\sqrt{(S^a_n(t_i))^2+(S^a_\lambda(t_i))^2}$ as long as $\big(M^{1/2}R^{3/2}_R(t)-\mathscr{S}\big)>0$, the same constraint we encounter for the solutions of the orbit equations of motion.

C.7 The Moving Triad Evolution

In the text, the resummed analytic expressions for the orbital equations of motion and spin precession we obtained are written in terms of the moving triad vectors $\{\boldsymbol{n},\boldsymbol{\lambda},\boldsymbol{l}\}$. To transform the complete results into a fixed frame, we follow the solutions to the evolution equations for the moving triad in [58, 66] for the 1.5PN order conservative dynamics and build the moving triad evolution for the radiative dynamics on quasi-circular orbits.

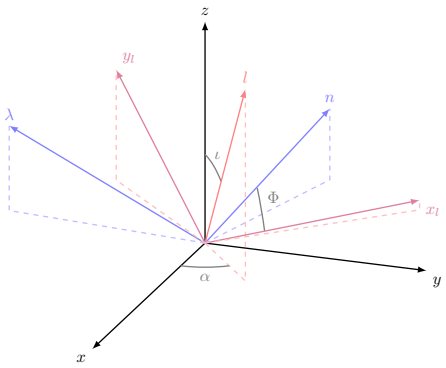

Figure C.1: Definitions of the Euler angle $\{\alpha, \iota, \Phi\}$ with respect to the moving triad $\{\boldsymbol{n}, \boldsymbol{\lambda}, \boldsymbol{l}\}$, the auxiliary moving frame $\{\boldsymbol{x}_l, \boldsymbol{y}_l, \boldsymbol{l}\}$, and the fixed lab frame $\{\boldsymbol{x}, \boldsymbol{y}, \boldsymbol{z}\}$.

We start by briefly summarizing the conservative moving triad evolution solution that relies fundamentally on the conservation of the total angular momentum $\boldsymbol{J}$. An orthonormal inertial frame $\{\boldsymbol{x}, \boldsymbol{y}, \boldsymbol{z}\}$ is then introduced with $\boldsymbol{J}/J$ as the fixed direction $\boldsymbol{z}$. Three Euler angles $\alpha(t), \iota(t), \Phi(t)$ are defined to specify the moving triad within the fixed frame as shown in Figure C.1. The azimuth α and the inclination ι are the standard spherical coordinates of the Newtonian angular momentum direction $\boldsymbol{l}$. The angle Φ is defined to be the angle between $\boldsymbol{n}$ and $\boldsymbol{x}_l$, where

$$\boldsymbol{x}_l = \frac{\boldsymbol{z} \times \boldsymbol{l}}{|\boldsymbol{z} \times \boldsymbol{l}|}, \qquad \boldsymbol{y}_l = \boldsymbol{l} \times \boldsymbol{x}_l, \tag{C.44}$$

forming the instantaneous orbital plane and with $\boldsymbol{l}$ to complete an auxiliary orthonormal basis $\{\boldsymbol{x}_l, \boldsymbol{y}_l, \boldsymbol{l}\}$.

In terms of the Euler angles, the relation between the moving triad $\{\boldsymbol{n}(t), \boldsymbol{\lambda}(t), \boldsymbol{l}(t)\}$ and the fixed Cartesian frame $\{\boldsymbol{x}, \boldsymbol{y}, \boldsymbol{z}\}$ can be written as

$$\boldsymbol{n} = (-\cos\Phi\sin\alpha - \sin\Phi\cos\iota\cos\alpha)\boldsymbol{x} + (\cos\Phi\cos\alpha - \sin\Phi\cos\iota\sin\alpha)\boldsymbol{y} + \sin\Phi\sin\iota\boldsymbol{z}, \tag{C.45a}$$

$$\boldsymbol{\lambda} = (\sin\Phi\sin\alpha - \cos\Phi\cos\iota\cos\alpha)\boldsymbol{x} + (-\sin\Phi\cos\alpha - \cos\Phi\cos\iota\sin\alpha)\boldsymbol{y} + \cos\Phi\sin\iota\boldsymbol{z}, \tag{C.45b}$$

$$\boldsymbol{l} = \sin\iota\cos\alpha\boldsymbol{x} + \sin\iota\sin\alpha\boldsymbol{y} + \cos\iota\boldsymbol{z}. \tag{C.45c}$$

The evolution solutions to the Euler angles up to linear order in spin are given by the components of the total angular momentum $\boldsymbol{J} = J_n(t)\hat{\boldsymbol{n}} + J_\lambda(t)\hat{\boldsymbol{\lambda}} + J_l(t)\hat{\boldsymbol{l}}$ as

$$\Phi + \alpha = \phi, \qquad \sin\iota = \frac{\sqrt{J_n^2 + J_\lambda^2}}{J}, \qquad e^{i\alpha} = \frac{J_\lambda - iJ_n}{J}e^{i\phi}, \tag{C.46}$$

where ϕ is the orbital phase, for which the resummed solution is given by (C.12) for the radiative binary orbits.

Finally, expressed in terms of some initial basis $\{\boldsymbol{n}_0, \boldsymbol{\lambda}_0, \boldsymbol{l}_0\}$ with corresponding Euler angles $\{\alpha_0, \iota_0, \Phi_0\}$, the moving triad $\{\boldsymbol{n}(t), \boldsymbol{\lambda}(t), \boldsymbol{l}(t)\}$ is given by

$$\boldsymbol{m} = e^{-i(\phi-\phi_0)}\boldsymbol{m}_0 + \frac{i}{\sqrt{2}}\left(\sin\iota e^{i\alpha} - \sin\iota_0 e^{i\alpha_0}\right)e^{-i\phi}\boldsymbol{l}_0 + \mathcal{O}(S^2) \tag{C.47}$$

$$\boldsymbol{l} = \boldsymbol{l}_0 + \left[\frac{i}{\sqrt{2}}\left(\sin\iota e^{-i\alpha} - \sin\iota_0 e^{-i\alpha_0}\right)e^{i\phi_0}\boldsymbol{m}_0 + \text{c.c}\right] + \mathcal{O}(S^2), \tag{C.48}$$

where $\boldsymbol{m} \equiv \frac{1}{\sqrt{2}}(\boldsymbol{n} + i\boldsymbol{\lambda})$ is a complex null vector.

The crucial point of this moving triad solution is the conservation of the total angular momentum and the ability to write out its components in the moving triad for all time, not the physical meaning to $\boldsymbol{J}$. In order to apply the triad solutions to a radiative motion where $\boldsymbol{J}$ can change, we find such a quantity that satisfies the requirements by observing the calculation of $\mathrm{d}\boldsymbol{J}/\mathrm{d}t$ for a conservative quasi-circular orbit. It is conventional to decompose $\boldsymbol{J} = \boldsymbol{L} + \boldsymbol{S}$, where $\boldsymbol{S}$ is the total spin specified by the choices of spin variables following [14], and $\boldsymbol{L}$ is the sum of the non-spinning Newtonian $\boldsymbol{L}_{\rm N}$ and the leading order spin-orbit contribution $\boldsymbol{L}_{\rm SO}$, given by

$$\boldsymbol{L}_{\rm SO} = \nu\left\{\frac{M}{r}\boldsymbol{n}\times\left[\boldsymbol{n}\times\left(3\boldsymbol{S} + \frac{\delta m}{m}\boldsymbol{\Delta}\right)\right] - \frac{1}{2}\boldsymbol{v}\times\left[\boldsymbol{v}\times\left(\boldsymbol{S} + \frac{\delta m}{m}\boldsymbol{\Delta}\right)\right]\right\}. \tag{C.49}$$

Written in terms of the moving triad components and taking the orbit radius and frequency as constants R and Ω for the quasi-circular approximation, the spin-orbit momentum becomes

$$\begin{aligned}\boldsymbol{L}_{\rm SO} =& \frac{1}{2}\nu R^2\Omega^2\left(\frac{m_2}{m_1}S_n^1 + \frac{m_1}{m_2}S_n^2\right)\boldsymbol{n} - \frac{\nu M}{R}\left(\left(\frac{m_2}{m_1}+2\right)S_\lambda^1 + \left(\frac{m_1}{m_2}+2\right)S_\lambda^2\right)\boldsymbol{\lambda} \\ &+ \left[\frac{1}{2}\nu R^2\Omega^2\left(\frac{m_2}{m_1}S_l^1 + \frac{m_1}{m_2}S_l^2\right) - \frac{\nu M}{R}\left(\left(\frac{m_2}{m_1}+2\right)S_l^1 + \left(\frac{m_1}{m_2}+2\right)S_l^2\right)\right]\boldsymbol{l}.\end{aligned} \tag{C.50}$$

For a conservative system without radiation, the time derivative to the sum $\boldsymbol{J} = \boldsymbol{L}_{\rm N} + \boldsymbol{L}_{\rm SO} + \boldsymbol{S}_1 + \boldsymbol{S}_2$ should vanish up to the Newtonian and leading spin order. By carrying out the detail calculation, we find that

$$\begin{aligned}\dot{\boldsymbol{L}}_{\rm SO} = &\left[\frac{1}{2}\nu R^2\Omega^2\left(\frac{m_2}{m_1}\dot{S}^1_n + \frac{m_1}{m_2}\dot{S}^2_n\right) + \frac{\nu M\Omega}{R}\left(\Big(\frac{m_2}{m_1}+2\Big)S^1_\lambda + \Big(\frac{m_1}{m_2}+2\Big)S^2_\lambda\right)\right]\boldsymbol{n}\\ &+\left[\frac{1}{2}\nu R^2\Omega^3\left(\frac{m_2}{m_1}S^1_n + \frac{m_1}{m_2}S^2_n\right) - \frac{\nu M}{R}\left(\Big(\frac{m_2}{m_1}+2\Big)\dot{S}^1_\lambda + \Big(\frac{m_1}{m_2}+2\Big)\dot{S}^2_\lambda\right)\right]\boldsymbol{\lambda},\end{aligned} \tag{C.51}$$

$$\begin{aligned}\dot{\boldsymbol{S}} = &-\frac{\nu M\Omega}{R}\Big[\Big(2+\frac{3m_2}{2m_1}\Big)S^1_\lambda + \Big(2+\frac{3m_1}{2m_2}\Big)S^2_\lambda\Big]\boldsymbol{n}\\ &+\frac{\nu M\Omega}{R}\Big[\Big(2+\frac{3m_2}{2m_1}\Big)S^1_n + \Big(2+\frac{3m_1}{2m_2}\Big)S^2_n\Big]\boldsymbol{\lambda},\end{aligned} \tag{C.52}$$

$$\dot{\boldsymbol{L}}_{\rm N} = -\frac{\nu M\Omega}{R}\Big[\Big(4+\frac{3m_2}{m_1}\Big)S^1_n + \Big(4+\frac{3m_1}{m_2}\Big)S^2_n\Big]\boldsymbol{\lambda}. \tag{C.53}$$

Thus the sum is

$$\begin{aligned}&\dot{\boldsymbol{L}}_{\rm N} + \dot{\boldsymbol{L}}_{\rm SO} + \dot{\boldsymbol{S}}\\ &= -\frac{\nu M}{R}\left[\left(\frac{1}{2}\frac{m_1}{m_2}\Omega_2 S^2_\lambda + \frac{1}{2}\frac{m_2}{m_1}\Omega_1 S^1_\lambda\right)\boldsymbol{n} + \left(\Big(2+\frac{m_1}{m_2}\Big)\Omega_2 S^2_n + \Big(2+\frac{m_2}{m_1}\Big)\Omega_1 S^1_n\right)\boldsymbol{\lambda}\right] \sim \mathcal{O}(v^2),\end{aligned} \tag{C.54}$$

which correspond to 1PN terms to be fixed by including higher-order orbital angular momenta. Notice that the time derivative of the spins in $\dot{\boldsymbol{L}}_{\rm SO}$ are completely canceled by $\dot{\boldsymbol{S}}$ and $\dot{\boldsymbol{L}}_{\rm N}$ at Newtonian order. Therefore we propose that for a radiative quasi-circular binary, the following quantity is conserved:

$$\begin{aligned}\mathscr{J} = &\sum_{a,b}\left\{\frac{1}{2}\nu\frac{m_b}{m_a}r(0)^2\omega(0)^2 S^a_n(t)\boldsymbol{n} - \frac{\nu M}{r(0)}\Big(\frac{m_b}{m_a}+2\Big)S^a_\lambda(t)\boldsymbol{\lambda}\right.\\ &\left.+\left[\frac{1}{2}\nu\frac{m_b}{m_a}r(0)^2\omega(0)^2 S^a_l(t) - \frac{\nu M}{r(0)}\Big(\frac{m_b}{m_a}+2\Big)S^a_l(t)\right]\boldsymbol{l}\right\}\\ &+\sum_{a,b}\nu M r(0)^2\omega(0)\boldsymbol{l} + \sum_{a,b}\boldsymbol{S}^a(t).\end{aligned} \tag{C.55}$$

Compared with the conservative expressions, we replace the constant orbital radius and frequency by the initial orbital radius and frequency. The conservative spin components are changed into the time-dependent resummed radiative spin component results. The time derivative of this quantity $\mathscr{J}$ is $\sim \mathcal{O}(v^4 S)$ but we are able to avoid the loss of total angular momentum due to non-spinning radiation at $\mathcal{O}(v^5)$. Using the substitution with $\mathscr{J}$ instead of $\boldsymbol{J}$ into the moving frame solutions (C.45- C.48), we can generate 3D-plot of the orbital radius evolution and animations of binary inspiral with spin orientation at every instant.

Bibliography

[1] S. Babak, R. Balasubramanian, D. Churches, T. Cokelaer, and B. S. Sathyaprakash. A Template bank to search for gravitational waves from inspiralling compact binaries. I. Physical models. *Class. Quant. Grav.*, 23:5477–5504, 2006.

[2] P. Ajith et al. A Template bank for gravitational waveforms from coalescing binary black holes. I. Non-spinning binaries. *Phys. Rev.*, D77:104017, 2008. [Erratum: Phys. Rev.D79,129901(2009)].

[3] Ian Harry, Stephen Privitera, Alejandro Bohe, and Alessandra Buonanno. Searching for Gravitational Waves from Compact Binaries with Precessing Spins. *Phys. Rev.*, D94(2):024012, 2016.

[4] Albert Einstein. Explanation of the perihelion motion of mercury from the general theory of relativity. *Sitzungsber. Preuss. Akad. Wiss. Berlin (Math. Phys.)*, 1915:831–839, 1915.

[5] HA Lorentz and J Droste. Collected papers of ha lorentz (vol. 5), 330p. *The Hague, Nijhoff*, 1937.

[6] Willem De Sitter. Einstein's theory of gravitation and its astronomical consequences. *Monthly Notices of the Royal Astronomical Society*, 76:699–728, 1916.

[7] Willem De Sitter. On einstein's theory of gravitation and its astronomical consequences. second paper. *Monthly notices of the royal astronomical society*, 77:155–184, 1916.

[8] A Einstein. Approximate integration of the field equations of gravitation (1916). translated in engel, a.(ed.) the collected papers of albert einstein, vol. 6, 1997.

[9] William L. Burke and Kip S. Thorne. Gravitational Radiation Damping. In *Relativity - Proceedings, Relativity Conference in the Midwest: Cincinnati, USA, June 2-6, 1969*, pages 209–228, 1970.

[10] Kip S Thorne and James B Hartle. Laws of motion and precession for black holes and other bodies. *Physical Review D*, 31(8):1815, 1985.

[11] Chad R. Galley and Adam K. Leibovich. Radiation reaction at 3.5 post-Newtonian order in effective field theory. *Phys. Rev.*, D86:044029, 2012.

[12] Richard W. O'Shaughnessy, J. Kaplan, V. Kalogera, and K. Belczynski. Bounds on expected black hole spins in inspiraling binaries. *Astrophys. J.*, 632:1035–1041, 2005.

[13] Scott A. Hughes and Roger D. Blandford. Black hole mass and spin coevolution by mergers. *Astrophys. J.*, 585:L101–L104, 2003.

[14] Lawrence E. Kidder. Coalescing binary systems of compact objects to postNewtonian 5/2 order. 5. Spin effects. *Phys. Rev.*, D52:821–847, 1995.

[15] Chad R. Galley and Ira Z. Rothstein. Deriving analytic solutions for compact binary inspirals without recourse to adiabatic approximations. *Phys. Rev.*, D95(10):104054, 2017.

[16] Adam K. Leibovich, Natlia T. Maia, Ira Z. Rothstein, and Zixin Yang. Second post-Newtonian order radiative dynamics of inspiralling compact binaries in the Effective Field Theory approach. 2019.

[17] Zixin Yang and Adam K. Leibovich. Analytic Solutions to Compact Binary Inspirals With Leading Order Spin-Orbit Contribution Using The Dynamical Renormalization Group. *Phys. Rev.*, D100(8):084021, 2019.

[18] Walter D. Goldberger and Ira Z. Rothstein. An Effective field theory of gravity for extended objects. *Phys. Rev.*, D73:104029, 2006.

[19] Albert Einstein, L. Infeld, and B. Hoffmann. The Gravitational equations and the problem of motion. *Annals Math.*, 39:65–100, 1938.

[20] Walter D. Goldberger and Andreas Ross. Gravitational radiative corrections from effective field theory. *Phys. Rev.*, D81:124015, 2010.

[21] Andreas Ross. Multipole expansion at the level of the action. *Phys. Rev.*, D85:125033, 2012.

[22] Chad R. Galley, David Tsang, and Leo C. Stein. The principle of stationary nonconservative action for classical mechanics and field theories. 2014.

[23] Chad R. Galley. Classical Mechanics of Nonconservative Systems. *Phys. Rev. Lett.*, 110(17):174301, 2013.

[24] John G. Baker, James R. van Meter, Sean T. McWilliams, Joan Centrella, and Bernard J. Kelly. Consistency of post-Newtonian waveforms with numerical relativity. *Phys. Rev. Lett.*, 99:181101, 2007.

[25] Joan Centrella, John G. Baker, Bernard J. Kelly, and James R. van Meter. Black-hole binaries, gravitational waves, and numerical relativity. *Rev. Mod. Phys.*, 82:3069, 2010.

[26] Sean T. McWilliams. Analytical Black-Hole Binary Merger Waveforms. *Phys. Rev. Lett.*, 122(19):191102, 2019.

[27] Thibault Damour, Piotr Jaranowski, and Gerhard Schafer. Nonlocal-in-time action for the fourth post-Newtonian conservative dynamics of two-body systems. *Phys. Rev.*, D89(6):064058, 2014.

[28] Thibault Damour, Piotr Jaranowski, and Gerhard Schafer. Conservative dynamics of two-body systems at the fourth post-Newtonian approximation of general relativity. *Phys. Rev.*, D93(8):084014, 2016.

[29] Piotr Jaranowski and Gerhard Schafer. Derivation of local-in-time fourth post-Newtonian ADM Hamiltonian for spinless compact binaries. *Phys. Rev.*, D92(12):124043, 2015.

[30] Laura Bernard, Luc Blanchet, Alejandro Bohe, Guillaume Faye, and Sylvain Marsat. Fokker action of nonspinning compact binaries at the fourth post-Newtonian approximation. *Phys. Rev.*, D93(8):084037, 2016.

[31] Laura Bernard, Luc Blanchet, Alejandro Bohe, Guillaume Faye, and Sylvain Marsat. Dimensional regularization of the IR divergences in the Fokker action of point-particle binaries at the fourth post-Newtonian order. *Phys. Rev.*, D96(10):104043, 2017.

[32] Tanguy Marchand, Laura Bernard, Luc Blanchet, and Guillaume Faye. Ambiguity-Free Completion of the Equations of Motion of Compact Binary Systems at the Fourth Post-Newtonian Order. *Phys. Rev.*, D97(4):044023, 2018.

[33] Laura Bernard, Luc Blanchet, Guillaume Faye, and Tanguy Marchand. Center-of-Mass Equations of Motion and Conserved Integrals of Compact Binary Systems at the Fourth Post-Newtonian Order. *Phys. Rev.*, D97(4):044037, 2018.

[34] Stefano Foffa and Riccardo Sturani. Conservative dynamics of binary systems to fourth Post-Newtonian order in the EFT approach I: Regularized Lagrangian. *Phys. Rev.*, D100(2):024047, 2019.

[35] Stefano Foffa, Rafael A. Porto, Ira Rothstein, and Riccardo Sturani. Conservative dynamics of binary systems to fourth Post-Newtonian order in the EFT approach II: Renormalized Lagrangian. *Phys. Rev.*, D100(2):024048, 2019.

[36] James B. Gilmore and Andreas Ross. Effective field theory calculation of second post-Newtonian binary dynamics. *Phys. Rev.*, D78:124021, 2008.

[37] Barak Kol and Michael Smolkin. Non-relativistic gravitation: from newton to einstein and back. *Classical and Quantum Gravity*, 25(14):145011, jun 2008.

[38] Andreas Ross. Multipole expansion at the level of the action. *Phys. Rev.*, D85:125033, 2012.

[39] Clifford Cheung, Ira Z. Rothstein, and Mikhail P. Solon. From Scattering Amplitudes to Classical Potentials in the Post-Minkowskian Expansion. *Phys. Rev. Lett.*, 121(25):251101, 2018.

[40] Chad R. Galley and Adam K. Leibovich. Radiation reaction at 3.5 post-newtonian order in effective field theory. *Phys. Rev. D*, 86:044029, Aug 2012.

[41] Luc Blanchet. Gravitational Radiation from Post-Newtonian Sources and Inspiralling Compact Binaries. *Living Rev.Rel.*, 17(1):2, 2014.

[42] A. Einstein, L. Infeld, and B. Hoffman. Progress in effective field theory approach to the binary inspiral problem. *Annals Math.*, 39:65, 1938.

[43] Laura Bernard, Luc Blanchet, Guillaume Faye, and Tanguy Marchand. Center-of-mass equations of motion and conserved integrals of compact binary systems at the fourth post-newtonian order. *Phys. Rev. D*, 97:044037, Feb 2018.

[44] Lawrence E. Kidder. Coalescing binary systems of compact objects to postNewtonian 5/2 order. 5. Spin effects. *Phys. Rev.*, D52:821–847, 1995.

[45] Rafael A. Porto. The effective field theorist's approach to gravitational dynamics. *Phys. Rept.*, 633:1–104, 2016.

[46] Clifford M. Will and Alan G. Wiseman. Gravitational radiation from compact binary systems: Gravitational waveforms and energy loss to second post-newtonian order. *Phys. Rev. D*, 54:4813–4848, Oct 1996.

[47] A. Gopakumar and Bala R. Iyer. Gravitational waves from inspiraling compact binaries: Angular momentum flux, evolution of the orbital elements, and the waveform to the second post-newtonian order. *Phys. Rev. D*, 56:7708–7731, Dec 1997.

[48] Walter D. Goldberger and Ira Z. Rothstein. An Effective field theory of gravity for extended objects. *Phys.Rev.*, D73:104029, 2006.

[49] Steve Drasco, Eanna E. Flanagan, and Scott A. Hughes. Computing inspirals in Kerr in the adiabatic regime. I. The Scalar case. *Class. Quant. Grav.*, 22:S801–846, 2005.

[50] Scott A. Hughes, Steve Drasco, Eanna E. Flanagan, and Joel Franklin. Gravitational radiation reaction and inspiral waveforms in the adiabatic limit. *Phys. Rev. Lett.*, 94:221101, 2005.

[51] Norichika Sago, Takahiro Tanaka, Wataru Hikida, and Hiroyuki Nakano. Adiabatic radiation reaction to the orbits in Kerr spacetime. *Prog. Theor. Phys.*, 114:509–514, 2005.

[52] Adam Pound, Eric Poisson, and Bernhard G. Nickel. Limitations of the adiabatic approximation to the gravitational self-force. *Phys. Rev.*, D72:124001, 2005.

[53] Bruce M Barker and Robert F O'Connell. The gravitational interaction: Spin, rotation, and quantum effects-a review. *General Relativity and Gravitation*, 11(2):149–175, 1979.

[54] Kip S. Thorne and James B. Hartle. Laws of motion and precession for black holes and other bodies. *Phys. Rev.*, D31:1815–1837, 1984.

[55] Katerina Chatziioannou, Antoine Klein, Neil Cornish, and Nicolas Yunes. Analytic Gravitational Waveforms for Generic Precessing Binary Inspirals. *Phys. Rev. Lett.*, 118(5):051101, 2017.

[56] Katerina Chatziioannou, Antoine Klein, Nicols Yunes, and Neil Cornish. Constructing Gravitational Waves from Generic Spin-Precessing Compact Binary Inspirals. *Phys. Rev.*, D95(10):104004, 2017.

[57] Lin-Yuan Chen, Nigel Goldenfeld, and Y. Oono. The Renormalization group and singular perturbations: Multiple scales, boundary layers and reductive perturbation theory. *Phys. Rev.*, E54:376–394, 1996.

[58] Luc Blanchet. Gravitational Radiation from Post-Newtonian Sources and Inspiralling Compact Binaries. *Living Rev. Rel.*, 17:2, 2014.

[59] KG Arun, Alessandra Buonanno, Guillaume Faye, and Evan Ochsner. Higher-order spin effects in the amplitude and phase of gravitational waveforms emitted by inspiraling compact binaries: Ready-to-use gravitational waveforms. *Physical Review D*, 79(10):104023, 2009.

[60] Sylvain Marsat, Alejandro Bohe, Luc Blanchet, and Alessandra Buonanno. Next-to-leading tail-induced spin–orbit effects in the gravitational radiation flux of compact binaries. *Classical and Quantum Gravity*, 31(2):025023, 2013.

[61] Lawrence E. Kidder, Clifford M. Will, and Alan G. Wiseman. Spin effects in the inspiral of coalescing compact binaries. *Phys. Rev.*, D47(10):R4183–R4187, 1993.

[62] Jeremy D. Schnittman. Spin-orbit resonance and the evolution of compact binary systems. *Phys. Rev.*, D70:124020, 2004.

[63] Karsten Ahnert and Mario Mulansky. Odeint–solving ordinary differential equations in c++. In *AIP Conference Proceedings*, volume 1389, pages 1586–1589. AIP, 2011.

[64] J. M. Martin-Garcia. xAct: Efficient tensor computer algebra for the Wolfram Language. https://www.xAct.es.

[65] Michael E. Peskin and Daniel V. Schroeder. *An Introduction to quantum field theory.* Addison-Wesley, Reading, USA, 1995.

[66] Luc Blanchet, Alessandra Buonanno, and Guillaume Faye. Tail-induced spin-orbit effect in the gravitational radiation of compact binaries. *Phys. Rev.*, D84:064041, 2011.